University of Stavanger

Faculty of Science and Technology

MASTER'S THESIS

Study program/ Specialization: MSc Petroleum Engineering / Reservoir Technology	Spring semester, 2011 Open
Author: Jan Morten Ferkingstad	..... (Author's signature)

Faculty supervisor: Professor Jann-Rune Ursin

External supervisor(s): Lene W. Andersen

Title of thesis:

Numerical Simulation of Productivity Effects by Hydraulic Fracturing in a Low Permeability Fluvial Reservoir in the North Sea

Keywords: Hydraulic Fracturing, Reservoir Simulation, Local Grid Refinement, Eclipse, Petrel, Fluvial reservoir	Pages: 85 + Appendix : 20 Stavanger, 15/06/2011

Acknowledgements

This thesis concludes the degree of Master in Petroleum Engineering at the University of Stavanger, with specialization on Reservoir Technology. The thesis was written for, and together with, Talisman Energy in Stavanger during the spring term 2011.

My intensions with this project were to get valuable experience using the reservoir simulator Eclipse and the modelling software Petrel, commonly applied in the industry, combined with the interest for hydraulic fracturing. In addition, the experience of being part of a team, and to work with an undeveloped field, were some of the reasons for choosing this subject.

Writing this thesis has been a challenging, exciting and outmost educational process which has given me the opportunity to do the practical work of a professional reservoir engineer. However, this thesis could never have been completed without the help and support from several individuals.

First of all, I would like to thank my supervisor at Talisman, reservoir engineer Lene W. Andersen. Her professionalism and encouragement have been an inspiration every day in the office. Thanks for all your guidance and motivational talks, and for letting me into the Talisman family.

I will also express my gratitude to the rest of the people at Talisman which has helped me with the thesis, especially the reservoir engineers Knut Olav Hettervik and Jørgen Leiknes. Both have been great consultants through interesting and helpful conversations. Thank You.

Thanks to the engineers at Schlumberger, Dag Bakkejord and Joel Robert, for answering all my questions regarding the software.

Finally, sincere thanks go to my professional supervisor at the University of Stavanger, Professor Jann-Rune Ursin, for motivational talks and guidance whenever needed. The thesis would never have been finished without your help.

Last but not least, my dearest greetings go to the love of my life, Katrine. Thanks for all your support and patience throughout this period, even though you were writing your own thesis. I wish you all the best!

Thank You All!

Regards

Jan Morten Ferkingstad, 15.06.2011

Abstract

A simulation study was performed on a recently discovered oil field. The operator is Talisman Energy, and the reservoir is complex in terms of disconnected fluvial channels, surrounded by a large majority of shale. The company was evaluating hydraulic fracturing of horizontal wells as a possible development strategy. Therefore, a simulation study was needed in order to estimate the increment in production by fracturing and to decide whether this field should be developed or not. The decision was made to numerically represent hydraulic fractures in the simulator using fine grid blocks, called Local Grid Refinement (LGR).

By using a small sector of the field reservoir model, two parallel horizontal wells were studied, one injector and one producer. Five scenarios were simulated where the aim was to get an understanding of how hydraulic fracturing could be optimised in the reservoir.

The first four scenarios studied two fractures in order to investigate the optimal distance between them, in terms of oil production, water breakthrough and sweep area. The position of the fractures was varied relatively in both wells and in one well only. The results indicated that there exist an optimal distance in the reservoir in regions of relatively equal permeability, but this distance is severely affected by flow barriers as shale and faults. The permeability variations, however, had less effect than expected. The main conclusion was that the optimal fracture setting varies throughout the reservoir. In general, fractures should not be placed too close to each other in order to avoid early water production, due to strong fracture interference. In addition, supporting fractures should be placed on the same side of a fault, sealing or not sealing, since this affects the communication.

The fifth and final scenario applied the conclusions from the other scenarios to optimise the multiple fracture placements in the two wells. Three transverse hydraulic fractures were placed in each well in order to give a realistic production estimate for one well couple. The results showed an increase in production, compared to a non-fractured case, of 400 000 Sm^3, which corresponded to 33% enhancement. In addition, the importance of high early production was identified, as the fracture performance dropped rapidly within the first years.

Uncertainty in the results exists, but hydraulic fracturing of parallel horizontal wells can severely improve the recovery in fluvial dominated reservoirs.

Table of Contents

List of Figures

List of Tables

1. Introduction

1.1 Background

Since its introduction to the petroleum industry in the late 1940's [1], hydraulic fracturing has evolved to become a common method for reservoir stimulation. As years have progressed, this technique has developed to fit with the increasing complexity of tight and low permeability reservoirs. This has resulted in the development of multiple hydraulic fracturing of horizontal wells.

Hydraulic fracturing is a complex and expensive process which requires careful planning and evaluation. To properly investigate the effect of this technique on a reservoir, hydraulic fractures with their designed properties must be analyzed in reservoir models through fracturing studies. Analytical solutions have made it possible to model the fractures, but in the recent years the need for numerical representations has been large in order to get accurate results and to follow the increasing complexity of new discoveries.

The international oil company, Talisman Energy, is considering to hydraulic fracture several parallel horizontal wells in a recently discovered oil field in the North Sea. The field is considered difficult to develop due to viscous oil and isolated fluvial channel-sands in the reservoir. This setting provides large variations in formation permeability and limited connectivity between the high porosity zones. In order to estimate the productivity enhancement from this strategy, a numerical simulation study is needed.

Numerical representation of hydraulic fractures has traditionally been performed by a gridding technique called Local Grid Refinement (LGR), where finer grid blocks are created around the wellbore geometry and the fractures. A new feature in Schlumberger's reservoir modelling software, Petrel, contains a feature which makes it possible to create hydraulic fractures in LGR within the program, and then directly export it to a reservoir simulator. This can potentially save time, as an alternative to manually create the grids.

This fracturing study is usually performed by service companies by detailed full field simulations, using internal models and templates. However, looking at the situation from an operator company point of view, these fracturing studies should ideally be done within the company, by the reservoir engineers themselves. This approach is therefore now considered by Talisman for the new discovery, in order to accurately estimate the possible gain in production from the planned development strategy. However, the physical aspects regarding the effects of fracturing of parallel wells in this type of reservoir is not fully understood, and the fracture placement must be evaluated in order to optimise the production.

1.2 Problem statement

The aim of this thesis was to explore the effects of hydraulic fracturing of parallel horizontal wells in a reservoir, dominated by fluvial deposition, in order to optimise the production in a possible Talisman development. The following topics were discussed:

- Can multiple hydraulic fractures effectively and accurately be simulated in a fluvial dominated reservoir, using local grid refinement and the available software Petrel?
- How should hydraulic fractures be placed in the wells in order to optimise the communication between them?

- Which factors affects the optimal fracture placement?
- How much can be produced based on optimal fracture placement in a multiple fractured development?

There were two main needs for this thesis to be done;

1) As the majority of the large oil fields in the North Sea has reached their peaks, the ability to develop new and complex reservoirs become important for global technology development, as well as growth and wealth of smaller oil companies. This will also be important for keeping up with the demand for oil in the world. This thesis may then be important as a guide for future discoveries.

2) The thesis is written and based on a real Talisman discovery in the North Sea, and the results of this study could be an important factor in the field development decision. It may also act as an analogue for future discoveries in the area.

1.3 Solution

The project was solved by using the Schlumberger reservoir modelling software Petrel Seismic to Simulation Software, version 2010.2 to create a sector model. The sector model was based on a small portion of the full field reservoir model of the Talisman discovery. By using this model, an analysis was performed evaluating the communication between two fractures in two parallel horizontal wells, one injector and one producer. The hydraulic fractures were modelled by using local grid refinement in the reservoir simulator, ECLIPSE 100 v2010.1.

By this approach, optimal placement of the hydraulic fractures was determined for the well couple. A final simulation was conducted where an optimised multiple hydraulic fracturing setting were compared to a non-fractured case.

The reservoir input data to the simulator was the same as for the full field model and the fracture properties were gathered from a fracture modelling study, conducted by Talisman.

1.4 Limitations

In order to have a good and clear definition of the thesis, as well as not being too wide, the scope of the study was settled by some limitations. The following topics were not considered or covered in this study:

- Tools applied during hydraulic fracturing
- Performance evaluation of high permeability units in the field
- Chemical aspects of hydraulic fracturing
- Performance simulations of alternative development strategies for producing low permeability reservoirs
- Acid fracturing

A general assumption that the reader has fundamental knowledge in both rock mechanics and reservoir simulation was made throughout this thesis. Therefore, such topics has not been considered in the report

1.5 The report

The study which has been performed is presented in the following report. The report consists of 10 chapters in addition to references, nomenclature and appendices.

Chapter 1 states the background, aim of thesis and the solution. Chapter 2 gives a brief introduction to the field discovery used in the thesis in terms of geology and planned development strategy. In Chapter 3, a basic introduction to the hydraulic fracturing process and the fundamental mechanics is given. Main methods to simulate hydraulically fractured horizontal wells and past work on the subject is investigated in Chapter 4. Chapter 5 concerns theory on available software used in the model.

Chapter 6 considers the main steps in how the simulation model was developed. Important assumptions and model input data are presented. Chapter 7 address the different simulations and scenarios performed during the study.

Chapter 8 presents all results from the simulations in form of graphs, plots and property maps. In addition, the results are evaluated and interpreted followed by a conclusion in each scenario. Problems encountered and simplifications to the model are explained. Possible sources of error are discussed at the end.

Chapter 9 summarize several conclusions from the results, while recommendations for further work are suggested in Chapter 10.

The appendices are present at the end of the report. These contain large illustrations and property maps which disturbs the readability of the report if included in the main chapters. In addition, plots of minor importance are located here. All figures in the appendices are referred to in the chapters.

2. The Field

This chapter presents available information about the discovered oil field. Important and relevant aspects regarding field history, geological setting and development strategy is addressed. The majority of the information has been retrieved from Talisman's internal database and employees, such that no reference is made unless other sources are used.

2.1 History

Talisman has discovered an oil field in the North Sea. A total number of four wells have been drilled, whereas the first well being the oil discovery. This well was formation tested, logged and cored before it was sidetracked as an appraisal well. One more appraisal well was drilled, tested, cored and sidetracked. All the available information which has been collected from the wells is:

- Three well tests
- Logs and cores in all wells

Based on this information, a geological model and a full field reservoir model were built.

2.2 Location

The field is located in the North Sea Central graben and the reservoir consists of rocks from late Triassic to middle Jurassic period. In this region, three main formations are evident in the reservoir. From top to bottom these are, in this report, referred to as Unit 1, Unit 2 and Unit 3. In the top of Unit 2 there is a sealing coal layer which prevents communication with Unit 1.

The regions on the field are divided into one eastern part and one western part, which are separated by a large fault. Whether this fault is sealing or not is not certain, but currently the engineers assume that it is sealing. Some minor faults are also present within the two regions.

2.3 Geology

2.3.1 Depositional environment

The whole system consists of a transgressive shoreface environment to a fluival channel system which can be illustrated by Figure 2-1.

The uppermost unit, Unit 1, consists of two sedimentological parts; an upper tide dominated delta deposition, and a lower wave dominated shoreface deposition. The deposition of Unit 1 is believed to have occurred by either storm waves or salt induced embayment. The facies found in Unit 1 are fine grained, silty sandstone in the lower shoreface region, which contains cross stratified structures created by waves. The tidal dominated delta part is mainly medium grained sandstone forming cross beds.

Figure 2-1: Illustration of a river-shoreline delta.

The middle unit, Unit 2, basically consist of meandering fluvial channels. The logs from the two wells in Figure 2-2 indicate a transgressive system where the top unit is a coastal swamp environment, moving into floodplain and more stacked fluvial channels with coal debris further down. From the logs it is evident that the thickness of Unit 2 varies strongly. The geologists believe that this is due to factors as base coal truncation on the transgressive event resulting in drifted and accumulated coal, or incision into the unit below where there is a large time gap.

The bottom unit, Unit 3, consist of two main facies. At the top, clean porous sandstone containing calcrete is evident. Calcrete is a carbonate rich, hard layer which is formed due to climatic fluctuations in an arid or semiarid environment [2]. These produce carbonate cement. At the bottom the system returns to a fluvial channel environment with floodplain mud. These channels have a wider geometry than the channels in Unit 2, which means that a layer-cake reservoir may be a sufficient interpretation.

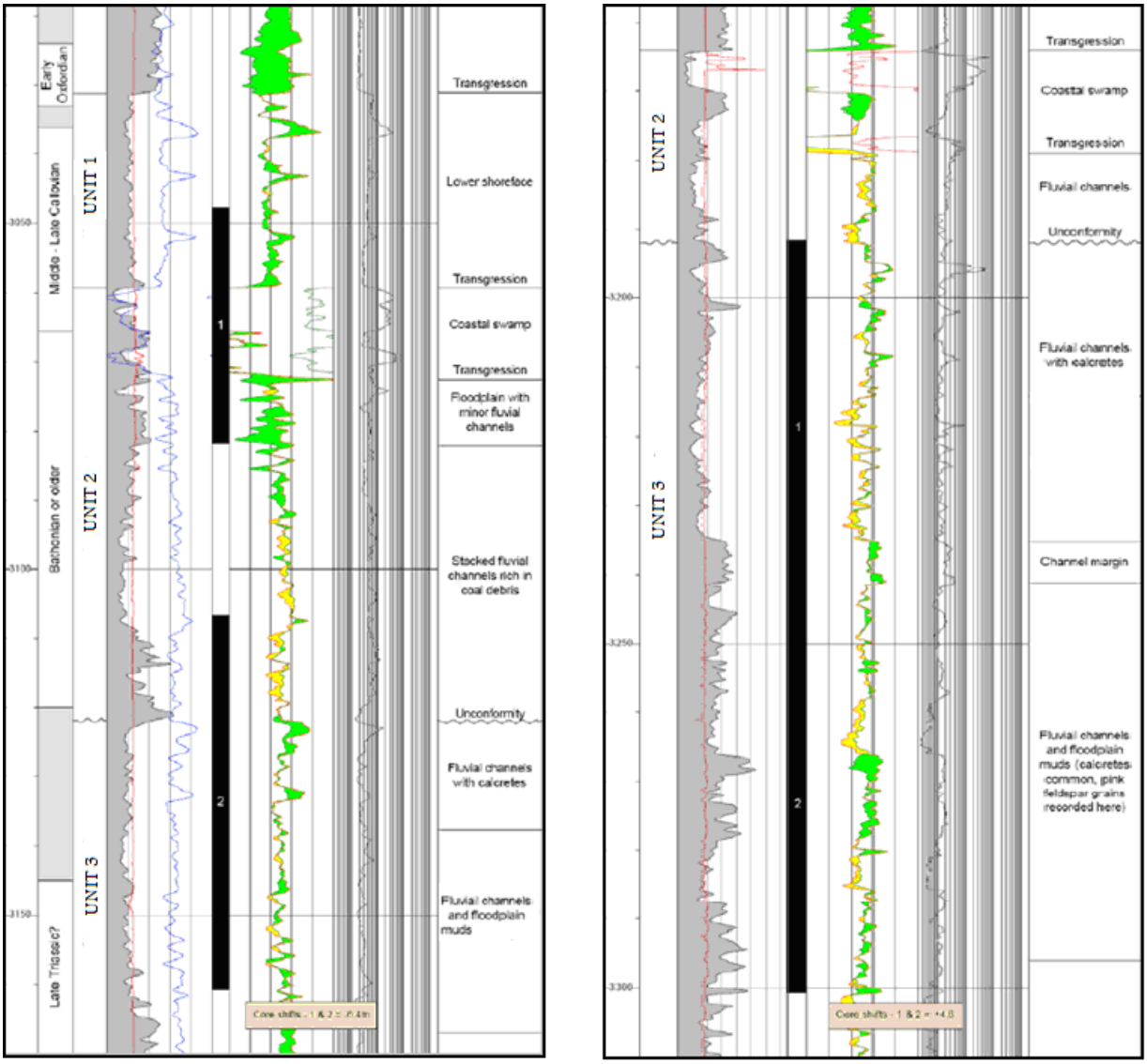

Figure 2-2: Field log and core data gathered from the two wells on the field.

2.3.2 Reservoir quality

Since Unit 1 consists of well sorted, uniform beach deposits, this layer has permeability values greater than for reservoir rocks where stimulation is needed for obtaining a good productivity. The coal layer seals the vertical communication between Unit 1 and the other units.

The fluvial channels in Unit 2 has moderately sorted, fine grained sandstone, while the uppermost fluvial channel zone in Unit 3 has poorly sorted, fine grained sands. Due to the calcrete, calcite cementation gives the zone low porosity. The quality is somewhat better in the lower fluvial zone, where the sand is moderate to poorly sorted and medium grained.

In general, this reservoir seems to be mainly dominated by fluvial channels surrounded by fine grained flood plain deposits. The channels may have permeability as high as 200 mD, while the surrounding shale deposits have permeability values from 0 to 5 mD. As a consequence, many of the good-quality sandstones are isolated and disconnected. This is the major issue causing questions about the profitability of developing this field.

2.3.3 In-situ stress

The in-situ stress measurements gathered in the area provides a North East – South West orientation for the minimum horizontal stress, and North West – South East direction for the maximum horizontal stress.

2.4 Development

2.4.1 Development strategy

Due to the complex reservoir in Unit 2 and 3, combined with the viscous oil, natural depletion may not be sufficient to produce these sections. Therefore, the engineers in Talisman are evaluating different methods for stimulating the production. The main method involves water injection for pressure support and hydraulic fracturing for connectivity enhancement.

The proposed strategy is mainly to drill several parallel and alternating horizontal injectors and producers in Unit 2 and 3, each having an azimuthal direction parallel to the minimum horizontal stress orientation. Based on cost estimates, the wells are to be hydraulically fractured with multiple transverse hydraulic fractures (*see Section 3.4.3*) in each well.

To ensure sufficient drawdown artificial lift may be performed by installing Electric Submersible Pumps (ESP). The ESP's has a pump pressure slightly above the oil bubble-point pressure such that occurrence of gas in the reservoir is prevented. This could potentially give good drawdown on a long term basis since the bubble-point pressure is relatively low compared to the high initial reservoir pressure.

If hydraulic fracturing becomes the final selection, horizontal sections will be completed as open-hole wells with sand-screens in order to avoid sand production. This gives the formation fluid opportunity to enter the wellbore, not only through the fractures, but also through possible high permeability zones intersected by the wellbores. One possible drawback with this completion design is that collapse may occur if the reservoir rock is unconsolidated or if the flow rates become too high.

In addition, the following alternative methods will be evaluated:

- Miscible gas injection to eliminate the oil surface tension by creating a highly mobile single phase in the reservoir
- Drill multilateral wells to increase the drainage area
- Deep gas lift

These methods do not exclude one another and could be combined. Gas lift may not be possible due to asphaltene issues and lack of gas availability. The scenarios studied in this thesis focused on the possible hydraulic fracturing strategy, and positive or negative interferences between the wells and fractures.

2.4.2 Risk of fracturing

Making transverse hydraulic fractures in horizontal wells, planned in a depletion strategy like this, provides a large risk of making fractures which coincides and extends all the distance between the wells. If this becomes the reality, a highly conductive path between the producer and the injector will be transferring the injected water directly to the producer, resulting in

only water being produced from this fracture. Therefore, it is not necessary true that hydraulic fracturing in the injectors will increase the production further. It may, as mentioned, rather decrease the production. In addition, the matrix in the fractured area would be bypassed.

3. Hydraulic Fracturing Theory

This chapter covers main important principles regarding hydraulic fracturing mechanics. For a more detailed description of the fracturing process, fracture mechanics and design the reader is advised to study reference [3].

3.1 Definition

A precise definition of hydraulic fracturing is given by Lake and Clegg [4]:

> *"Hydraulic Fracturing is a process of pumping a fluid into a wellbore at an injection rate too great for the formation to accept in a radial flow pattern"*

As the definition states, the formation is hydraulically fractured by exceeding the formation strength.

There are two main scenarios for creating hydraulic fractures [5]. One is to unintentionally fracture the formation during drilling. This is due to high Equivalent Circulating Density (ECD), caused by too high mud weight or pump rate. The other case is to intentionally fracture the formation, either during drilling to determine the fracture gradient of the formation, or during/after development to increase the productivity of the reservoir and wells. The last part gives rise to two important and distinct terms, reservoir stimulation and damage removal, which will be discussed in the following.

After a time of production in a reservoir, the permeability tends to be reduced in the area close to the well. This near-well effect is called damage and result in higher pressure drop through this zone, limiting the inflow performance and the wellbore productivity. This damage is expressed with a skin factor, S, and the extra pressure drop caused by damage must be added to the performance equations. The skin pressure drop is defined as [3]:

$$\Delta p_s = \frac{q\mu}{2\Pi kh} S \tag{3.1}$$

The skin factor can take both negative and positive values, as well as zero. Positive skin values indicate damage and permeability reduction, which again reduces the rates. Skin equal to zero means undamaged reservoir. Negative skin indicates that the permeability and connectivity is greater than initial, hence the productivity is increased beyond the natural state of the reservoir.

Reservoir stimulation only refers to techniques giving negative skin values at the end of treatment [3]. Processes like acid treatment, only reducing skin to a positive number, are defined as damage removal. Hydraulic fracturing is a technique within the reservoir stimulation category.

3.2 Applications

One of the main objectives for hydraulic fracturing is to increase the reservoir productivity. By, for instance, studying the pseudo-steady state solution for the productivity index, one can easily determine the factors that must be altered in order to maximise the production [6].

$$PI = \frac{q}{\bar{p} - p_{wf}} = \frac{2\Pi kh}{\ln \frac{r_e}{r_w} - \frac{3}{4} + S} \tag{3.2}$$

From Equation 3.2 the productivity is enhanced by:

- Increasing the flow potential, kh
- Increasing the wellbore radius, r_w
- Reducing the skin factor, S

These factors may be altered by creating hydraulic fractures. By increasing the flow potential, a highly conductive fracture enhances connectivity between reservoir and wellbore. The wellbore radius is increased by maximizing the wellbore contact-area with the reservoir through hydraulic fractures. The skin is reduced by creating fractures in order to bypass damaged zones near the wellbore, and connect the well to distal parts of the reservoir.

All in all, hydraulic fracturing in the oil industry is mainly performed in order to [4]:

- Enhance productivity in low permeability reservoirs
- Enhance productivity of damaged reservoirs
- Connect natural fractures to the wellbore
- Increase the reservoir drainage area
- Establish vertical communication in layered reservoirs

In this thesis hydraulic fracturing was applied for productivity enhancement in a low permeability reservoir to establish lateral and vertical connectivity.

3.3 The fracturing process

The hydraulic fracturing process for reservoir stimulation is, in fact, rather simple [3]. It involves heavy pumping of a fracturing fluid down the well at larger rates than the rate of fluid escape into the formation. Thereby, the hydraulic effect exceeds the strength of the formation and a fracture is created. Consequently, the fracturing fluid disappears into the formation through the fracture. If the pump rate is kept larger than the rate of fluid loss, the fracture will propagate further into the formation and increase the wellbore contact area with the formation. When pumping ceases, the fracture will close and no further effect would be seen. To prevent this from happening, a highly resistant material, called proppants, is injected together with the fluid. This creates porosity in the fracture as well as sufficient fracture conductivity. After the proppants have been placed, the pressure is relieved and the well is shut in for a period. The shut-in period allows the fracture to close around the proppants and for the injected fluid to leak off. Afterwards, the fracture has gained properties important for

reservoir flow and production enhancement. The properties are given below and illustrated for a fractured horizontal well in Figure 3-1.

- Propped fracture width, w
- Fracture half-length, x_f
- Propped fracture height, h_f
- Fracture permeability, k_f

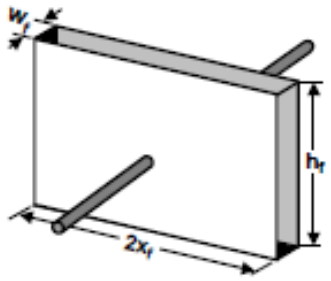

Figure 3-1: Geometry of a vertical transverse hydraulic fracture [22].

A quantity which becomes important in fracturing design is the fracture conductivity, F_c;

$$F_c = k_f w \tag{3.3}$$

The effective conductivity of the fracture is frequently measured in milli-Darcy feet (mDft) or milli-Darcy meters (mDm). Furthermore, it is more convenient in many cases to use the dimensionless fracture conductivity;

$$F_{cD} = \frac{k_f w}{k x_f} \tag{3.4}$$

Here, k is the formation permeability. The dimensionless fracture conductivity is defined in reference [3] as; *"the ratio of the ability of the fracture to carry flow, divided by the ability of the formation to feed the fracture"*.

Equation 3.4 is used to optimise the fracture performance [7]. A desired dimensionless conductivity is kept constant, as well as optimal fracture half-length and reservoir permeability. The focus is then on maximizing the fracture permeability and width. This is done by choosing appropriate materials and treatment procedures.

3.4 Fracturing principles

3.4.1 Fracture initiation and propagation

A general rule can be given for hydraulic fractures; a fracture always propagates in a symmetric plane, directed perpendicular to the minimum in-situ stress [3]. Commonly this stress is horizontal, creating a vertical fracture. For other cases, for instance where the vertical overburden stress component is the least in-situ stress, the fracture becomes horizontal.

Fracture initiation, however, occurs in the direction of least resistance, which is not necessarily directed perpendicular to the minimum in-situ horizontal stress. In horizontal or deviated boreholes initial fracture direction depends on the wellbore azimuth. Wellbores with azimuths oriented parallel and perpendicular to the minimum in-situ stress create fractures normal and parallel to the wellbore, respectively. If the wells are not in alignment to the horizontal stresses, fractures will initiate in the direction of least resistance, which may seem random. Further out in the formation, the fractures locate the in-situ stress, re-orientate and propagate according to the general rule. [5]

3.4.2 Fracture confinement

The vertical and horizontal propagation of a fracture is dependent on the formations above and below the zone to be hydraulically fractured [8]. If a fracture is created in a thin sand zone with coal or shale layers above and below, these will have larger horizontal stresses than in the sand due to larger Poisson's ratio. The vertical fracture growth thus terminates in these tight stress barriers. Therefore, the fracture becomes confined within the sand zone and extends deep into the formation. This fracture is then called a confined hydraulic fracture and will have an elliptical shape as shown in Figure 3-2A.

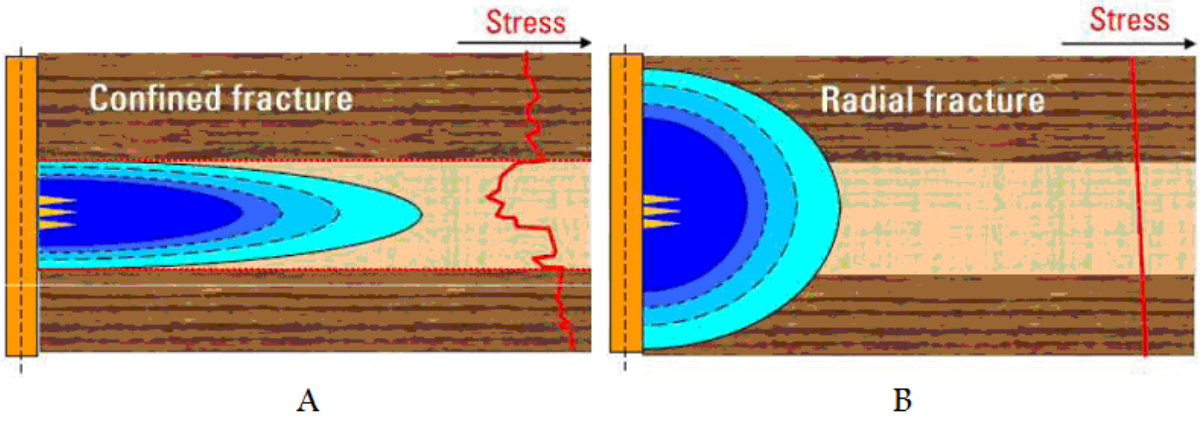

Figure 3-2: Confined (A) and unconfined, radial (B) hydraulic fracture and respective stress gradients [6].

If the fracture is initiated in a large, thick sand reservoir, having a uniform stress gradient, it will not be confined and grows upwards instead of outwards. This fracture is then called radial hydraulic fracture and will have a circular shape as shown in Figure 3-2B [6]. Fracture confinement can be explained by the following equation [9]:

$$\sigma_h = \frac{\upsilon}{1-\upsilon}\sigma_v \qquad (3.5)$$

Equation 3.5 states that the minimum horizontal stress (σ_h) in a formation is dependent on Poisson's ratio (υ) and the overburden stress (σ_v). Therefore, in tight formations where large Poisson's ratio occur, the least horizontal stress becomes larger than in porous sandstone, which typically has a ratio of 0.2 – 0.25 [9]. This result in the horizontal stresses in the stress barriers pressing against each other, thus terminating further vertical fracture growth.

In addition to contrasts in horizontal stress, other factors important for fracture confinement are pump pressure and differences in elastic properties and rock strength. If the pump pressure during hydraulic fracturing becomes large enough, the least horizontal stress in the stress barriers is not sufficient to terminate the fracture. [5]

3.4.3 Fracturing of horizontal wells

As stated before, the type of hydraulic fracture created is dependent on the azimuthal direction of the wellbore. Ideally, the well should be drilled along the direction of the three principal stresses (σ_h, σ_H, and σ_v) [8]. For a horizontal well this means wellbore orientation parallel or perpendicular to the least horizontal stress. These settings create to two types of hydraulic fractures in horizontal wells; transverse and longitudinal fractures.

A horizontal well drilled normal to the least in-situ horizontal stress direction would create a vertical fracture going along the wellbore. This is called a *longitudinal* hydraulic fracture. If, however, the well is drilled parallel to the least horizontal stress orientation, a vertical fracture plane will form perpendicular to the wellbore. This type is called a *transverse* hydraulic fracture and several of those can be made in a well [10]. This is frequently referred to as multiple hydraulic fracturing. Figure 3-3 illustrates the two fracture types.

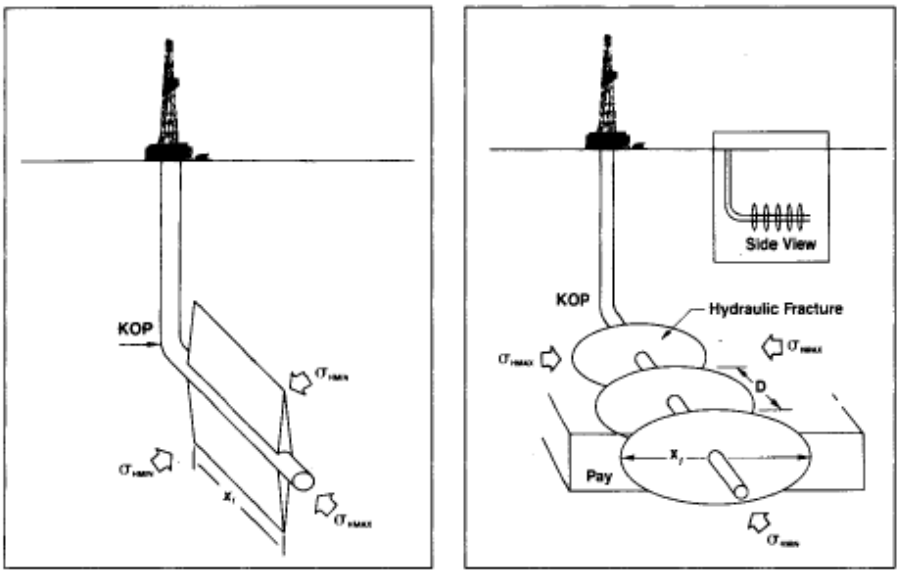

Figure 3-3: Longitudinal (left) and transverse (right) hydraulic fractures in horizontal wells [21].

3.4.4 Factors affecting fracture performance

The performance of hydraulic fractures after production has started, i.e. in the post-fracturing phase, is affected by factors related to the proppant mechanical strength and relative permeability effects from fluids flowing through the fracture. These factors normally have a negative effect on the fracture conductivity and should be accounted for in the planning process. The main factors are described in the following.

Non-Darcy effects

In cases where the hydraulic fractures provides high flow rate, most typically in gas reservoirs, the production may be reduced by an increase in pressure drop within the fracture. This is due to inertial effects and turbulence where the fluid accelerates and decelerates in a tortuous flow path [11]. The flow no longer follows Darcy's law, but is expressed through non-Darcy effects and Forchheimer's equation.

Fracturing fluid damage

After the treatment, the viscous fluid used for fracturing, is present in the fracture and a filter cake is created on the rock surface [12]. These will reduce the conductivity and the initial production will be fracturing fluid only.

Multiphase effects

When the flow inside a fracture alters from single phase flow to multiphase flow, by for instance water/gas breakthrough or production below bubble-point pressure, the relative permeability is affected. This effect is extremely important on productivity in gas condensate wells [13].

4. Simulation of Hydraulic Fractures in Horizontal Wells

When performing a simulation study of hydraulic fracturing, petrophysical data and stress measurements are used as input to a hydraulic fracture design model. This model then predicts the important fracture parameters as conductivity, height, width and half-length. These properties are then transferred to the reservoir simulator and assigned to the grid blocks representing the hydraulic fracture in the reservoir model. There are several methods for hydraulic fracture representation and the following chapter address some of them in a literature survey of past work of multiple hydraulic fracturing simulations in horizontal wells.

4.1 Past work and methods

In the last decades, many simulation studies of hydraulically fractured horizontal wells have been published [13-26].

Karcher et al. (1986) studied productivity enhancement of hydraulic fractures in a horizontal well compared to a vertical well in 1986. Pseudo-steady state flow equations were used in a finite difference simulator which confirmed that horizontal wells should be placed normal to the hydraulic fractures. This could increase the productivity up to 10 times the productivity of a vertical well.

Schulte (1986) calculated the bottom-hole pressure (BHP) in a fractured gas reservoir using finer grid blocks along the fracture, both near the wellbore and the fracture tips. It was stated that long term production is severely reduced when the inflow interval is much smaller than the fracture height.

Larsen and Hegre (1994) developed analytical models for all flow regimes in multiple fractured horizontal wells which should solve the complexity of choosing correct models for fracture representation.

Hegre (1996) discussed the effect of both transverse and longitudinal hydraulic fractures in horizontal wells. He studied the effect of grid block size with respect to long term production using finite conductivity fractures. He stated that a hydraulic fracture should, in general, be modelled explicitly by using small, highly conductive grid cells representing the fracture and relatively small grid cells near the fractured area, to capture the transient pressure behaviour of single wells. He also recommended increasing the grid block width describing the fracture, and correspondingly decreasing the fracture permeability, keeping the fracture conductivity constant. This was mainly to reduce numerical stability problems and simulation time.

Hegre also gave a review of *the equivalent effective wellbore radius concept*. This is an analytical method and the traditionally simplest technique for describing hydraulic fractures in reservoir simulators. The method is based on analytical solutions of the Paceman formula [27] and the concept is that fractured horizontal wells are modelled as standard non-fractured vertical wells, with no further geometrical representation. This is done by establishing an equivalent wellbore radius of the vertical well which corresponds to the fractured horizontal well, given directly from dimensionless charts. Hegre states that this method is a simple way of modelling fractures and may be sufficient for some reservoir management purposes.
Ding (1996), in addition to *Hegre (1996)*, proposed methods for hydraulic fracture representations which include the use of coarser grid blocks as an alternative to fine grid cells near the wells and fractures. Ding used numerically calculated productivity indices and

equivalent transmissibility values around wells and fractured grid blocks. Hegre recalculated the transmissibility value between the neighbouring blocks and the block containing the fracture, using the average pressure. In addition, the well connection factors between wellbore and cells, in which the wellbore is completed, were adjusted. This is referred to as *the transmissibility corrected method.*

Ehrl et al. (2000) conducted a full field study of a tight gas field in order to determine the productivity increase from fracturing of horizontal wells. They used two levels of fine grid blocks outside wells and fractures. The fracture permeability was assigned to the fractured grid blocks by keeping the designed fracture conductivity constant and using the grid block width, as stated by Hegre.

Wan et al. (2002) investigated multiple fractured horizontal wells using a semi-analytical model, which combines analytical solutions of the well pressure with numerically calculated grid block pressures in order to determine the equivalent effective wellbore radius. The study was limited to fractures within one grid block.

Iwere et al. (2006) conducted a full field fracturing study using fine grid blocks in a reduced volume of the reservoir model, in order to determine flow models in a coarse grid based on effective properties. This method gave accuracy close to the fine grid method.

Sadrapanah et al. (2006) discussed advantages of fine-grid explicit modelling of hydraulically fractured horizontal wells and applied it to a field model. They stated the importance of gradual grid refinement towards the wellbore to avoid numerical stability issues, as well as the need for numerical modelling of layered reservoirs to represent realistic flow behaviour.

Fjærstad et al. (2008) represented hydraulic fractures in a new simulator by using unstructured, refined grid blocks in the well and fractured area. Explicit fracture modelling was performed to capture fluid flow into and inside the fracture. The refinement around the wells gave accurate pressure description and breakthrough observations.

Abacioglu et al. (2009) applied a coarse grid method which treats the hydraulic fractures as infinite conductivity line sources, such that the elliptical drainage pattern around the fracture was captured.

Soleimani et al. (2009) modelled fractured wells using a Near Wellbore Simulator and a sector model. Unstructured and refined grid was applied in the fractured area.

In the recent years, a need of combining fracture design software and reservoir simulators has resulted in development of tools, which automatically transfer the gridded hydraulic fractures and their properties from the fracture design model to the reservoir simulator [28-30]. This development eliminates time-consuming, manual work as well as many factors which impacts fracture performance, are accounted for.

Throughout the papers, three main simulation methods for representing hydraulic fractures in horizontal wells have been presented;

- Fine grid around fracture and wells using Local Grid Refinement (LGR)
- Equivalent Effective Wellbore Radius method
- Transmissibility Corrected Method

Each method involves positive and negative aspects which should be evaluated. Using the LGR method, large degree of accuracy is gained since accurate pressure distribution and fluid movement is captured towards the wellbore and fractures. In addition, factors affecting the fracturing performance can be modelled inside the fracture. Water or gas breakthrough and coning effects are also described accurately using fine grid blocks. The main problem with the technique is the long simulation time for full field studies. Full field simulations often have many wells, and if each fractured well should be represented by LGR, too many grid blocks would result in a slow and ineffective simulation [20]. In addition, manual construction of local grid is time consuming, but some simulators or modelling software has the ability to create the grids automatically [19].

The equivalent wellbore radius method, compared to the LGR method, is more flexible regarding large scale simulations. The fractures are represented without refining the coarse grid; hence a more efficient field simulation can be run. However, this method has one important limitation; the effective wellbore radius must be smaller than the pressure equivalent radius of the grid cell [15]. In other words this means that the fractured horizontal wellbore must be located within one single areal grid block. This limits the use of this method in cases where long wells and relatively small grid blocks must be applied. In addition, the fracture geometry is not represented, making flow analyses around fractures difficult.

The transmissibility corrected method is also using the original, coarse grid blocks in model to represent hydraulic fractures. Therefore, it becomes applicable for large field simulations. The only problem is that the transmissibility multipliers used in the simulation must be computed and validated based on a fine grid model, using LGR. Therefore, this model is most effective in cases where it is easy to include LGR, and where software or correlations compute the adjusted parameters.

5. Available software

This chapter provides theory on two techniques available in the reservoir simulator Eclipse and modelling tool Petrel; sector modelling and hydraulic fracture representation by local grid refinement. For workflows, the reader is referred to the Petrel user manual with reference [31] and the Eclipse user manual with reference [32].

5.1 Sector modelling

In general, a full field reservoir model is used to simulate and predict fluid movement and production of the entire field. Sometimes, however, simulations not affecting the whole reservoir are performed. This can be for instance single well studies which has a small drainage area compared to the field area. In such cases, full field simulations will reduce the efficiency of the study, since many more grid blocks than needed are simulated.

As an alternative to the full field simulation, Eclipse offers the use of flux boundaries. This means that a large model can be reduced to a smaller model, based on sector boundaries specified by the user. This eliminates the grid blocks outside its volume and thereby allows the user to perform simulations on a small part of the full field model only.

In order to create a sector model, certain boundary conditions must be specified. There are three possible alternatives of creating boundary conditions in the model [31]:

1. Capture the fluid flux through the boundaries by running a full field simulation.
2. Capture the pressure in the boundary grid blocks by running a full field simulation.
3. Use a no flux boundary condition such that the boundaries create an isolated reservoir.

The two first alternatives provide boundary conditions based on a large field scale which means that the entire field model must be run. The full field model provides fluid flux and pressure conditions on the boundaries which are written to a file. This file is then used as input to the reduced sector model to get the most likely fluid movement and pressure behaviour across the boundary grid blocks. The third alternative is the simplest and state that no fluid flows through the boundaries. In other words, a no flow boundary is created and the sector becomes closed.

Petrel provides an interface which can create the sector model, eliminating manual editing of the Eclipse run files. The keywords which are exported to Eclipse from Petrel to simulate the sector model are given in Table 5-1.

Table 5-1: Keywords in Eclipse used for sector modelling.

Data file section	*Keyword*	*Meaning*
GRID	DUMPFLUX	Used in the full field run to tell the simulator to capture the fluid flux across the sector boundaries.
	USEFLUX	Used in the sector model run to activate flux option and to import the flux file created from the full field run.
	FLUXREG	Tells the simulator which regions in the full field model that is active. Active regions define the sector model.
	FLUXNUM	Define the regions in the full field model which is to be run as a sector model.
	FLUXTYPE	Specifies the type of boundary conditions which are to be used in the sector model (FLUX or PRESSURE)
	USENOFLO	Activates the no flow boundary condition and overwrites the FLUXTYPE keyword

It should be mentioned that a sector model only will give results based on the sector; hence the boundary conditions used are only approximations. A sector model simulation should therefore never be compared to a full field simulation run [31].

5.2 Hydraulic fracturing by Local Grid Refinement (LGR)

As mentioned, LGR is a technique within Eclipse which basically involves splitting of coarse grid blocks into smaller cells, in order to achieve a more detailed simulation in sensitive areas. This is the most common and accurate technique used for hydraulic fracture representation. The workflow for simulating hydraulic fractures by LGR in Eclipse is a time consuming process and different variants may be proposed. However, there are some general elements which must be included [32].

***Grid type*:** A type of LGR must be chosen. Eclipse offers three main types of grids; radial, cartesian and unstructured (PEBI) refinement. Traditional representations of fractures are made using cartesian refinement. The principle is to split the coarse grid blocks, called *host* or *global cells*, in the area of interest into boxes of smaller cells, having squared geometry along I, J and K direction of the model. A uniform cartesian grid refinement is illustrated in Figure 5-1A.

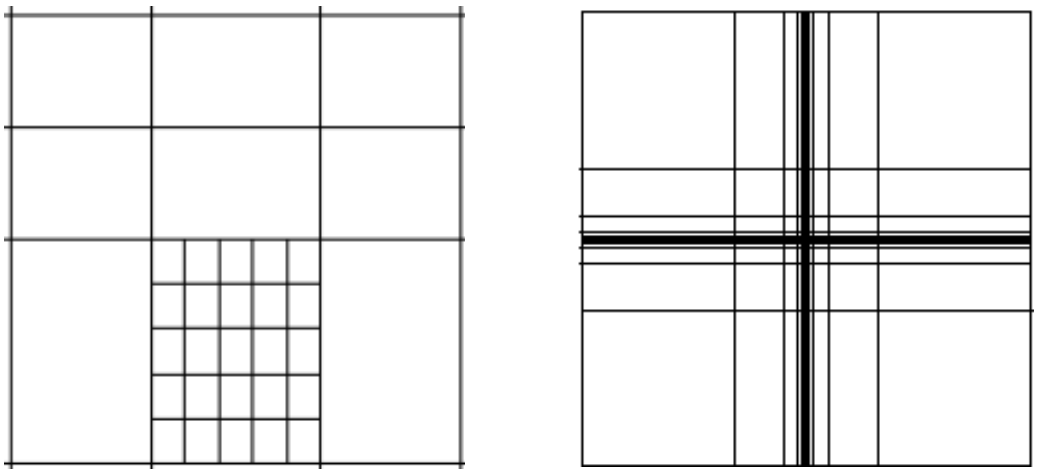

(A) (B)

Figure 5-1: Example of uniform (A) and gradual (B) cartesian LGR [22, 32].

***Grid block size*:** Refined grid cells must be defined for both the wellbore and fracture. Along the wellbore the local grids may be traditionally squared or gradually fining towards the well. The fracture LGR must be represented by gradual refining towards the centre-blocks. Only the thin centre-blocks represent the fracture and the block width must be given a value large enough to avoid numerical problems. Therefore, the actual fracture width cannot be used. Figure 5-1B illustrates a gradual LGR representation which could be, for instance, both the well and fracture.

Local grid block properties: If nothing else is specified, Eclipse automatically transfers the properties of the host cell to all the refined cells within. This is usually sufficient for the refinement along the wellbore and around the fracture. Inside the fracture, however, important parameters as permeability and porosity are different than for the host cells. This is where the output from the fracture design is applied. If constant fracture conductivity is assumed, then fracture permeability corresponding to a desired fracture grid width can be adjusted and specified in the model [33]. Using subscripts f and G for fracture and grid block respectively, the following relation applies:

$$k_f w_f = k_G w_G \tag{5.1}$$

Using a known grid width, the adjusted fracture grid permeability becomes:

$$k_G = \frac{k_f w_f}{w_G} \tag{5.2}$$

Amalgamation: Amalgamation of several local grid refinements can be made for horizontal and deviated wells. By amalgamation means that smaller refinements can be made along the wellbore in a zigzag pattern instead of having one single, large LGR. This reduces the amount of local cells and, consequently, simulation time. For well paths not aligned along I or J axis, amalgamation can severely reduce the amount of grid cells. Figure 5-2 shows an example of two amalgamated refinements.

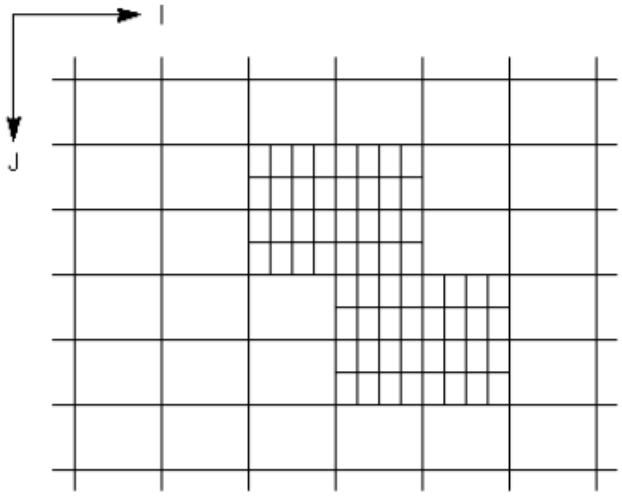

Figure 5-2: Two amalgamated refinements [32].

Time steps*:* Two types of time stepping are available when simulating LGR. The default and traditional type is by the use of *local time steps*. Refined grids often require shorter time steps than coarse grids. Local time stepping allows each local grid or amalgamation to be solved at individual time steps. This means that the global grid can run at longer time steps, without having to wait for the local grid to progress. The other method is called *"LGR in-place"* and provides a fully implicit solution of local and global grid blocks, i.e. they are solved simultaneously at the local time step. The problem with the first type is that stability issues may occur due to the explicitness of the solution. Global and local grid cells provide boundary conditions for each other; hence a fully implicit solution is not obtained. The second type has one problem: it may reduce efficiency of the simulation process. If small cells are used, small time steps are required to solve the LGR. Consequently, the global grid is delayed by waiting for the local grids to run. However, a stable simulation is obtained.

Important restrictions to the use of LGR in Eclipse that may become a problem and must be kept in mind are [32]:

- LGR's are not allowed to overlap, but they can touch
- LGR's cannot extend beyond a specified boundary, i.e. be in different flux regions
- A well cannot be completed in both global and local grid cells

The main keywords used in Eclipse, and their location in the simulation data-file, are provided in Table 5-2 for simple LGR-representation of hydraulic fractures.

Petrel has a feature which allows the user to create LGR around the wells and the hydraulic fracture automatically. This feature eliminates time consuming manual work when placing fractures, creating local grids, completing wells in the local grids and modifying properties in each fine grid cell.

The refinement levels must be specified for both well and fracture and the LGR's are then exported to Eclipse. Instead of using modified permeability values through PERMX, PERMY and PERMZ in Table 5-2, Petrel computes transmissibility multipliers which are present in the SCHEDULE-section by the keywords MULTX, MULTY and MULTZ. The difference from the manual approach is that the transmissibility values, which are defined in GRID-section, are modified using the multipliers in the fractured area. In addition, smaller pore volumes are calculated and assigned to the LGR's containing the fracture using MULTPV in the EDIT-section. [31]

Table 5-2: Keywords used for hydraulic fracture representation in Eclipse by LGR

Data file section	***Keyword***		***Meaning***
RUNSPEC	LGR		Activate LGR option in the model
GRID	CARFIN / ENDFIN		Activates / ends a LGR
		BOX	Activates property assignment to the LGR
		HXFIN, HYFIN, HZFIN / NXFIN, NYFIN, NZFIN	Specifies relative refinement levels or grid block sizes in the LGR
		PERMX, PERMY, PERMZ, PORO	Assigns directional permeability and porosity values to the LGR
	AMALGAM		Combines several LGR's into one group
SCHEDULE	WELSPECL		Defines a well in the LGR
	COMPDATL		Completes a well in the LGR
	LGRLOCK		Deactivate local time stepping, i.e. LGR and global grid will be solved simultaneously

6. Simulation Model

This chapter describes important assumptions, procedures and input data applied when building the simulation model.

6.1 Modelling method

In order to simulate hydraulic fractures in an existing full field model, an appropriate technique had to be chosen to effectively represent the fractures. Of the methods described in Chapter 4, local grid refinement was applied together with a sector model to build the model. The reason for this choice was to capture the whole fracture geometry. For parallel injecting and producing wells, the fracture geometry were believed to be one of the main important factors for optimal fracture setting in terms of water breakthrough. Petrel software offers automatic construction of LGR and sector models, which made this project suitable for the limited time available.

6.2 Assumptions

Due to the complexity of simulating hydraulic fractures using LGR, the model was built based on the following initial assumptions:

1) The largest stress in the reservoir is the overburden stress; hence only vertical fractures can be formed.

2) All hydraulic fractures have equal properties.

3) Fracture plane is two 180 degrees spaced wings along the J-direction, perpendicular to the wells.

4) Thermal, geo-mechanical and fluid filtrate effects are neglected.

5) Friction inside the wellbore is neglected, due to lack of lift curves.

6) All local grid blocks, except for the fracture grid, inherit properties from their host cells

7) No flow occurs at sector boundaries

6.3 Full field model

A full field reservoir model was provided by Talisman Energy which was history matched to the well tests performed in the appraisal wells. The model has been created based on a geological model, where Unit 1, 2 and 3, along with the coal layer, was included. The geo-model was based on the interpretations of the depositional environment explained in Section 2.1. The model dimensions are maximum 6500 m along the x-axis (East-West direction) and a maximum of 4300 m along the y-axis (North-South direction). The model consist of a 112 x 124 x 126 grid (nI x nJ x nK) giving a total number of 1749888 grid blocks, where each grid block has the dimension of 50x50x1 m. The x- and y-axis does not coincide with the I- and J-axis of the grid. The reservoir is slightly over-pressured and located at 3000 mTVD. Figure 6-1 shows a map view of the top layer in the full field model. The colour code indicates vertical depth.

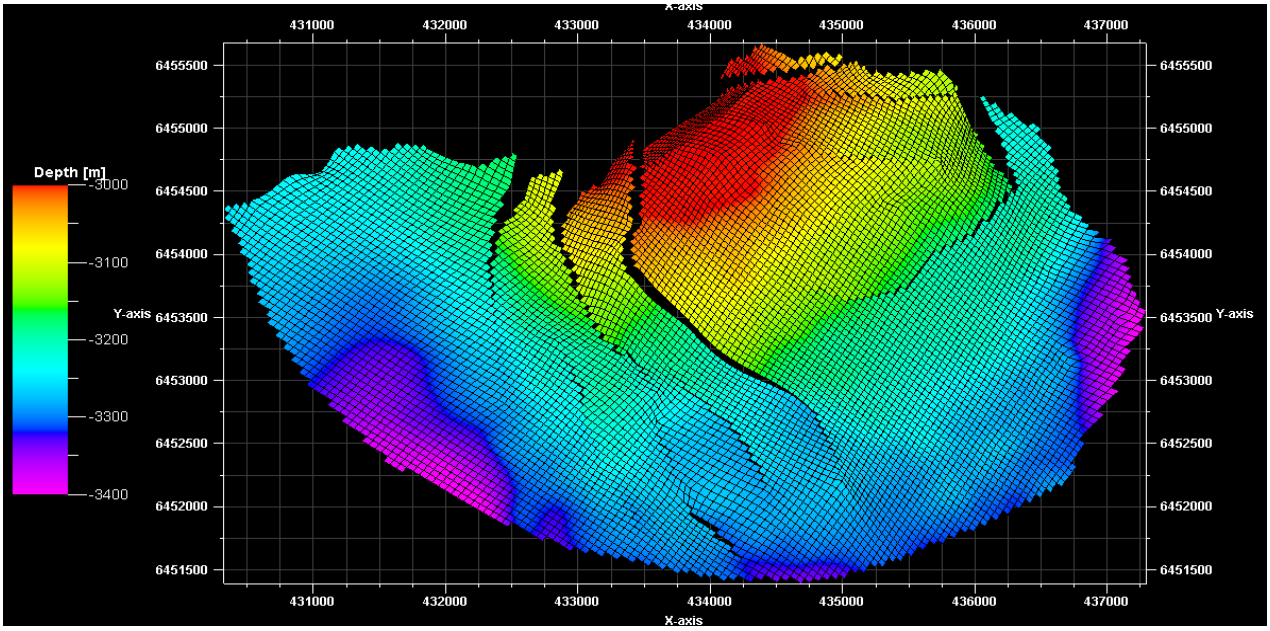

Figure 6-1: Petrel illustration of full field model along layer K=1.

6.4 Model Description

6.4.1 Wells

Two horizontal wells were placed in the full field model by creating lines between points, using Petrel. They were constructed along a thin and relatively continuous sand layer in order to achieve decent production from the perforations, in addition to the multiple hydraulic fractures. The wells were parallel and oriented along the direction of the least in-situ horizontal stress presented in Section 2.3.3. This would in reality, according to Section 3.4.3, create transverse fractures during the fracturing process. One well injected water (INJ) and the other produced reservoir fluid (PROD). The horizontal distance between them was set to 500 m, which were in agreement with the planned strategy. The well data are given in Table 6-1.

Table 6-1: Properties of the horizontal wells present in the model

Property	***Producer***	***Injector***
Top of horizontal section (mTVD)	*3106*	*3141*
Bottom of horizontal section (mTVD)	*3128*	*3178*
Length of horizontal section (mMD)	*2176*	*2194*
Inclination (deg)	*85 - 95*	*85 - 95*
Diameter (in)	*8.5*	*8.5*

6.4.2 Sector model

The full field model was reduced to a smaller model, having an area of 1000x2500 m^2 and 370 554 grid blocks. This was done by the sector modelling feature described in Section 5.1, in order to reduce the amount of grid blocks to a minimum. The sector modelling was

performed in Petrel, using a polygon surrounding the two wells. The parts of the reservoir outside the polygon were excluded entirely. Figure 6-2 illustrates the location of the two horizontal wells and the sector model created around them for a certain layer.

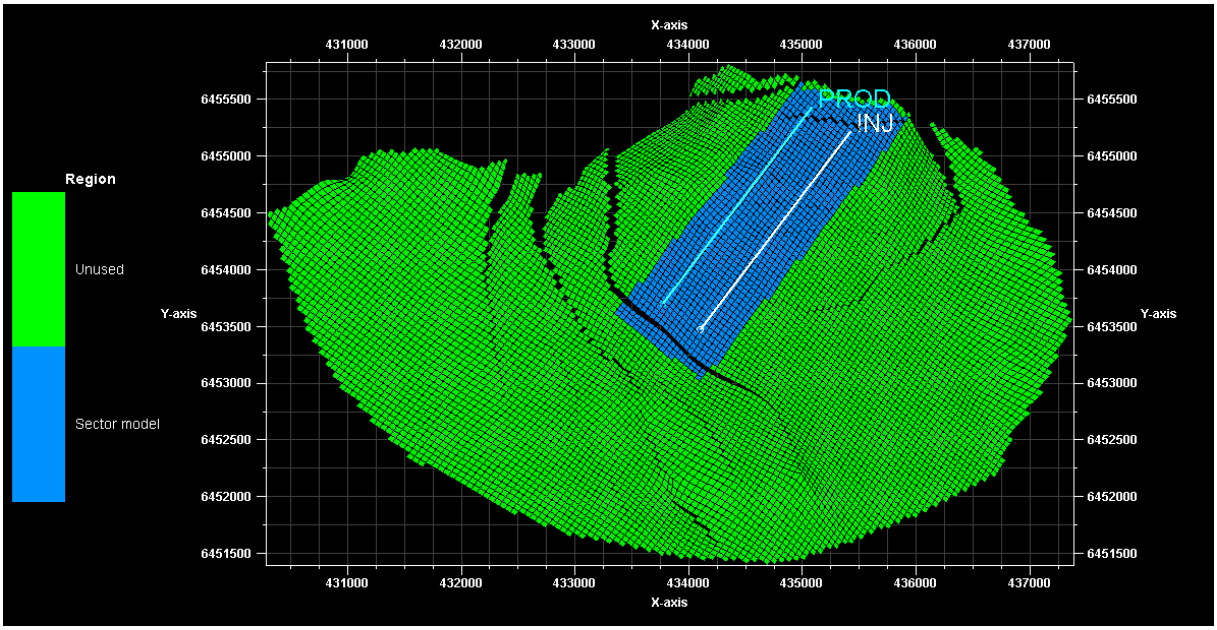

Figure 6-2: Sector grid (blue) and around one injector (white) and one producer (light blue).

To investigate the interference between wells and fractures in a possible field development scenario, where many wells are placed in parallel couples, a possible boundary was assumed to be in the middle between the two wells. Therefore, sector boundaries were placed at 250 meter horizontal distances to both wells. Since this thesis only considered the effect of fractures in a relation between two wells, there was no point in running the full field case to capture either pressure or flux boundaries. By this approach, it was assumed that a no-flow condition would occur at the sector boundaries; hence option (3) in Section 3.3.1 was applied.

The vertical extent of the sector model was limited to the zones considered important in this study. This means that only Units 2 and 3 were included. Therefore, the top boundary was the base of coal layer and the bottom boundary, base of Unit 3.

Figure 6-3 shows the initial state of the sector model in 3D-view and the active grid blocks present. The colour code indicates oil saturation.

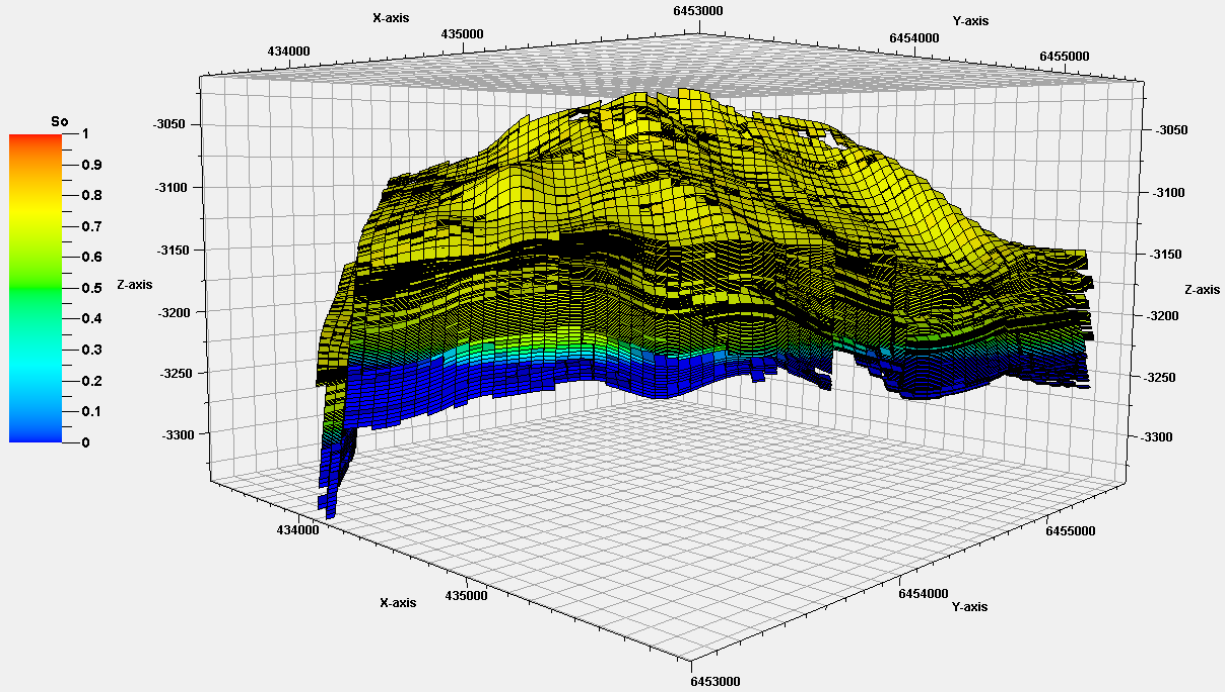

Figure 6-3: Active grid blocks and initial oil saturation in the sector model.

6.4.3 Hydraulic fractures

Hydraulic fractures were created in Petrel using a completion design event. Each fracture in the model followed a plane along the J-direction by default, perpendicular to the wellbore, representing transverse hydraulic fractures. The amount of coarse grid blocks within each fracture LGR varied due to the non-linear layers in the model, caused by faults and dipping structures.

The properties assigned to each hydraulic fracture were based on an internal fracture design study, performed by Talisman and Schlumberger. Based on logs, lithology and stress measurements from the exploration wells, the suitable fracture properties for this reservoir were established. The fracture properties used as input to the model are given in Table 6-2.

Table 6-2: Hydraulic fracture input parameters to the model

Parameter	***Value***
Fracture permeability (mD)	*1000*
Total fracture length (m)	*200*
Fracture height (m)	*30*
Propped fracture width (in)	*0.25*

The fracture properties were calculated as average values from the study, except from the fracture permeability. The average permeability was originally 100 000 mD, but due to large

occurrence of numerical problems experienced during the simulations, it had to be reduced to 1000 mD. This is discussed further in Chapter 8.

6.4.4 Local grid refinement and grid sensitivity

Locally refined grid blocks were created around the wells and in the fractured area by using the LGR feature in Petrel. The degree of refinement along the wells and in the fracture was determined using sensitivity analyses, combined with trial and error.

6.4.4.1 Wellbore refinement

The wellbore refinement is specified in Petrel as N_x x N_y x N_z, meaning level of refinement in I, J and K-direction respectively. As an example, a global grid block having the dimension of 50 x 50 meters, has a refinement level equal to 1, hence $N_x = N_y = 1$. By refining the block to a set of 1 x 1 meter grid blocks, the refinement level becomes $N_x = N_y = 50$.

A sensitivity analysis was performed in a non-fractured scenario with LGR around the producer only, to quickly establish the optimal wellbore refinement. The refinement levels were increased between 2 and 10, giving 25 to 5 meter dimensions along I and J-direction for the refined blocks. Refinement in K-direction was not needed since the grid blocks initially were sufficiently refined in this direction (1 meter). The different refined runs used in the sensitivity analyses are given in Table 6-3.

Table 6-3: Sensitivity scheme for wellbore LGR determination

N_x	N_y	N_z
2	*2*	*1*
4	*4*	*1*
6	*6*	*1*
8	*8*	*1*
10	*10*	*1*

Cumulative oil production and computer simulation time were used as decision criterion through a compromise. The optimal refinement shows small changes in production, compared to finer grid blocks, as well as having significantly less simulation time.

The results from the sensitivity analysis are given in Figure 6-4 and 6-5 respectively. Figure 6-4 shows cumulative oil production through simulation period of 5 years (1800 days), while Figure 6-5 illustrates the corresponding cumulative running time for the same period.

The 6 x 6 x 1 refinement showed little change in production, compared to finer LGR's, and provided an effective simulation time. Therefore, this refinement was selected to be used in the simulation model. It should be mentioned that the 10 x 10 x 1 refinement terminated after 4 years of simulation.

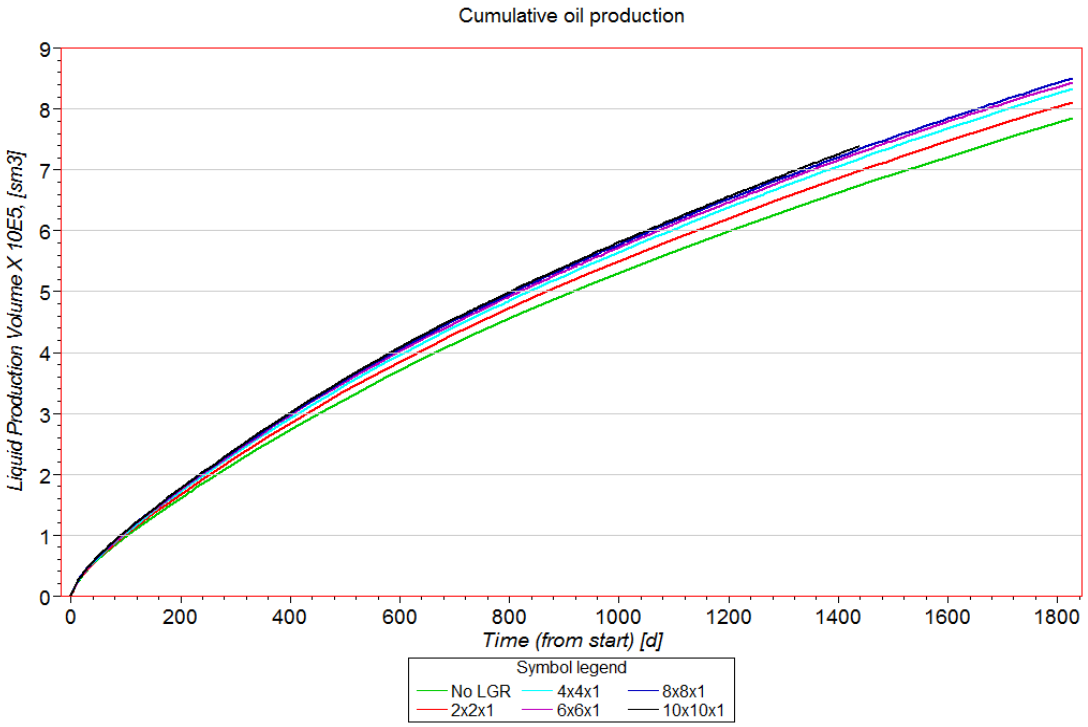

Figure 6-4: Cumulative oil production for wellbore LGR sensitivity analysis.

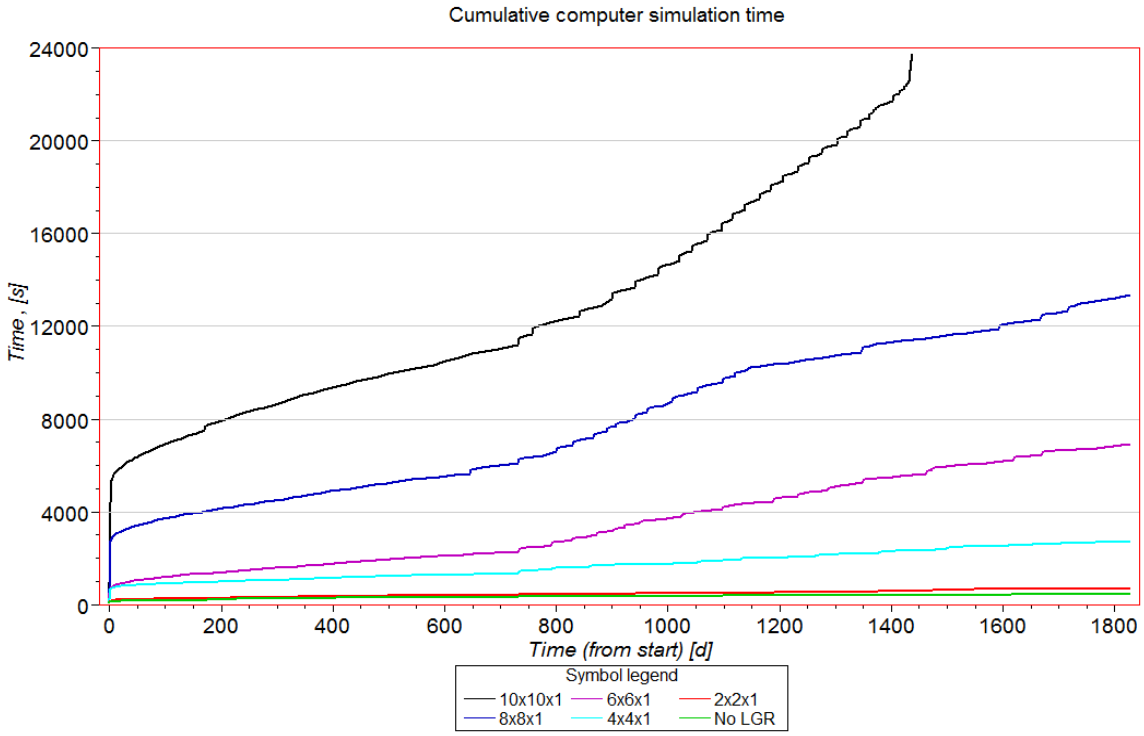

Figure 6-5: Computer simulation time for wellbore LGR sensitivity analysis.

6.4.4.2 Fracture refinement

The LGR representation of the hydraulic fractures in Petrel is given by:

- Refinement perpendicular to the fracture (I-direction)
- Refinement parallel to the fracture (J-direction)
- Fracture width

The fracture refinement selection was based on trial and error, combined with the need for fine grid in all directions. No refinement was used in the direction perpendicular to the fracture, such that $N_y = 1$. The reason is that the linear flow into the fracture was the interesting part. Flow along the axis of the fracture was assumed not to make any contribution to accuracy. It was, however, discovered that a large amount of numerical problems occurred when N_y was increased beyond 1.

The refinement along the I-direction was determined to be $N_x = 9$. This means that the centre grid blocks of the fracture LGR, representing the hydraulic fracture itself, is surrounded by 4 gradually refining levels towards the centre. The width of the centre-blocks was set to 2 meters, in order to reduce numerical problems as suggested by *Hegre* in Chapter 4. Both the fracture and wellbore LGR used in this study is illustrated in Figure 6-6. The centre-blocks in the fracture LGR, representing the hydraulic fracture, are indicated by a black line.

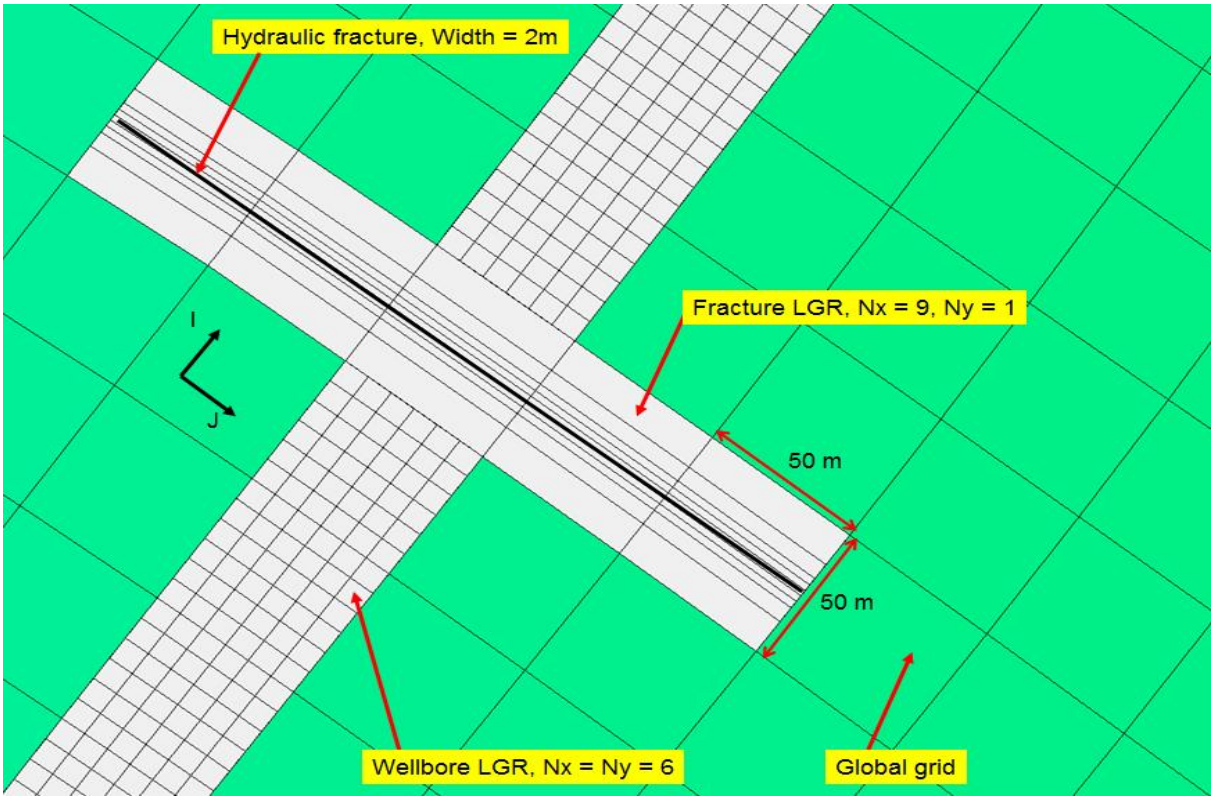

Figure 6-6: Fracture and wellbore LGR used in the model.

6.5 Model Input Data

Due to the complexity and large amount of data present in the full field model, only the essential parameters are given in this report. Input data stated as important concerns porosity, formation permeability and net-to-gross ratio. These are provided together with well, fracture and time control data.

6.5.1 Porosity

Each global grid block within the sector model was assigned to one porosity value. The range varied between 0 and 23 %. The histogram in Figure 6-7 shows the percentage of grid blocks having a certain porosity value. The majority had porosity between 12 and 15 % and the mean was around 13%.

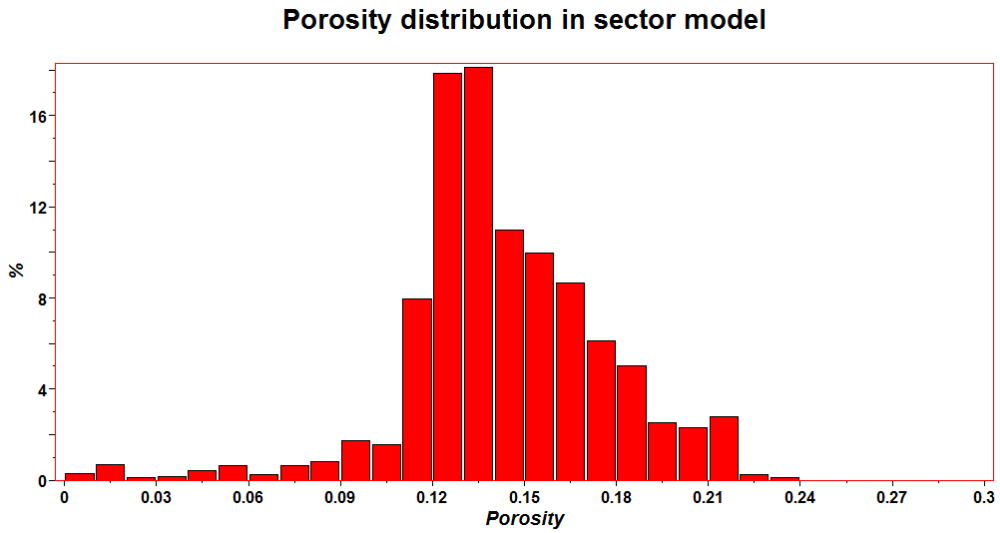

Figure 6-7: Porosity distribution in the model.

6.5.2 Permeability

Like porosity, formation permeability in the model varied significantly throughout the reservoir. The good sand zones had values exceeding 100 mD while the surrounding shale was likely to be non-permeable. In order to simplify, the permeability was equal in all directions for each grid block. Figure 6-8 shows the permeability distribution in the model. The majority of the grid blocks had permeability values less than 10 mD, mostly around 3 mD. Based on these values, relatively low permeability regions were considered less than 3 mD, intermediate regions around 10 mD, and high permeability regions above 20 mD.

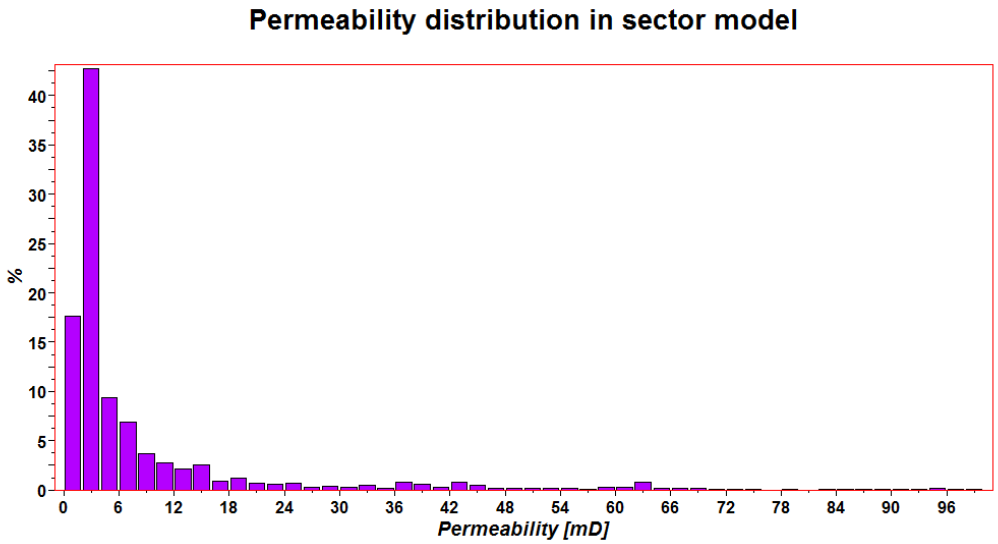

Figure 6-8: Permeability distribution in the model.

6.5.3 Net-to-Gross ratio

The Net-to-Gross ratio is the height of producible sand relative to the total thickness, and is used to convert from gross to net thickness. In the model, one value between 0 and 1 was assigned to each grid block in the model. The majority of them were in the lower end of the scale, describing the shale, with ratios from 0 to 0.05. The good sands were grouped around 0.95 to 1 and accounted for about 20 % of the grid blocks. Figure 6-9 shows the distribution.

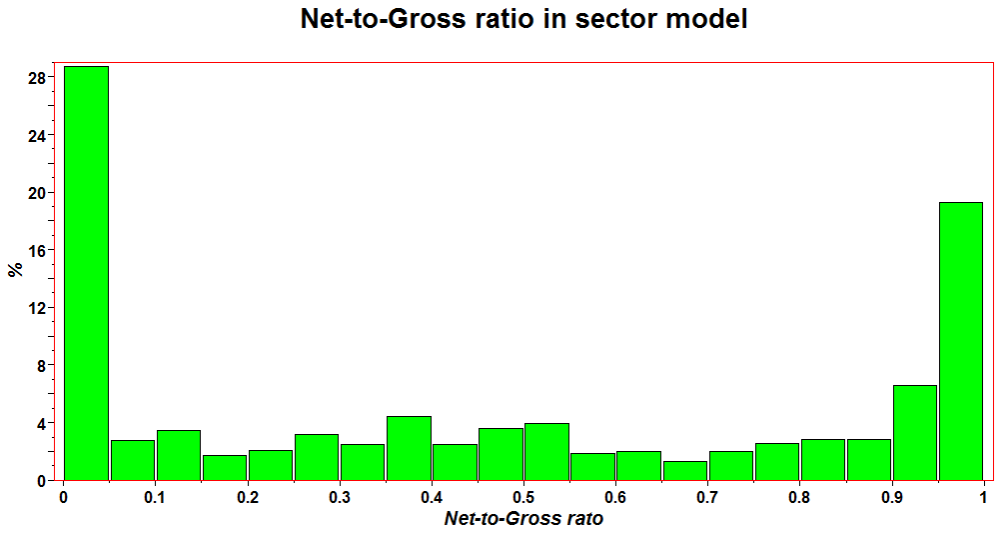

Figure 6-9: Net-to-Gross ratio distribution in the model.

6.5.4 Wells and completion

The two horizontal wells in the model were completed with casing and perforations along the entire sections, in order to represent open-hole completions. A casing diameter of 8.5 inches was applied to represent a typical wellbore diameter. This means that Eclipse reads connections along the entire well section, including the hydraulic fractures. A skin value equal to zero was assumed in both wells.

Production control was set to 60 bars bottom hole pressure (BHP) in order to represent the ESP pump pressure. The injector was set to inject at 500 bars BHP to give sufficient pressure support. In addition, to avoid initially high production and injection rates creating numerical problems, water and oil control rates of 500 Sm^3/d and 2000 Sm^3/d were put on the injector and producer respectively, while reaching the limiting BHP.

6.5.5 Hydraulic fractures

The model contained large amounts of inactive grid blocks where the Net-to-Gross ratio or porosity was equal to zero. These were inactive in order to represent tight shale blocks, which did not contribute to flow. Consequently, by placing fractures and well connections in such blocks, they become ignored in Eclipse. Therefore, each block within the fracture LGR's was made active to prevent Eclipse from ignoring it. In addition, a more flexible placement of the fractures was established. The blocks were made active by manually assigning Net-to-Gross ratios and porosity values to each cell within the fracture LGR's. The values were estimated averages based on Figure 6-7 and 6-9; hence a porosity value of 0.13 and a Net-to-Gross ratio of 0.4 were applied.

6.5.6 Time control

To avoid convergence problems, keywords TUNING and TUNINGL were applied to limit the time step lengths of global and refined grid during the simulation. The maximum time step length for the global grid was 5 days while the refined grid used 0.5 days.

To reduce simulation time, the LGRLOCK keyword was disabled, hence local time stepping was applied.

7. Scenarios

The simulation model developed in Chapter 6 was applied to five different scenarios. Scenario 1 was a base case study for a non-fractured setting. In order to understand the effects of hydraulic fracturing in this reservoir, Scenario 2 to 4 was conducted. The analysis was evaluating various settings containing two fractures only. Scenario 5 applied the results from the other scenarios to optimise the setting in a multiple-fractured scenario. Scenario 2 consisted of five cases. Figure 7-1 shows a schematic overview of the investigated scenarios. The scenarios are addressed more in detail in the following.

7.1 Scenario 1: Non-fractured wells

A base case scenario, where none of the wells were fractured, was simulated in this scenario. The sensitivity to permeability variations in the reservoir was investigated by comparing the base case with three other runs, each one having a constant formation permeability of 1, 10 and 50 mD. This detected how sensitive the formation was to permeability changes and thus the potential for hydraulic fracturing.

7.2 Scenario 2: Two injecting fractures

The communication between two hydraulic fractures, one in each well, were analysed in Scenario 2. A total of five cases were run, each case having six runs, where the horizontal, longitudinal[1] distance (d) between the producing and injecting fractures, referred to as fracture distance, was given values from 0 to 700 meters. This distance was measured along the wellbores and is only the separation between the fractures. The setting is illustrated in Figure 7-2A and the distance is measured relative to the fracture closest to the wellbore toe, at all times.

The two first cases investigated the optimal fracture distance and the effect of relative movement of the fractures. In Case 1, the producing fracture was moved while the injecting fracture was kept in a fixed position. In Case 2, the setting was switched where the producing fracture remained in a fixed position, while moving the injecting fracture. The objective was to investigate and detect an optimal fracture distance.

The three other cases evaluated different factors and their effects on the optimal fracture distance. Case 3 investigated permeability effects by running simulations for all distances, having a constant formation permeability of 10 mD. Case 4 analysed the effects of changes in fracture length. In addition to the fracture half-length of 100 meters, values of 75 and 125 meters were simulated for all distances. Case 5 studied the effect of changes in the injector BHP. The pressure was reduced by 50 bars, from 500 to 450 bars, and then compared with each other for all distances.

7.3 Scenario 3: Two fractures in the injector

The effect of horizontal fracture spacing (s) in the injector was studied in Scenario 3 by varying the horizontal distance between two injecting fractures for 100 to 500 meters. Five runs were simulated. The producing well was remained non-fractured for all runs. The objective was to understand fracture interference and to detect optimal fracture spacing in the

[1] Measured as horizontal distance along the wellbore azimuth

injector, in terms of early oil and water production combined with sweep area. The fracture setting is illustrated in Figure 7-2B.

7.4 Scenario 4: Two producing fractures

The effect of horizontal fracture spacing (s) in the producer was studied in Scenario 4 by varying the horizontal distance between two producing fractures for 100 to 500 meters. Five runs were simulated. The injecting well was remained non-fractured for all runs. The objective was to understand fracture interference and to optimal fracture spacing in the producer, in terms of oil and water production combined with drainage area. The fracture setting is illustrated in Figure 7-2C.

7.5 Scenario 5: Multiple-fractured wells

The planned field development strategy, with multiple hydraulic fractures in both wells, was run based on the results achieved in the Scenario 2 to 4. Three hydraulic fractures were placed in each well. The objective was to get an optimised estimate of the oil production from one well couple. This run was compared to the base case results in Scenario 1.

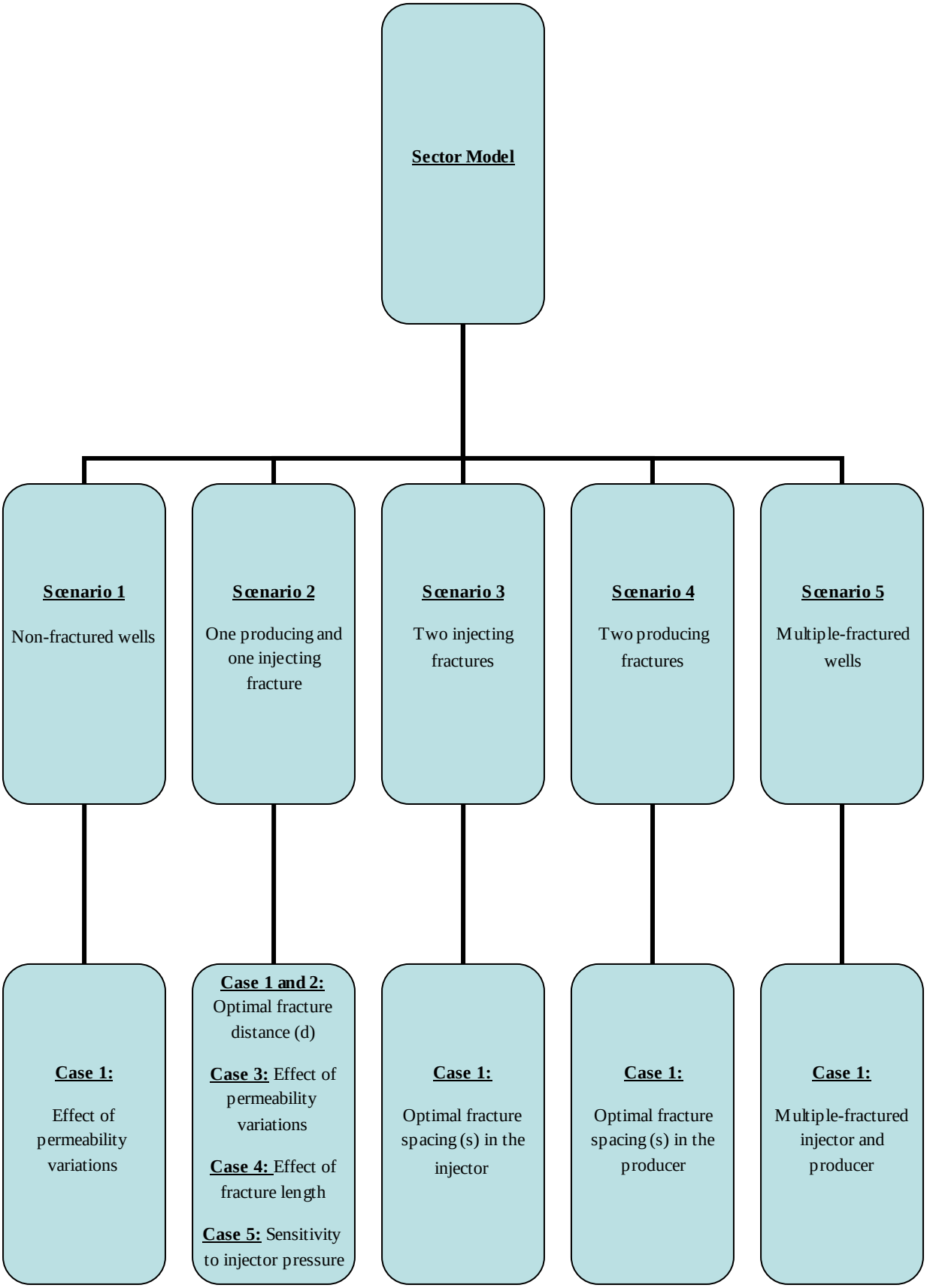

Figure 7-1: Schematic overview of the main scenarios performed in this thesis.

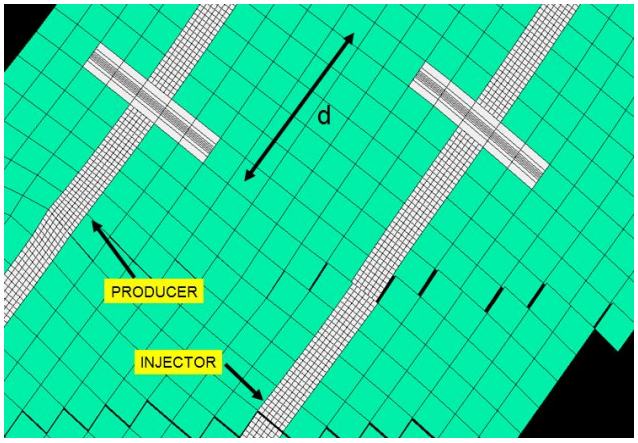

(A)

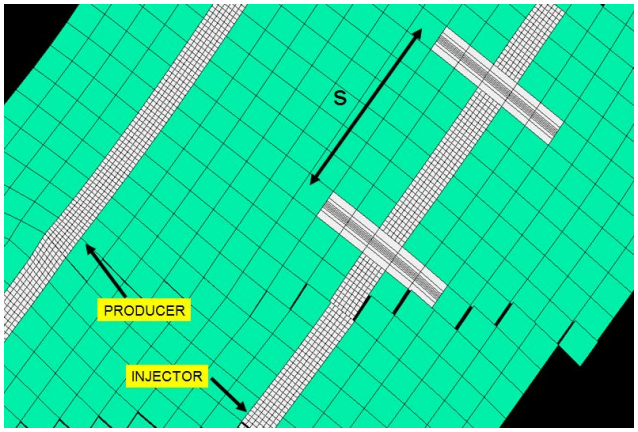

(B)

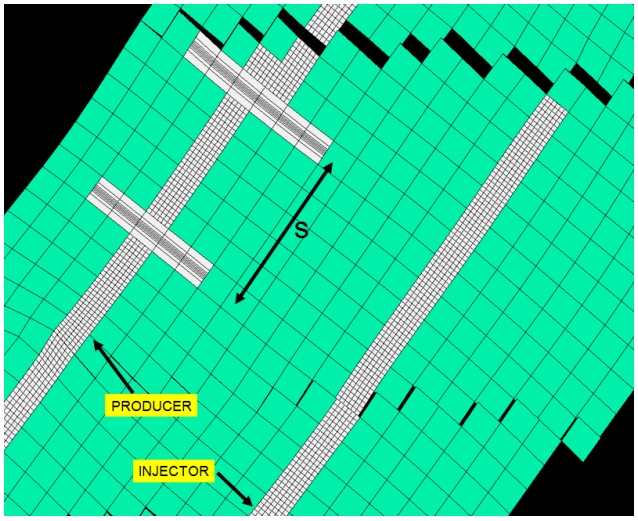

(C)

Figure 7-2: Fracture setting in Scenario 2 (A), Scenario 3 (B) and Scenario 4 (C).

8. Results and Discussion

This chapter provide results from all scenarios conducted in the analysis. For each scenario and cases the expected outcome is addressed, followed by presentation of the results and interpretations. Findings are reported in a summary for each scenario. At the end of the chapter, possible sources of uncertainty and error are discussed together with problems encountered during the simulations. To reduce amount of grid blocks and simulation time, Scenarios 2 to 4 were simulated with LGR and perforations in the toe sections of the wells. Therefore, the analysis was performed in these sections only; hence much lower production will be evident, compared to scenarios 1 and 5.

Saturation and pressure maps for the different scenarios can be found in their respective Appendices.

8.1 Scenario 1: Non-fractured wells

8.1.1 Case 1: Effect of permeability variations

In order to understand the ability of the reservoir to produce hydrocarbons by water injection, a non-fractured scenario was conducted. A base case run consisting of a strongly heterogeneous setting, in terms of permeability, was compared to 3 homogeneous runs where the constant permeability was given relatively low (1 mD), intermediate (10 mD) and high (50 mD) permeability. Unfortunately, the high permeability run had so many numerical problems that it terminated after about a half year of production. However, it was still possible to investigate the sensitivity to permeability variations in the model. Although the permeability was altered, the rest of the input data remained unchanged for all runs. Therefore, the amount of inactive grid blocks was constant throughout these simulations.

Figure 8-1 shows the oil production rates (solid lines) on the primary y-axis and the cumulative production (dotted lines) on the secondary y-axis through a simulation period of 5 years (1825 days), for the four runs conducted. The cumulative production is given in terms of a 10^6 multiplier. The rapid decrease in oil production rates from 2000 Sm^3/d in the beginning was due to the BHP control on the producer. Initially the well was on rate control, but changed to BHP almost instantly. By keeping constant pressure, the rates naturally decreased with time.

It is evident that for the high permeability run, good production was easily obtained; hence the BHP control was not reached. This gave a constant production rate of 2000 Sm^3/d until termination. The base case heterogeneous run produced more oil than the low permeability run, but less than the intermediate permeability case.

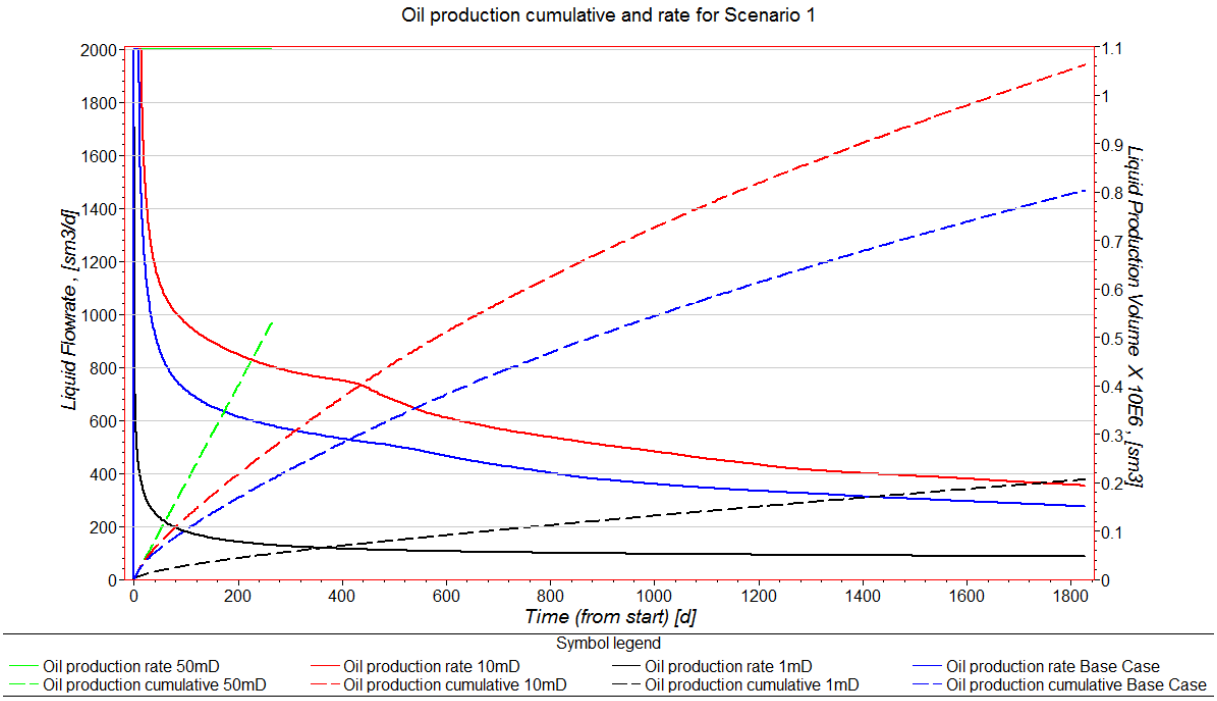

Figure 8-1: Effect of permeability variations on oil production in non-fractured scenario.

These results indicate that high production rates are easily obtained for high permeability zones in the reservoir. However, the large difference in production between 10 mD and 1 mD, combined with the base case model between them, may indicate that this reservoir is highly sensitive to permeability heterogeneity in terms of oil production. The flow towards the producer is thus affected by tortuous and variable flow paths, meaning that the reservoir theoretically should significantly benefit from connectivity enhancement, by, for instance, hydraulic fracturing.

Figure 8-2 shows the water cut (solid) and cumulative water production (dotted) for the same four runs. Here, an increase in formation permeability gave earlier water breakthrough and higher cumulative water production. The intermediate permeability run produced water faster than the base case. For the low permeability run, no water was produced after 5 years.

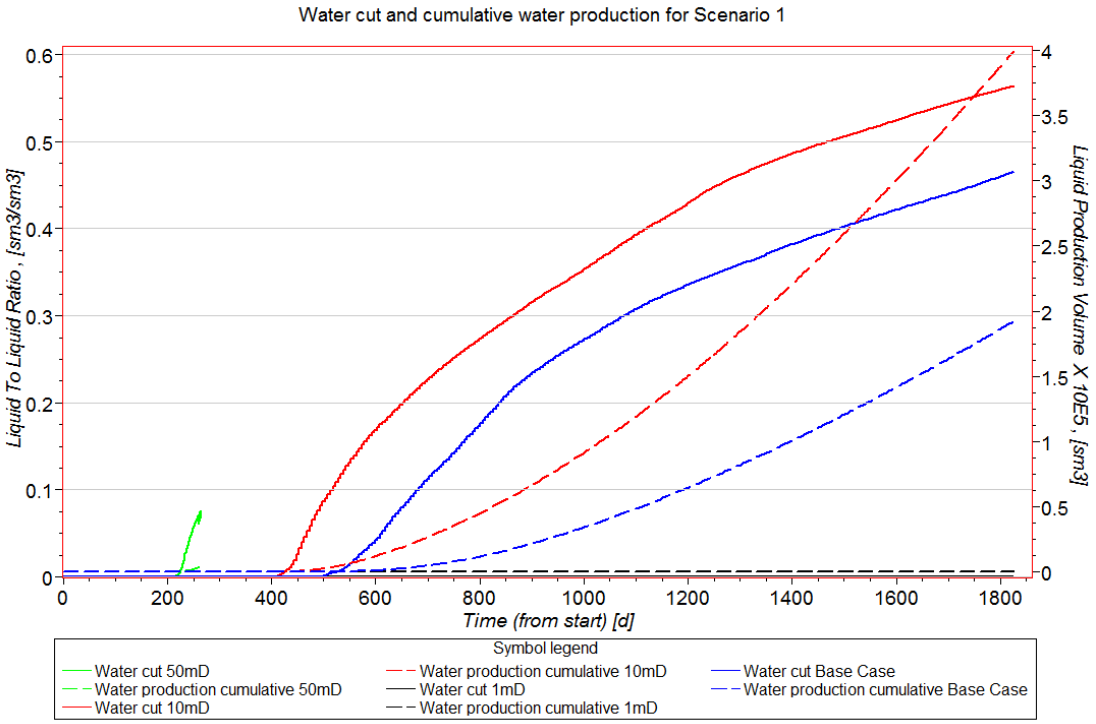

Figure 8-2: Effect of permeability variations on water production in a non-fractured scenario.

Figures A-1 to A-3 in Appendix A show integrated saturation maps in the sector model after 3 years of production for the base case, intermediate and low permeability case. The two wells are identified by PROD and INJ for the producer and injector, respectively, which are located in the toe sections (upper right corner). Red to blue colours indicates high to low water saturation. It is clearly visible that the potential sweep area was equal for all runs. The 10 mD case, however, provided a slightly more effective water sweep than the base case. For the 1 mD case, the injected water had not broken through in the producer, but as seen from the map, the same area as the other runs were swept. The limitation, however, are time requirements, in terms of early oil production. In all runs the injection started out as circular patterns in the regions of active perforations. As the time progressed, the small circles were united creating a more elliptic pattern. The effect was a large area with potential for efficiently sweep.

8.1.2 Summary of Scenario 1

The following conclusions are collected from the analysis in Scenario 1:

- The production in the reservoir is sensitive to changes in formation permeability.
- The reservoir has potential for increase in productivity by connectivity enhancement, by, for instance, hydraulic fracturing.

8.2 Scenario 2: One producing and one injecting fracture

One fracture was placed in both the injecting and producing well. The goal was to study the communication between two fractures in two different wells, for different wellbore longitudinal distances (d). In addition, the effect of fracture length, formation permeability and injection pressure was investigated.

8.2.1 Case 1: Optimal fracture distance (d) by moving the producing fracture

Seven runs were performed where each run had different horizontal distances between the fractures along the wellbore. The distance was varied by keeping the injecting hydraulic fracture in a fixed position near the wellbore toe, while moving the producing fracture towards the wellbore heel. Distances of 0 to 500 meters, as well as 700 meters, were simulated.

The expected findings from this case were that an optimal distance should be evident, where the fractures work together in order to maximise the production. In addition, large distances should negatively affect early production, due to delay in pressure communication between the fractures. In a case of narrowly to aligned fractures (d=0 m) early water production was expected due to a more or less united flow path, hence water being directly moved from the injector to the producer, via the fractures. This was expected to be evident in terms of reduced oil production.

Figure 8-3 shows oil production rates and cumulative production for the runs after 3 years of simulation. In addition, a base, non-fractured case was included to determine the effectiveness of a fracture couple. The cases of d=300m and d=400m had highest oil production. For wider and narrower distances, the production was reduced. The case of aligned fractures produced least amounts of oil. By comparing cumulative oil production for d=300m with the non-fractured case, the production increased by more than 150 000 Sm^3, confirming that multiple hydraulic fracturing severely improves productivity in this reservoir.

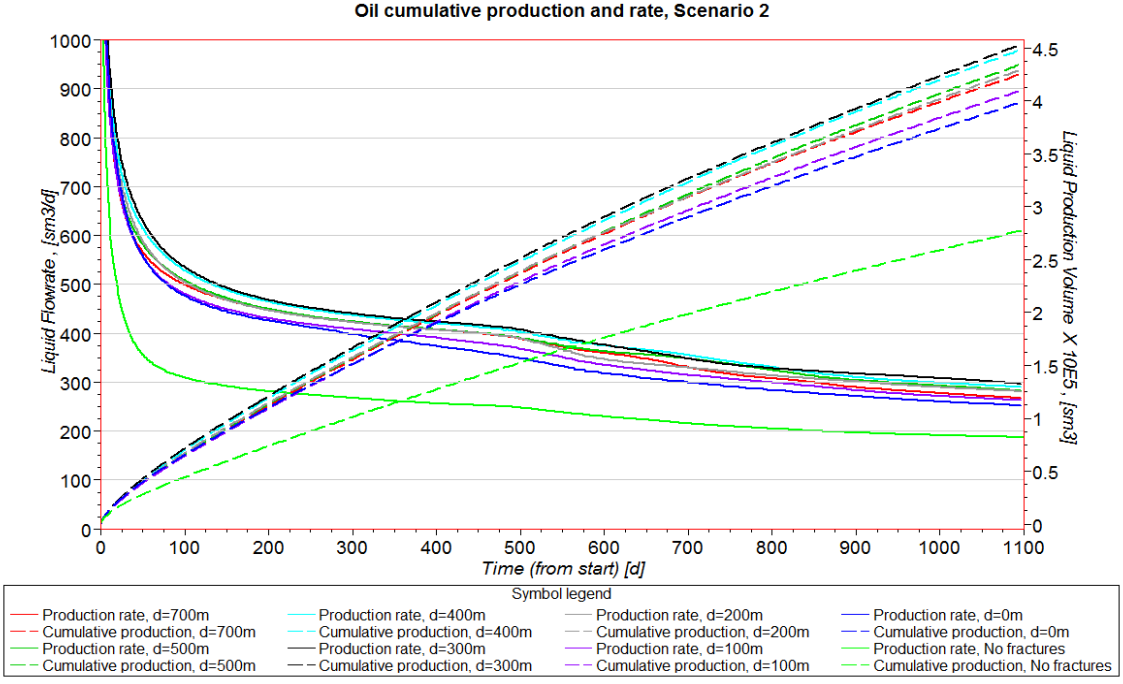

Figure 8-3: Oil production for different fracture distances by moving the producing fracture.

The results indicate that there exists a regional maximum distance beyond which the efficiency, in terms of early oil production, is reduced. The fact that production was reduced in this area as the distances decreased below 300 meters, are in agreement with the expectations stating too much fracture influence for narrowly distanced fractures. This means that the water sweep significantly reduces outside the fractured area between the wells, since the water moves from the injecting to the producing fracture. The result is therefore that the perforations become important in other parts of the wells after water breakthrough, in order to produce the remaining oil. For wider distances, the reduced production was probably not due to fracture interference, as for narrower placement, but rather the opposite; lack of interference.

Furthermore, the water-cut in Figure 8-4 indicate that water breakthrough occurred for all the runs at approximately the same time. However, the case of aligned fractures (d=0 m) clearly produced water at an earlier point, and at higher rates than the others. For d=300m the water production was lowest, while d=700m produced second most water.

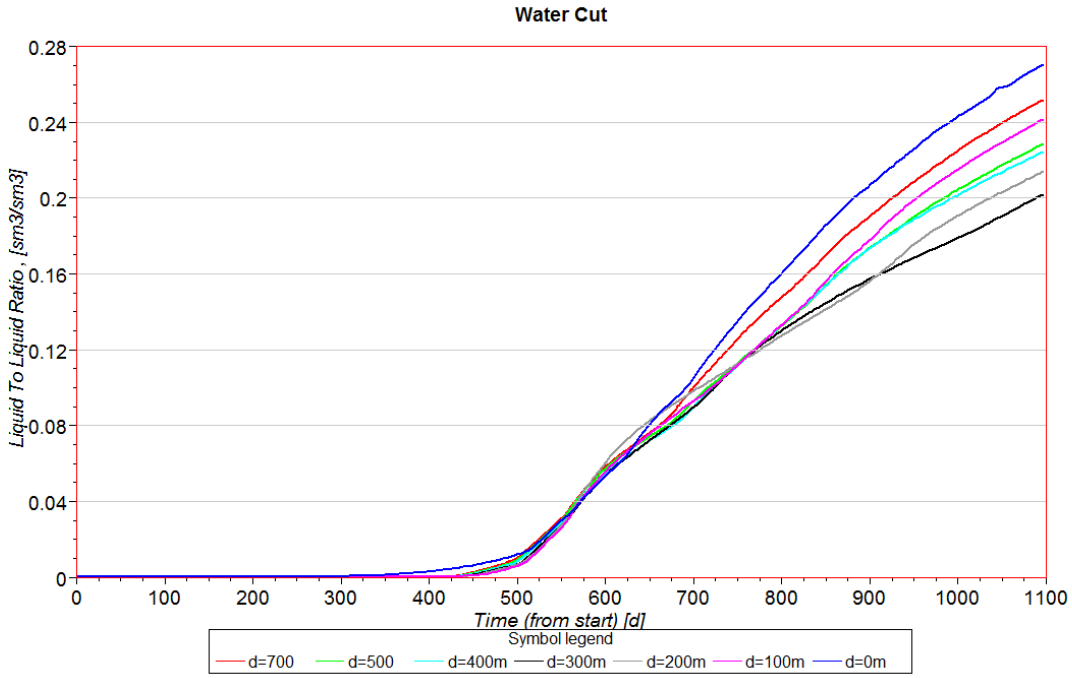

Figure 8-4: Water cut for different fracture distances by moving the producing fracture.

The observed behaviour, in terms of water production, is to some degree in accordance to what was expected. The effect of aligned fractures, by direct water transfer from the injector to the producer, resulted in early water production and a large part of the injected water afterwards following this path. However, this effect was also expected to be observed for distances as d=100m as well, but the amounts of water produced were closer to that for greater distances. In addition, the fact that the largest distance, d=700m, also produced much water indicate that local permeability variations could play an important role, in terms of water behaviour. On the other hand, the differences in produced volumes were not enormous by looking at the scale on the water cut. However, the difference does say something about the fracture relation for narrower distances.

Since all distance-runs had water breakthrough occurring at approximately the same time, this indicate that breakthrough occurs first in the area of the fractured injector, and the amount of

water produced is dependent on the location of the producing fracture. The high water cut for d=700m may indicate that the producing fracture was placed in a highly conductive region, consequently providing high connectivity with the injecting perforations right across it. The other runs were fractured in zones of lower permeability.

To investigate where the water was produced from, after water breakthrough, water saturation profiles along a layer, intersected by both wells in the fractured regions, were created for 300 and 700 meters distance after 2 years of production. This time of simulation is right after the curves separate on Figure 8-4. The maps are given in Figure B-1 and B-2 in Appendix B.1 along the layer K=89. The producer and injector are indicated by light blue and white lines, respectively. Both the wellbore and fracture LGR's are shown and the black squares are inactive grid blocks. Blue to red colours indicate high to low water saturations, respectively. The figures states that the water production was different due to the fracture at d=300m being placed in a region with less connectivity, compared to wider distances, which clearly had a more rapid increment of water production.

The effect of fracturing the injector, on vertical communication in the reservoir, was investigated by creating a cross-section between the two wells, showing water saturation after 3 years of production. Figures B-3 to B-6 in Appendix B.2 shows the cross-sections for 0, 300 and 700 meters distance, as well as the non-fractured case. The dotted lines indicate the location of the fractures in both wells. The view is from the side of the injector

From these vertical sections it is evident that the non-fractured case only injected water into a thin layer; hence limited vertical communication occurred. For the fractured runs it can be seen to the right in the figures that the entire fracture height in the injector contributed to connect different layers, and vertical communication was established. The large area of high water saturation in the lower layers, indicate that the case of d=300m provided the best setting, in terms of sweep, at this time of production. However, the run of d=700m had a larger volume of oil between the fractures, which could be swept if the production time was extended. Nonetheless, a part of the reason for hydraulic fracturing is to achieve high, early production rate, and 700 meter distance was too wide to obtain this.

The effect on vertical communication, by fracturing the producer, was studied by pressure maps created for the same four runs after 3 years of production. The maps are given in Figures B-7 to B-10 in Appendix B.3 and shows pressure distribution along the horizontal layer K=47, located above the main reservoir penetrated by the wells. The layer is within the vertical extent of both fractures and illustrates the drainage area created by the producing fracture. Yellow to blue colours represent high to low pressure, respectively. Both well and fracture LGR's are visible in the figures.

The main result is that vertical pressure communication was established. It is interesting to see that the pressure was maintained high in the same regions around the injecting fracture, independent of the location of the producing fracture. This states that the injector provided a continuous pressure support in the whole layer, and a large drawdown towards the producer was achieved. In addition, the drainage radius in the producing fracture seems larger for the 300 meter run, compared to both 0 and 700 meters, in terms of extent of blue colour. This again indicates that 300 meter distance could be the best distance in this region. The non-fractured run clearly shows low-pressure regions in the whole layer, probably due to initially communicating layers being connected to the producer, as well as lack of pressure support

from a non-communicating injector. The results provide the possibility for an optimal fracture distance at 300 meters.

8.2.2 Case 2: Optimal fracture distance (d) by moving the injecting fracture

The runs performed in Case 1 kept the injecting fracture in a constant position while the producing fracture was shifted along the wellbore, to give the different distances. To investigate the optimal fracture distance, the reversed setting was analysed. This means that the producing fracture was kept in a constant position, while the injecting fracture was shifted along the wellbore for the same distances as in Case 1.

Due to the variations in reservoir properties, a change in optimal fracture distance and production, compared to Case 1, was expected.

Figure 8-5 shows the oil production rate and cumulative production for all the reversed runs. Firstly, compared to Figure 8-3 in Case 1 it is evident that the cumulative production after 3 years had been reduced for all runs in Case 2. In addition, the difference between highest and lowest run, in terms of production, was narrowed. Based on the early rates it is clear that d=100m was the optimal fracture distance for this setting.

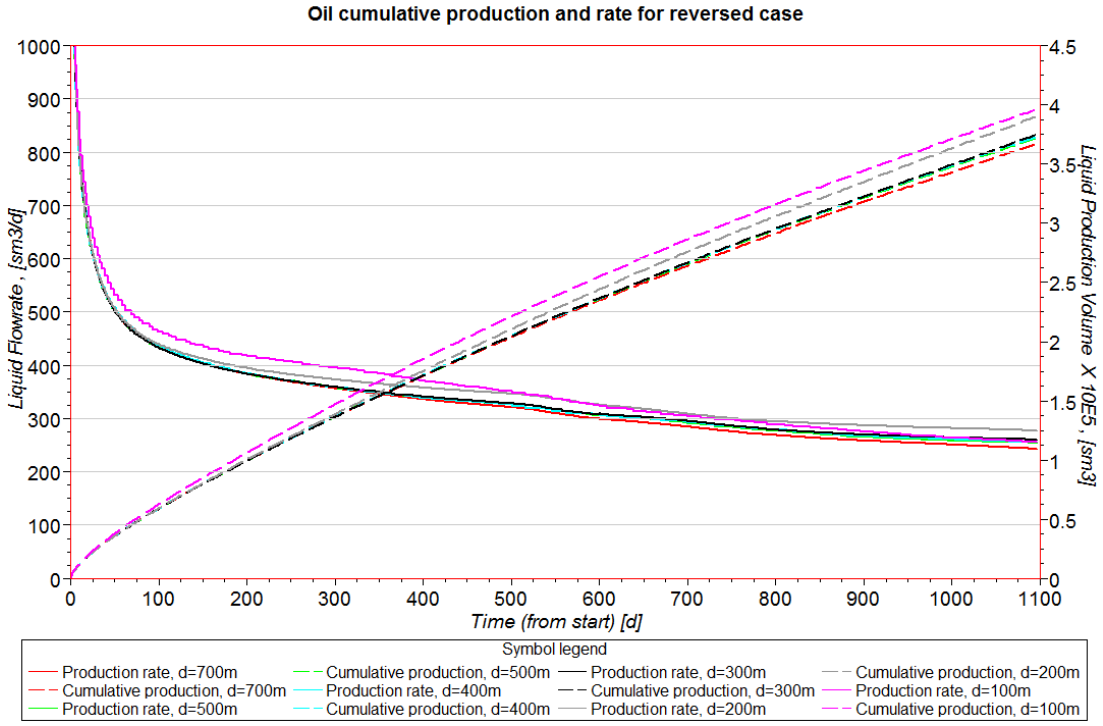

Figure 8-5: Oil production for all fracture distances by moving the injecting fracture.

Figure B-11 to B-16 in Appendix B.4 shows separate oil production plots for each fracture distance in Case 2, compared with the original results from Case 1. These results clearly state that the production for each distance beyond 100 meters was significantly reduced in the reversed setting. The reduction is smallest for d=100m, implying that this distance was least affected by the reversed setting, and equal rock properties could be present around both fractures in this area.

All in all, there seems to be a dependency in the model whether if the injecting or producing fracture is moved. Therefore, the relative position of both fractures becomes important.

8.2.3 Case 3: Effect of permeability variations on optimal fracture distance

In both Cases 1 and 2, the results showed reduced production as the distance increased beyond a certain value. In addition, the volumes produced were significantly lower by moving the injecting fracture, rather than the producing. The reasons for these results were investigated in Case 3.

Based on own experience using the model, the reduction in fracture performance for larger distances could be due to the following:

1. The fractures or wells were in different permeability regions such that either the injected or the produced fluid flowed slower than the other; hence improper communication between the fractures was obtained.

2. Too great distance between the fractures resulted in delayed communication, and the injecting fracture did not provide sufficient pressure support to obtain high, early production in the producing fracture.

3. Large occurrence of flow barriers as shale or inactive grid blocks, pinch outs and non-continuous layers or sealing faults resulted in limited communication between the fractures.

To investigate the effect of the first point, permeability variations, a permeability map was made. This map is given in Figure 8-6 and shows the vertical sum of permeability values within the sector model, in the toe section of the wells. The map was filtered such that only the layers within the vertical extent of both fractures were included. The colour code end-points indicate low-permeability (blue) and high-permeability (red) regions. The producer (PROD) and injector (INJ) are shown as two parallel lines. The fractures at d=0 m, d=300m, d=500m and d=700m in both wells are indicated by red lines.

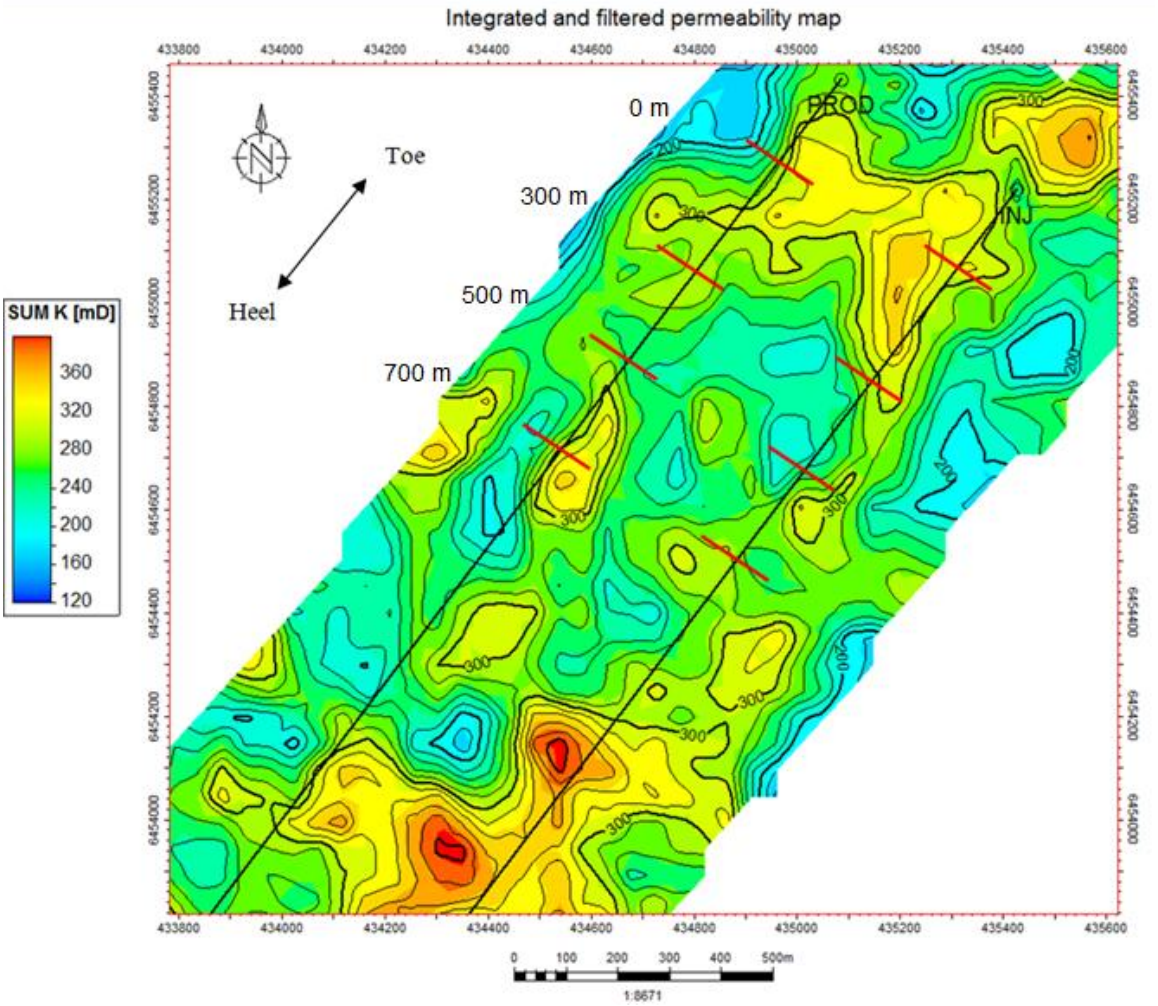

Figure 8-6: Integrated permeability map between layers K=44 and K=101.

From the map it is evident that the permeability contrasts between the injecting and producing fracture increased as the producing fracture was moved further towards the heel. For the runs of d=0m to d=200m, it seems that the fractures were in the same permeability region. For d=300m the integrated permeability slightly reduced and for d=500m the permeability contrast between the injecting and producing fracture were even more dominant. At 700 meters distance, the producing fracture was in a region with higher permeability, such that good communication with the injecting perforations right across provided sufficient pressure support, independent of the injecting fracture.

By moving the injecting fracture towards the heel, as in Case 2, the high permeability regions seem to include the 300 meters distance. However, this region is somewhat narrower there than around the producer, hence reduced effect of fracturing the injector beyond 400 meters could be evident. On the other hand, distances up to 300 meters in both wells seems to lie within the same permeability region. Such distances are thus more connected and would give higher production than longer distances. These different permeability regions could potentially affect the optimal distance between the fractures in this reservoir.

However, to investigate the impact of permeability variations on fracture distance, Case 1 was repeated where the formation permeability was set to a constant value of 10 mD. This was

done to eliminate the effect of permeability contrasts and, if dependent on this, the rates would become equal.

The results are given as oil production rates and cumulative oil production in Figure 8-7 for fracture distances of 0 to 700 meters. The results show that there still was difference in production. However, the optimal distance now had moved from 300 meters to 400 and 500 meters distance.

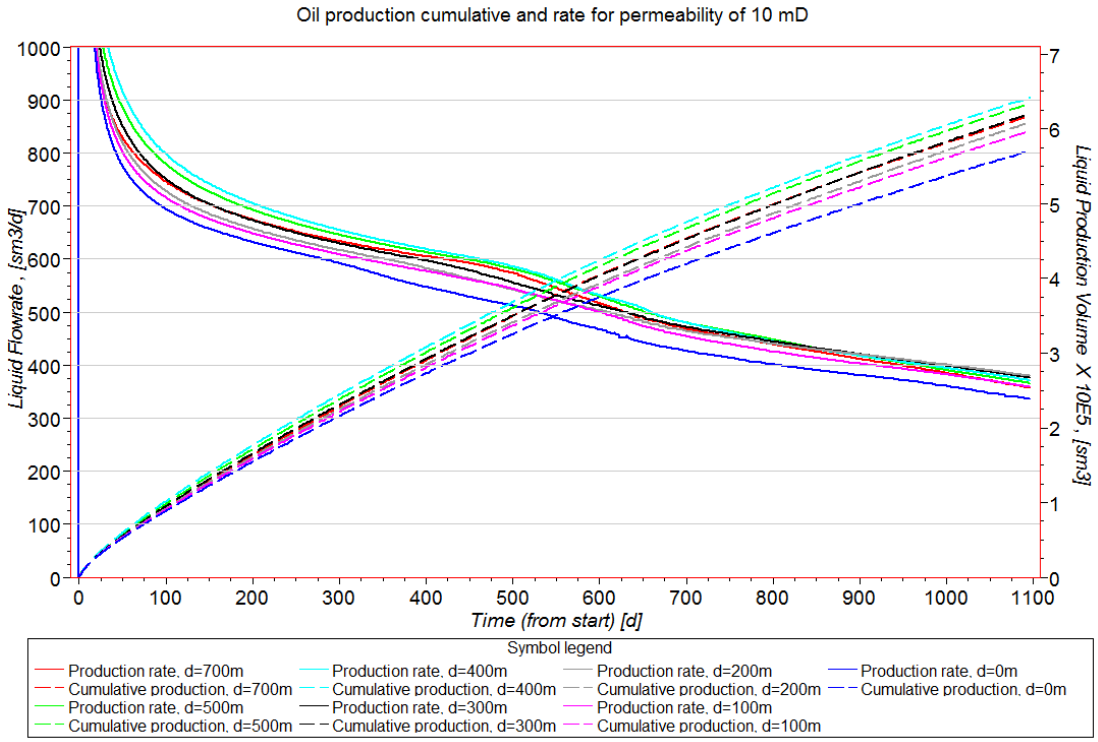

Figure 8-7: Oil production for different fracture distances with constant formation permeability of 10 mD.

The results above indicate that different permeability regions are not the main factor determining the optimal distance in the reservoir. The distance itself may contribute more, in terms of delay in pressure communication, as well as isolated regions due to shale.

The amount of inactive shale blocks in the model was equal whether varying or constant permeability was applied. If all grid blocks in the model had been activated, and the rates had become more similar, this could indicate dominating effects of inactive grid blocks and isolated regions. However, the main issue in this reservoir is to connect different isolated zones. Therefore, frequent occurrence of flow barriers could explain the observed variations in production for several distances. Such simulations for this reservoir are recommended for future work.

On the other hand, 3 faults in the fractured region were evident in the model and are shown in Figure 8-8 by a horizontal layer along the wells. In both wells, the fractures at 0, 300, 500 and 700 meters distance, for Case 1 and 2, are illustrated by the brown squares.

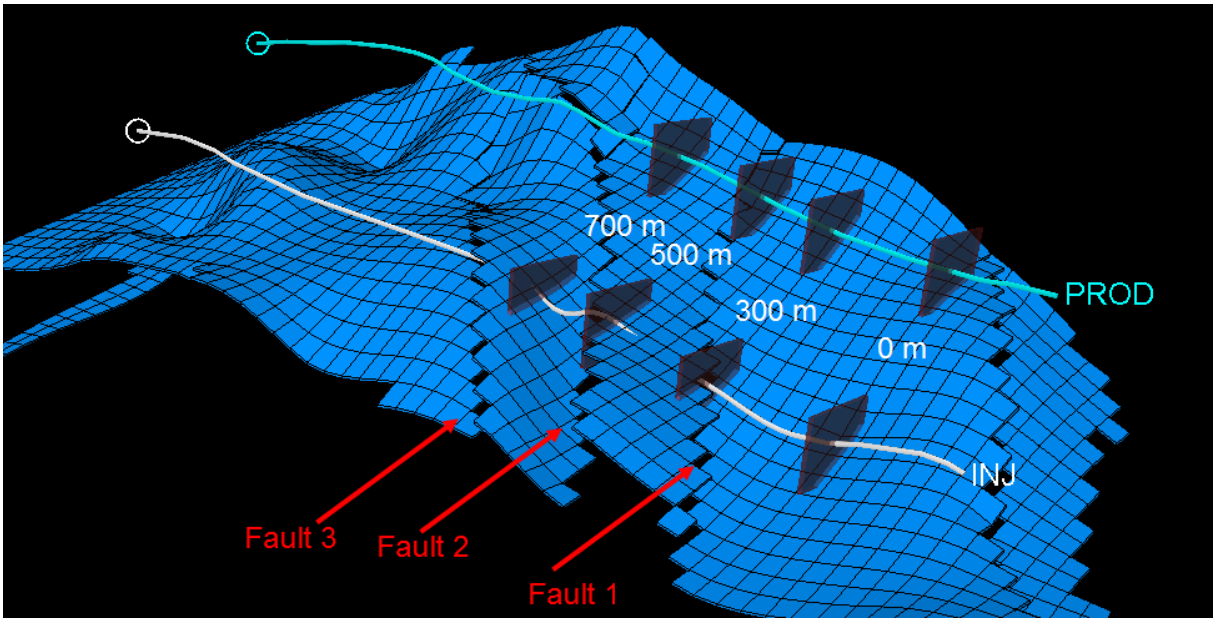

Figure 8-8: 3D view of faults in the model along horizontal layer K=89.

For Case 1, it is clear from the figure that the producing fracture, at distances less than 500 meters, was in direct communication with the injecting fracture since Fault 1 intersects the producer at around 550 meters distance. The presence of this fault could reduce the communication between the producing fracture at 700 meters and the injecting fracture at fixed position of 0 meters. However, according to Figure 8-6, the high permeability region around the producing fracture could, as mentioned, be more in connection with the injecting perforations across it. This may explain the high oil and water production observed for d=700m in Case 1.

Fault 1 intersects the injector around the fracture at d=300m. This means that for the runs in Case 2, fractures at narrower distances than 300 meters were in communication with the producing fracture at 0 meters; hence the oil production was highest for these runs (Figure 8-5). The injecting fractures at d=500m and d=300m distance was located between Fault 1 and 2 and may had reduced communication with the producing fracture. This could explain the drop in performance, going from Case 1 to Case 2.

For a distance of d=700m, the producing fracture was separated from the injecting fracture in Case 1, by Fault 1 only. In Case 2, however, both Fault 1 and Fault 2 were between the fractures and could have prevented the fractures from communicating. This could be one of the factors giving less production for Case 2 at 700 meters.

Since the analysis was disturbed by the faults at around 300 meters distance, the optimal distance in an un-faulted region could likely be longer. This was not feasible in this study, but should be investigated in the future.

Based on this, flow barriers, rather than permeability contrasts, could be the main factor affecting fracture performance. Therefore, supporting fractures should be placed on the same side of a fault.

8.2.4 Case 4: Effect of fracture length

The actual length of a fracture in a reservoir may not necessarily be the one found in a modelling study. According to Section 3.4.2, the length is dependent on the presence of stress barriers around the well and could vary significantly throughout the reservoir. Whether such variations in length are important for production in this reservoir was investigated in Case 4.

Expected findings from this case would be that performance of narrowly placed or aligned fractures is critical to fracture length. Long fractures would increase the risk of getting water directly from the injecting to the producing fracture, as described in Case 1, consequently decreasing the sweep efficiency between parallel wells. For widely spaced fractures, fracture lengths were not believed to be as critical, unless the wells are closely placed and high permeability zones easily provides connection between the producing fracture and perforations in the injector.

Figures 8-9 to 8-11 show oil production rates and cumulative for the runs of 0, 300 and 700 metres distance between the fractures, using the fracture setting as for Case 1. In addition to the fracture half-length of 100 meters, half-lengths of 75 and 125 meters were applied in the runs. For simplicity, the fracture height was kept constant at 30 meters.

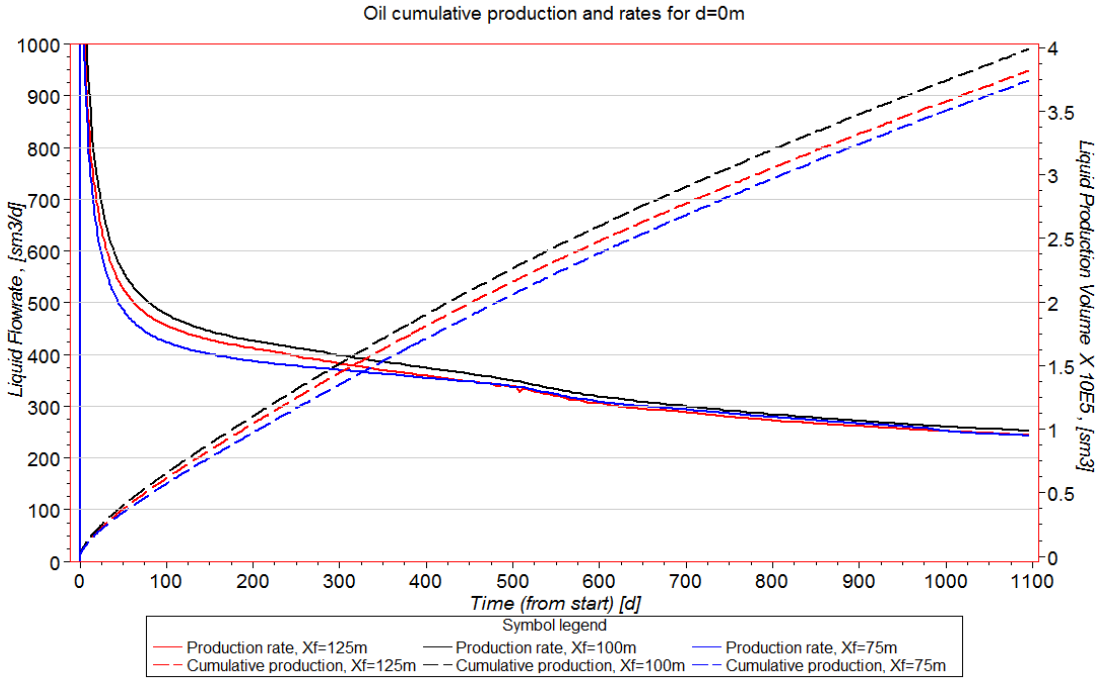

Figure 8-9: Oil production for different fracture lengths for d=0m.

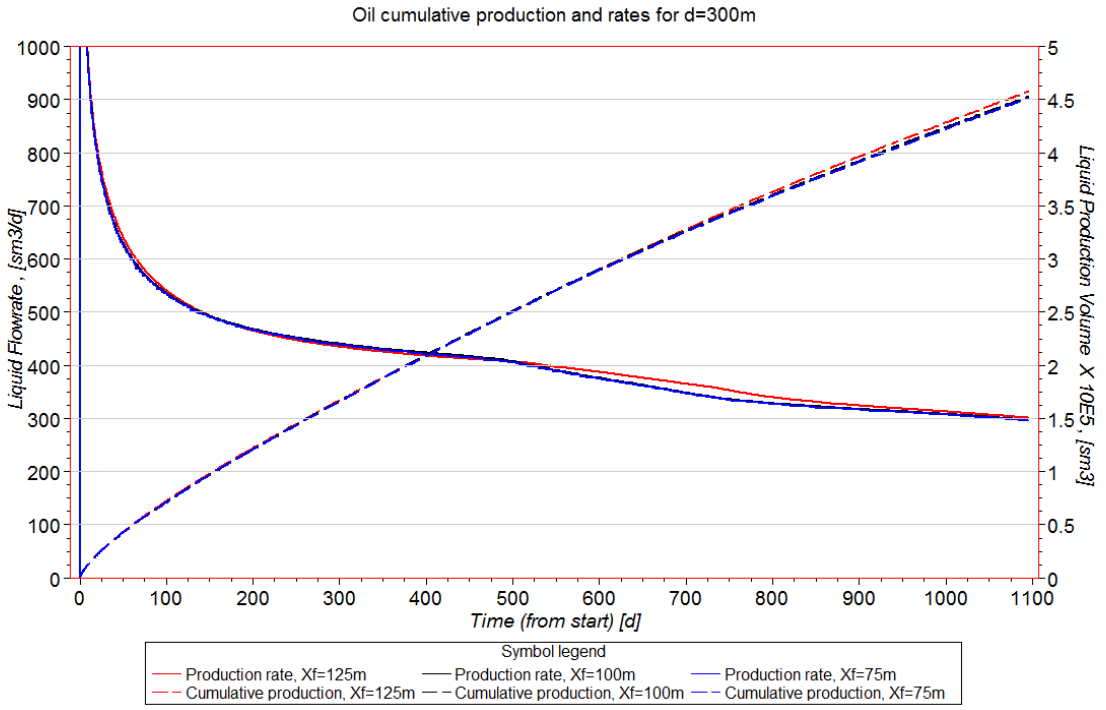

Figure 8-10: Oil production for different fracture lengths for d=300m.

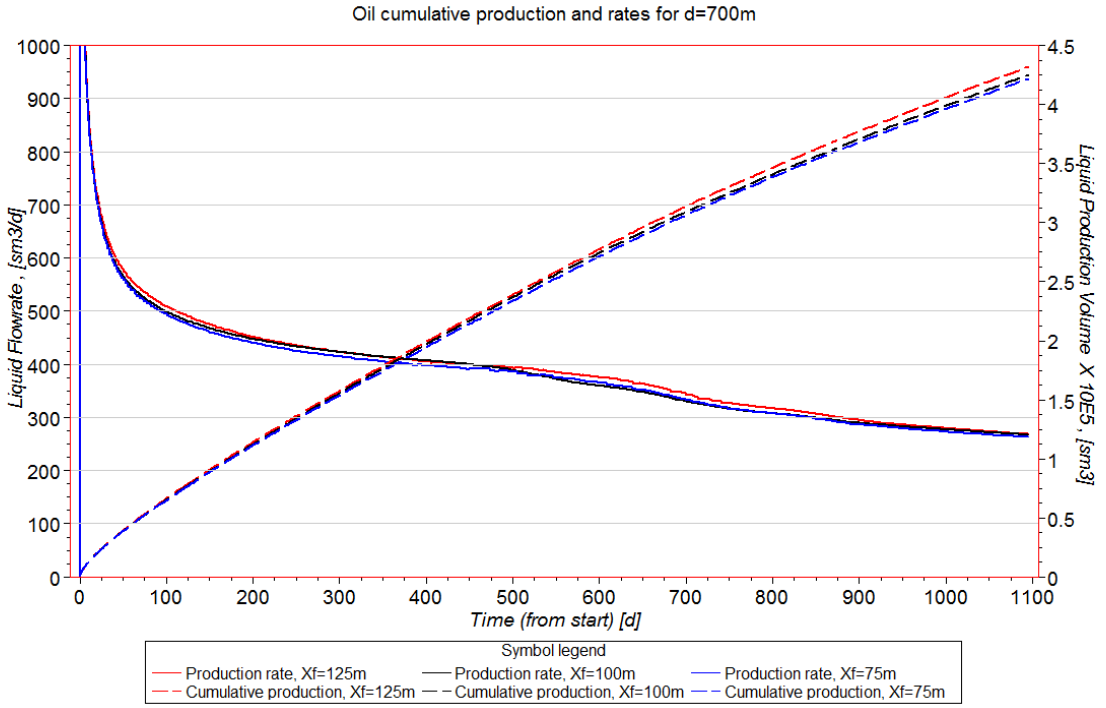

Figure 8-11: Oil production for different fracture lengths for d=700m.

The results show minor effects of fracture length on oil production. For the run where the fractures were aligned, it seems that the production was negatively affected if both longer and shorter half-lengths than 100 meters occurred. This indicates that the applied half-length of

100 meters was, by coincidence, the optimal fracture half-length for this reservoir section. For the other cases, the fracture lengths did not affect the production significantly. This makes sense according to the expectations where, due to the large fracture distance, the amounts of oil displaced by water were not different as fracture length changed.

The water cut for d=0m is given in Figure 8-12. The water behaviour was almost identical for 100 and 125 meter half-lengths and the water production was less for 75 meters. This supports the expectations that shorter fracture lengths reduce the risk of getting early water breakthrough for narrowly spaced fractures. However, maybe due to local permeability variations, the reduced fracture length had the largest effect on both water and oil production.

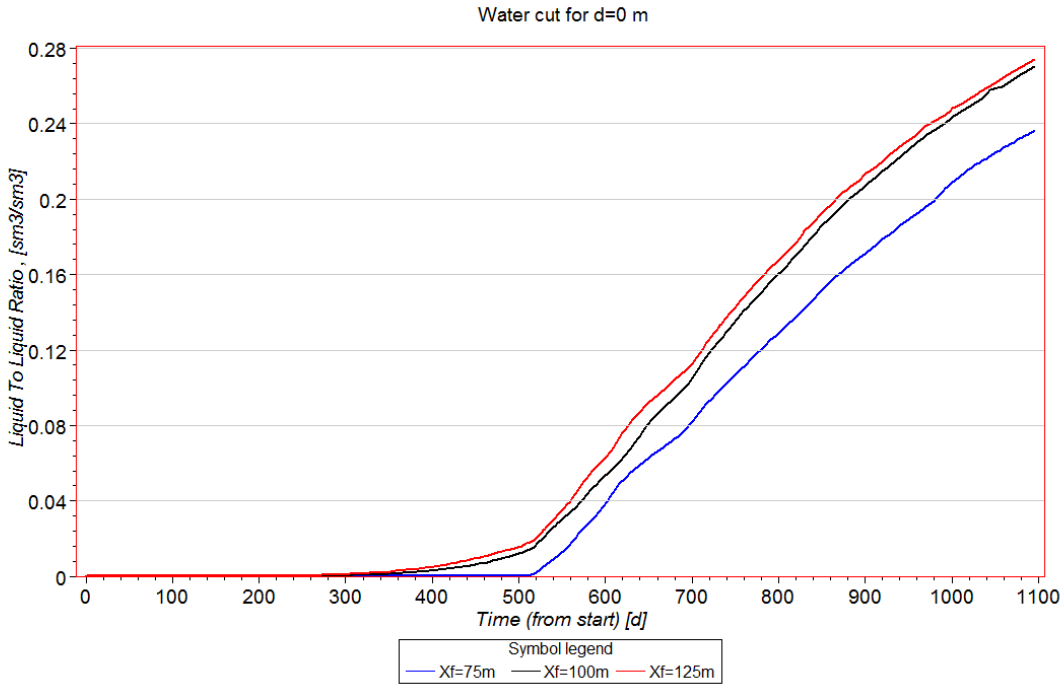

Figure 8-12: Water cut for different fracture lengths for d=0m.

The conclusion from this case is that the fracture length only affects narrowly placed and aligned fractures in this reservoir.

8.2.5 Case 5: Sensitivity to injection pressure

The applied control pressure on the injector of 500 bars was only an estimate, made to give sufficient pressure support. In a realistic case, the pressure could be higher or lower depending on the pumps and formation. To test whether such changes in pressure has an effect on production and optimal fracture distance, an analysis was performed in Case 5. Unfortunately, due to numerical problems at higher pressure, only a reduction in pressure could be performed.

The logically expected outcome of this study was that a reduced BHP in the injector would decrease the pressure support; hence less oil production should be evident and the two fractures had to be placed closer, in order to optimise the communication.

The pressure was reduced by 50 bars, to 450 bars for the fracture settings in Case 1. The results regarding oil production rates and cumulative production are given in Figure 8-13. The

figure shows that the largest production still occurred for 300 and 400 meters distance. Now, in addition, d=700m also had highest production. The least oil production occurred for the aligned fractures, and then gradually increased for 100 and 200 meters distances.

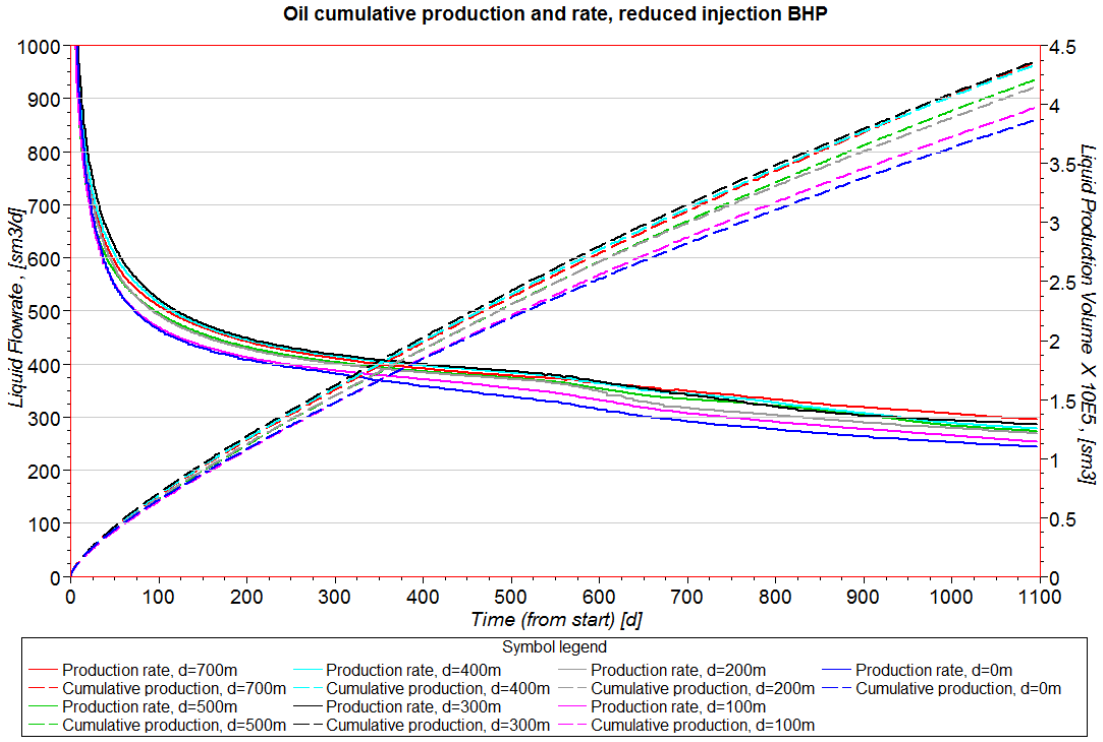

Figure 8-13: Oil production for different fracture distances by reduced injector bottom-hole pressure.

In terms of volumes produced, the reduction in injection pressure decreased the production with around 10 000 Sm^3 for all runs after 3 years, compared to Case 1. The plots comparing each run in Case 1 with the reduced BHP-runs are given in Appendix B.5, Figures B-17 to B-23. Based on these figures, all runs, except from d=700m, had a small decrease in oil production. The 700 meters run, however, increased the late production for lower BHP.

The main conclusion to draw from this is that minor reductions in injection pressure have small effects on the optimal distance, but an overall reduction in volumes produced. The observed increase in production for d=700m could be due to delay in water breakthrough and better sweep. In addition, the producing fracture at this distance was located in a high permeability zone, according to Figure 8-6; hence the production would be larger than for other distances if the pressure was decreased. In general, less pressure is needed to push the fluid towards the producer for this distance.

Theoretically, if the injection pressure was increased by 50 bars, to 550 bars, a similar minor change in production could be seen. For high permeability regions, however, the increased pressure could lead to more water going to the producing fracture and less oil being swept. This is a theory recommended to be studied in the future.

However, changes in injector BHP seems to only affect production volumes, not optimal fracture distance.

8.2.6 Summary of Scenario 2

The following conclusions can be made from the analysis considering one injecting and one producing fracture in two parallel horizontal wells, in a fluvial dominated reservoir:

- Hydraulic fracturing increases production in this reservoir
- Vertical communication is established
- Narrowly placed and aligned fractures affect oil production negatively in terms of early water production and reduced sweep efficiency.
- Widely distanced fractures increase the risk of reduced early high oil production rates due to either delay in pressure communication or presence of flow barriers.
- Optimal distance between one injecting and one producing fracture could be between 300 and 400 meters.
- Permeability variation is not the main factor determining the optimal fracture distance (d) between two parallel horizontal wells.
- Hydraulic fractures supporting each other should not be separated by flow barriers, such as faults.
- Fracturing of high permeability regions in two parallel horizontal wells, in a fluvial reservoir, can reduce the sweep efficiency if the wells are close, and the high permeability region extends through both wells.
- The relative placement between one injecting fracture and one producing fracture affects the oil production.
- Changes in fracture length only affects narrowly spaced fractures in terms of oil production.
- Small changes in injection pressure do not significantly affect optimal fracture distance, only the oil production.

8.3 Scenario 3: Two injecting fractures

8.3.1 Case 1: Optimal fracture spacing (s) in the injector

The next part of the analysis was to investigate the effect of fracture spacing between two fractures in the injector only. The main aim was to determine how the communication between them developed for different permeability regions and horizontal distances. The horizontal distance (s) between the two fractures was varied between 100 and 500 meters by keeping the near-toe fracture in a fixed position (same position as for Case 1 in Scenario 1) and shifting the other fracture towards the wellbore heel (Figure 7-2B). Five runs were conducted where the fracture spacing was increased by 100 meters in each run.

The expected findings in this study, concerning fracture communication, were that narrowly spaced fractures would interfere and unite outside the wellbore. A high conductivity path, where much of the injected water goes into, could then be created. This would reduce the sweep efficiency of the injecting well and less oil would be produced.

If the spacing was too large, the sweep could also be negatively affected due to lack of fracture communication. This could be due to closely placed wells, in which the circular sweep pattern of each fracture having radii quickly exceeding the distance between the wells. As a consequence, ineffective sweep of the remaining oil between the fractures could be the case. Therefore, ideally, the optimal fracture spacing in a homogeneous reservoir should be two times the distance between the wells. Then the two circular sweep patterns would unite at the same time as breakthrough occurred in the producer. However, this theory is only for a homogeneous reservoir with non-fractured producer. If both wells were fractured, the drawdown from an additional producing fracture could shift the optimal fracture spacing to larger values. In addition, the reservoir heterogeneity could also change the optimal fracture spacing.

Figure 8-14 shows the oil production rates and cumulative production for all the runs in Scenario 3. It is obvious that there was no difference in early oil production as the fracture spacing increased. After about 500 days of production, however, the production rates dropped for all runs, but the cumulative production shows that the case of s=300m produced 10 000 Sm^3 more than the other runs after 3 years (1095 days).

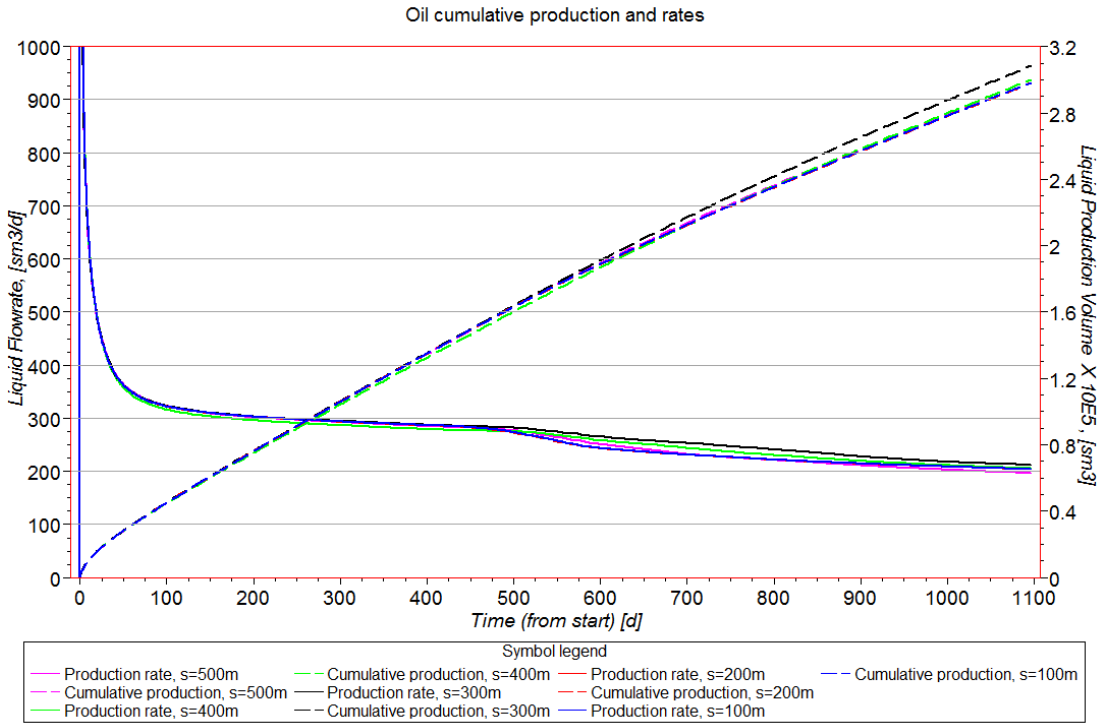

Figure 8-14: Oil production for different fracture spacing in the injector.

The results could indicate that the area around 300 meters spacing had larger productivity. However, the rate was decreasing less than the others, meaning that an effect contributed to support the production at this distance. Therefore, at 300 meters spacing, the two fractures may work together more sufficiently to optimise the production. On the other hand, the small changes in cumulative production indicate that the permeability variations and flow barriers, discussed in Scenario 2, are likely to have contributed. Therefore, no general conclusions can be drawn from this.

To further discuss the fracture interference, the amount of injected water was investigated. Figure 8-15 shows water injection rates for the different runs. It is clear that for s=400m the rates were lower than for the other runs. 100 and 300 meters spacing injected at highest rates.

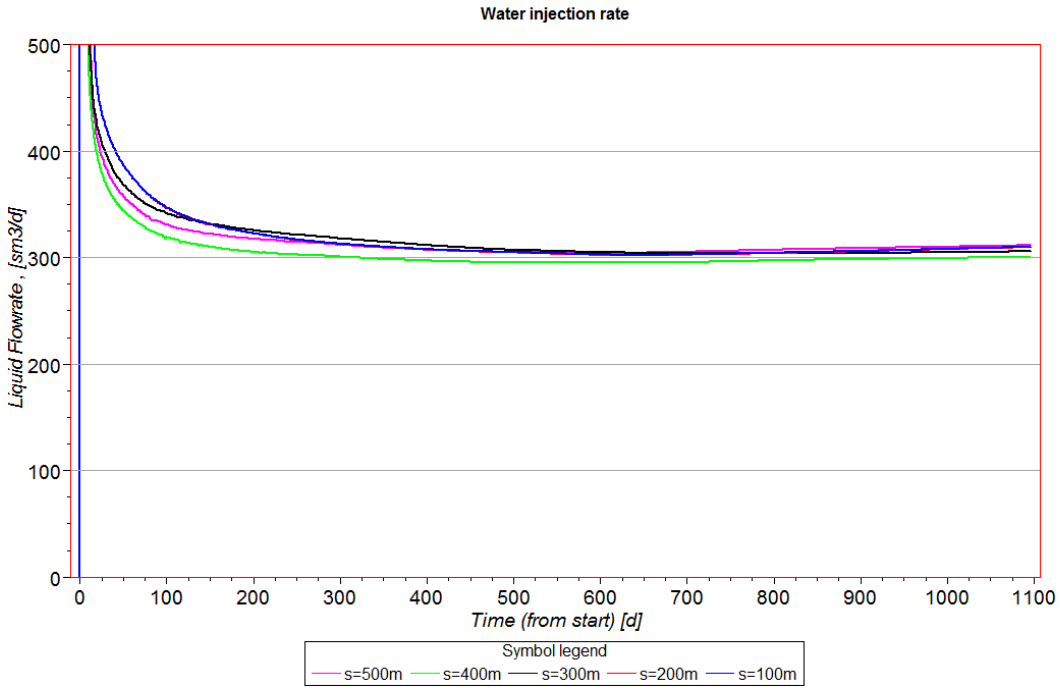

Figure 8-15: Water injection rates for different fracture spacing in the injector.

This indicates that s=100m was too close in this case. The fractures interfered and more water had to be injected to obtain the constant BHP in the injector. For the other runs, however, there seems to be too high degree of randomness in the results to draw any other conclusions regarding fracture spacing. The low rate for s=400m might be due to one fracture being in the lower permeability regions (between 500 and 300 m in Figure 8-6). This would result in less water being injected to maintain 500 bars BHP in the injector.

Figure 8-16 shows the water cut and the cumulative water production for the different runs. The runs for 100 and 200 meters spacing overlaps entirely, such that only the blue lines are visible. The results reveal a major effect regarding water breakthrough; earliest water production for 100, 200 and 500 meters fracture spacing.

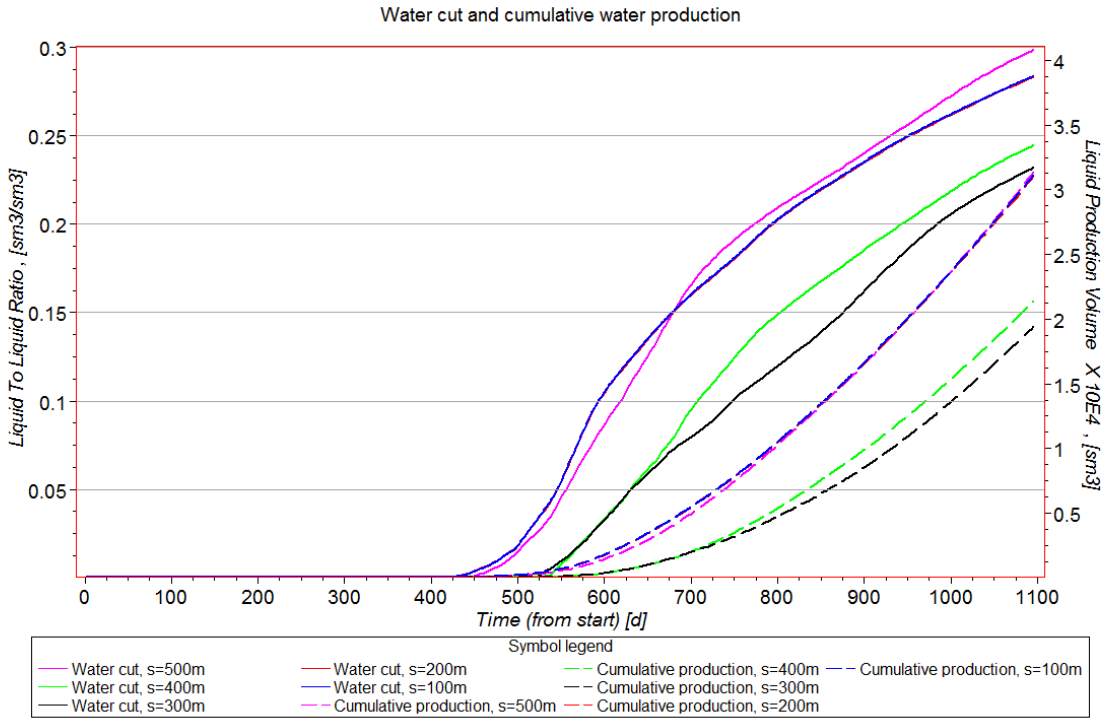

Figure 8-16: Water production for different fracture spacing in the injector.

The reasons for early water breakthrough were further investigated by creating water saturation maps of the toe section of the wells. These are given in Appendix C, Figures C-1 to C-6 and illustrate contour maps where the contours describe the vertically integrated water saturation values in the vertical extent of the fracture LGR's. Red to blue colours indicates low to high water saturation respectively, equivalent to high and low oil saturation. The two fractures are located in the areas where circular patterns occur, for all runs. The maps show saturation after 3 years of production, at the end of the simulation period. All runs are present as well as the non-fractured base case, to illustrate the effect on sweep.

The main result is that around each fracture a circular pattern was formed, displacing the oil towards the producer. As the distance between the fractures increased, a larger area was swept by the injected water. In addition, it is clearly visible that the injecting perforations alone also contributed further up in the well, in terms of a blue circle close to the heel section.

For closely spaced fractures, 200 meters and less, they interfered and created one strongly conductive path, where the majority of the injected water went. This is clear from the dark blue circles. For such distances, too strong interference occurred. The non-fractured case had a low integrated saturation value, which probably was due to the limited vertical extent of the well itself. Therefore, the importance of hydraulic fracturing in the injector is clearly evident.

According to the maps, fracture spacing of 300 and 400 meters had swept largest areas at the end of simulation, where s=300m had most uniform water distribution. For s=400m, the majority of the water seemed to be flowing into the near-toe fracture. This may be due to the fault separating the two fractures for this spacing.

At 500 meters the fractures were too widely spaced, resulting in water breakthrough across both fractures before the two sweep circles joined, leaving less swept regions between them even at late times.

Based on the runs, larger volumes are swept by increasing fracture distances, but taking into account the distance between the two wells, a too wide spacing will provide a large radial sweep pattern around each fracture until water breakthrough in the producer. At optimal spacing the water has displaced all the oil between the fractures at time of water breakthrough. This could explain the equal increase in water production observed for s=100m and s=500m, hence too narrow and too wide distance between the fractures in the injector should be avoided. However, the high water production could also be due to high permeability regions near the fractures. The relationship between well spacing and fracture spacing should be investigated in the future to determine the effect on optimal fracture setting.

8.3.2 Summary of Scenario 3

The main findings regarding optimal spacing between two injecting fractures can be summarized as follows:

- Evaluation of fracture spacing in the injector is important for avoiding early water production.
- Narrowly spaced fractures will increase the chance of early water breakthrough and reduced sweep efficiency.
- An optimal spacing of around 300 meters is evident in the reservoir, but will be affected by flow barriers.

8.4 Scenario 4: Two producing fractures

8.4.1 Case 1: Optimal fracture spacing (s) in the producer

The same comparison as for the injector was conducted for the producer in Scenario 4. Five runs were simulated where each run increased the producing fracture spacing by 100 meters, up to 500 meters. In this case the injector was non-fractured and the aim was to determine how multiple producing fractures would communicate and interfere through different distances. The near-toe fracture was kept in a fixed position, as in Case 2 of Scenario 2, while the other fracture was moved towards the wellbore heel (Figure 7.2C).

This study was expected to show that each fracture has a certain circular drainage area. To secure and optimise early oil production, in terms of high rates, an optimal distance between them should be evident where the fractures together create a wide, rectangular and effective drainage pattern between the wells. In such areas the pressure drawdown is maximised by the pressure support from the injector. Since this case considered fractured producer only, fracturing the injector would probably disturb the results and shift the optimal spacing towards larger values. This theory is based on that an injecting fracture would provide more pressure support; hence wider spacing in the producer would increase the drainage area and reduce risk of early water breakthrough from the injecting fracture.

Figure 8-17 shows oil production rates and cumulative production for the different runs in this scenario. It is evident from the figure that the early production rates differed around 100 Sm^3/d after 100 days of production, between the highest and lowest rate. It is also clear that the two narrowest spaced runs, at 100 and 200 meters fracture spacing, produced least amounts of oil during the simulation. The rest produced almost the same amounts, with 400 and 500 meters spacing entirely overlapping.

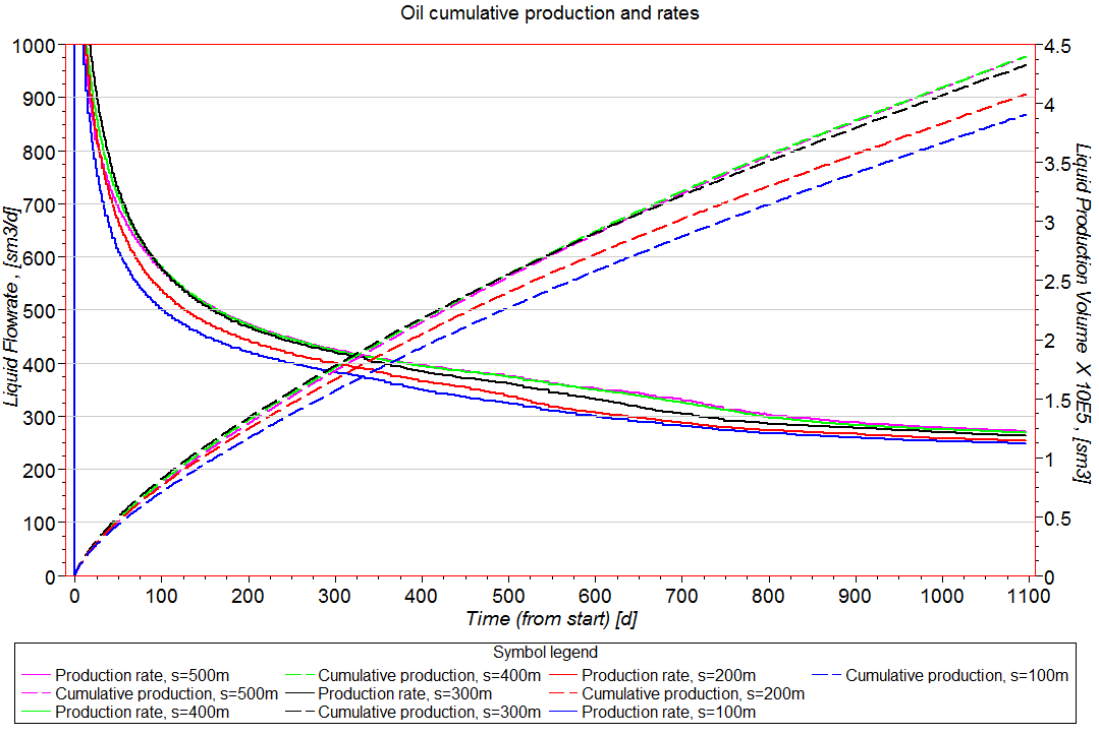

Figure 8-17: Oil production for different fracture spacing in the producer.

These results indicate what was suspected; narrowly spaced fractures in the producer negatively affect the fracture efficiency. The reason for this limit on performance is probably due to the same interference principle as for Scenario 3. The producing fractures act as one single fracture, providing large drawdown in the fractured area. This pulls the local oil and injected water towards the fractures, and the result becomes a direct pathway from the injector to the producer. The oil further out is not reached by the effective drainage radius of each fracture.

On the other hand, by only moving one fracture, the chances of getting into an entirely different permeability region is large. The differences in production could be due to each fracture affecting two isolated regions. However, the faults in Figure 8-8 did not separate the fractures if the spacing was less than 500 meters, such that flow barriers are unlikely to explain the observed difference. The permeability map in Figure 8-6 indicates that different permeability regions were present for spacing larger than 300 meters. Based on this, the producing fractures should not be narrower than 300 meters before the production is affected negatively, by interference and presence of equal formation properties around both fractures. Spacing between 400 and 500 meters seems to maximise the production.

Figure 8-18 shows water cut and cumulative water production for all the runs. It is visible that earlier water breakthrough occurred for narrowly spaced fractures (100 and 200 meters). In addition, it is evident for 400 and 500 meters that the amount of produced water rapidly increased after breakthrough, and ended up at the same rates as for closer fractures. However, the optimal spacing seems to lie in the region between 400 and 500 meters. This could, of course, be greater if longer distances were simulated, but as mentioned before, distances around 700 meters probably would be too much affected by high permeability regions, such that the result would not be representative for sections closer to the toe. Therefore, a maximum of 500 meters distance was simulated.

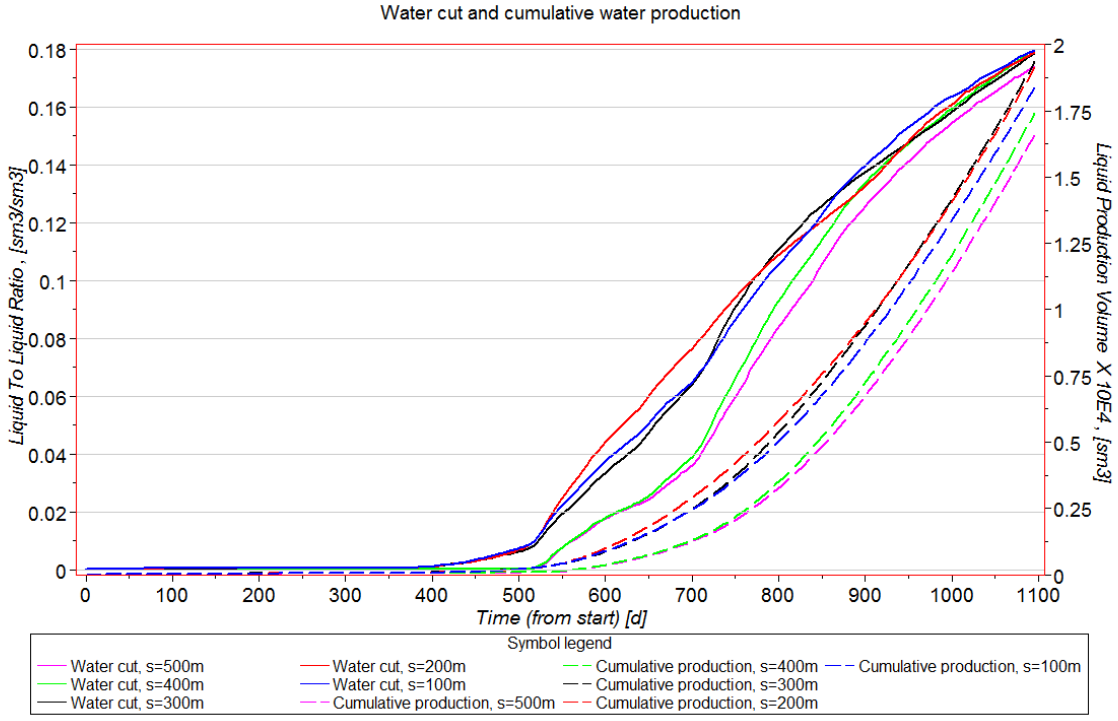

Figure 8-18: Water production for different distances between two producing fractures.

Appendix D.1, Figures D-1 to D-6 shows the average pressure distribution in the fractured areas after 3 years of production for the different runs, including the non-fractured case. Blue to red colours indicates low to high pressure.

It is evident that the non-fractured case had very limited drawdown. After 3 years of production the pressure difference between the injector and producer were only 100 bars, but uniform along the entire interval. For the fractured runs, a large drawdown of 200 bars is observed and communication with the injector was established. As the spacing increased, the drainage area significantly improved and the expected rectangular-shaped area between the wells is visible in the figures. This indicates increased connectivity in the fractured regions.

8.4.2 Summary of Scenario 4

The conclusions regarding optimal spacing of two producing fractures are summarized in the following:

- Narrow spacing in connected regions of equal permeability negatively affect early oil production and increase risk of early water production, compared to wider distances.
- Wider the spacing, larger the drainage area.
- Optimal spacing in this reservoir is around 400 to 500 meters.

8.5 Scenario 5: Multiple-fractured wells

This scenario consisted of one run where both wells were hydraulically fractured in a multiple fracture setting. The aim was to optimise oil production from the producer by placing several hydraulic fractures in both wells, according to the results obtained in the previous analyses.

8.5.1 Case 1: Multiple-fractured injector and producer

Based on the analyses performed in the previous sections, the following points were considered for the parallel wells in the sector model:

- Scenario 2 indicated that one injecting and one producing fracture should not be aligned, i.e. not placed along the same J-plane or any plane overlapping within 200 meters horizontal distance, due to risk of early water breakthrough and reduced sweep efficiency.

- The longitudinal distance between one injecting and one producing fracture should not exceed 400 meters. Larger distances negatively affected early oil production due to delay in pressure communication and presence of flow barriers.

- If a fracture in one of the wells is surrounded by faults, the supporting injecting fracture should also be placed within this region, if the faults intersect both wells.

- Scenario 3 stated that injecting fractures should be spaced more than 300 meters to avoid too early interference between them.

- Scenario 4 indicated that producing fractures should be spaced more than 300 meters, in order to avoid negative interference and to maximise drainage area for each fracture.

- By comparing total amount of oil produced, Scenario 3 produced around 300 000 Sm^3 in 3 years time which was at least 100 000 Sm^3 less than for Scenario 2. This states that a producing fracture should be located between two injecting fractures in a multiple fracturing case.

- By comparing the fracture setting in Scenario 4 with the setting studied in Case 1 of Scenario 2, it was evident that Scenario 2 produced 20 000 Sm^3 more for the 300 meters distance. This indicates that the best effect of multiple hydraulic fracturing could be accomplished if the fractures are placed in an alternating injecting and producing fracture setting along the wellbore longitude, rather than clusters of producing or injecting fractures.

Due to the amount of numerical problems frequently occurring in this model, a maximum of 3 fractures in each well was possible to run, without reducing the injector BHP and get injection pressure equal to reservoir pressure. The fractures were placed in the same area as for the previous analyses, extending towards the wellbore heel. This was mainly to avoid significantly differences on optimal fracture spacing. In addition, the heel sections were more connected, such that less effect of hydraulic fracturing would be seen there.

Instead of limiting the perforated interval, as in the analyses, the entire horizontal sections were open to flow. The fractures were placed as illustrated in Figure 8-19. One producing fracture with one supporting injecting fracture was placed within each faulted region.

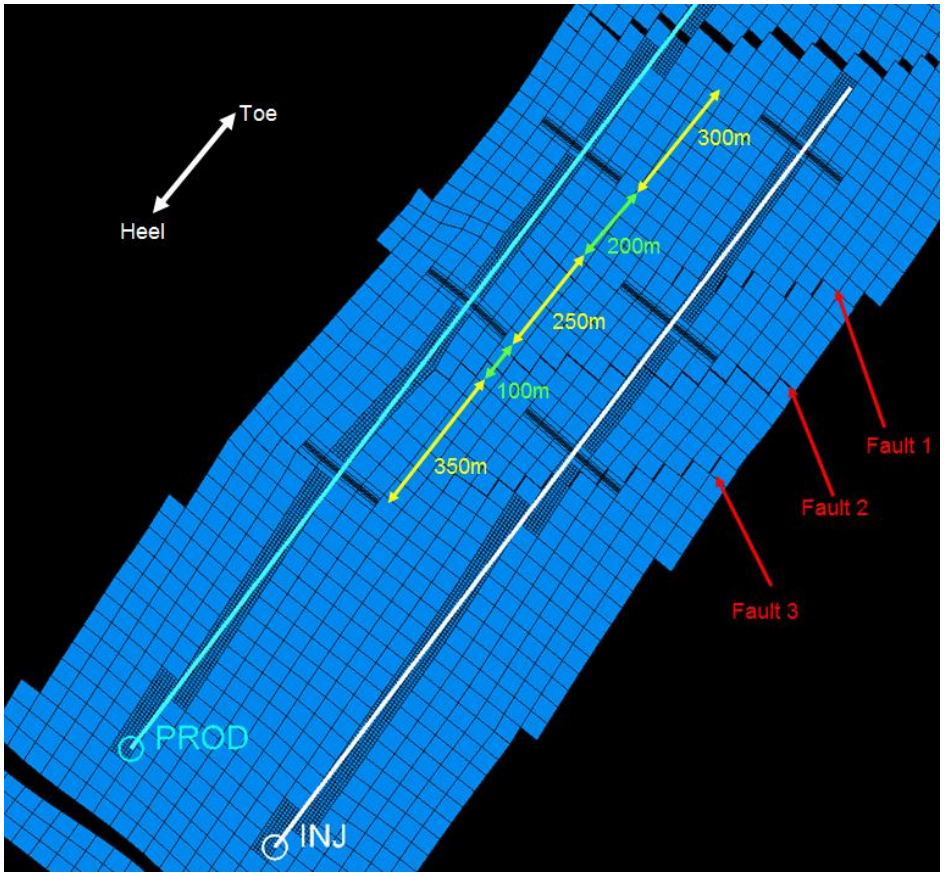

Figure 8-19: Three multiple hydraulic fractures in the injector and producer.

Figure 8-20 shows the same permeability map as in Figure 8-6, but contains the multiple fractured setting, indicated by red lines, not representing the full fracture length. The faults are indicated by blue lines. The region closest to the toe was having a more or less uniform permeability around both wells, such that a horizontal distance of 300 meters between the near-toe fracture couple would be sufficient.

The neighbouring region, between Fault 1 and 2, contained two supporting fractures. The distance between them was set to 250 meters in order to achieve maximum fracture distance within this faulted region. As a consequence, a distance of 200 meters from the injecting fracture down to the producing fracture in the previous region, was applied. This would be too narrow if the properties were equal on both sides of Fault 1. However, due to Fault 1 partly disconnecting the two regions, combined with the results from Case 2 in Scenario 2 stating that the injecting fracture could be placed closer to the heel than the producing fracture at shorter distances, 200 meters would be sufficient to delay water breakthrough in this region.

In the third region, between Fault 2 and 3, the distance between the producing and injecting fracture was set to 350 meters to be in accordance with the optimal distance. Fault 3 did not extend to the producer; hence this would not significantly affect flow between the fractures. In addition, the producing fracture were placed in a low permeability region surrounded by very high permeability, and probably well connected, regions.

The spacing between the fractures in each well (s) was kept between 300 and 500 meters. This was optimal according to the analyses in Scenario 3 and 4, in terms of oil produced by the producer and area swept by the injector.

One drawback with this setting was the close distance of 100 meters between the producing and injecting fracture on each side of Fault 2. However, taking into account the disturbance in flow due to the fault, and that relatively large permeability contrasts separate them, early water breakthrough here was not of main concern.

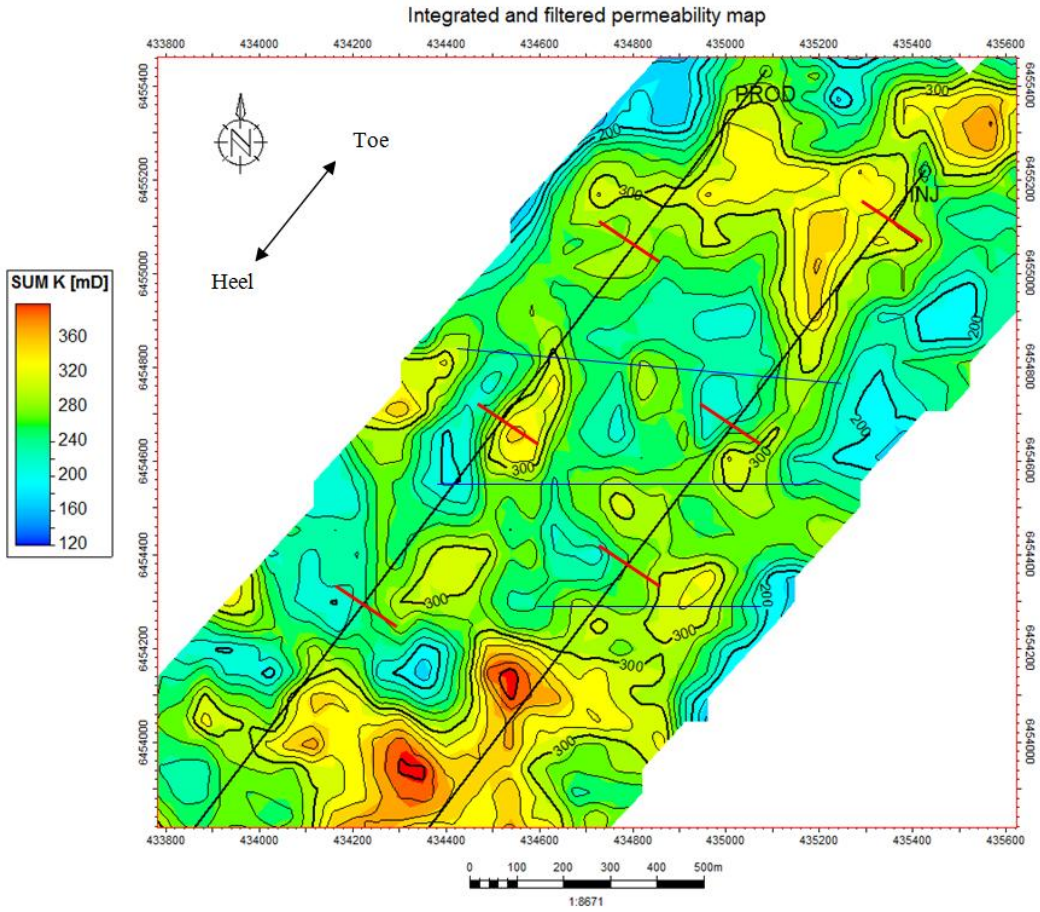

Figure 8-20: Integrated permeability map between layers K=44 and K=101 for multiple-fractured scenario.

The simulation of the multiple fractured run was carried out using the same control parameters as for the non-fractured case in Scenario 1. The simulation period was extended by two years, compared to the previous scenarios; hence 5 years prediction was run.

Figure 8-21 shows the oil production rate and cumulative production for the multiple and non-fractured scenarios. It is evident that the fractured case, with the optimal setting, satisfied the requirements of high, early production rate within the first years. The fractures had their largest efficiency within approximately the first year (400 days), before the efficiency started to decrease rapidly. At the end of the simulation period, there was nearly no remaining effect of the fractures, in terms of production rates, which is also evident from the almost identical slopes of the cumulative production. The end-points on the oil cumulative production plot shows a difference in volumes produced of almost 400 000 Sm^3 (2.5 million Sbbl) which corresponds to 33 % extra production by fracturing this well-couple.

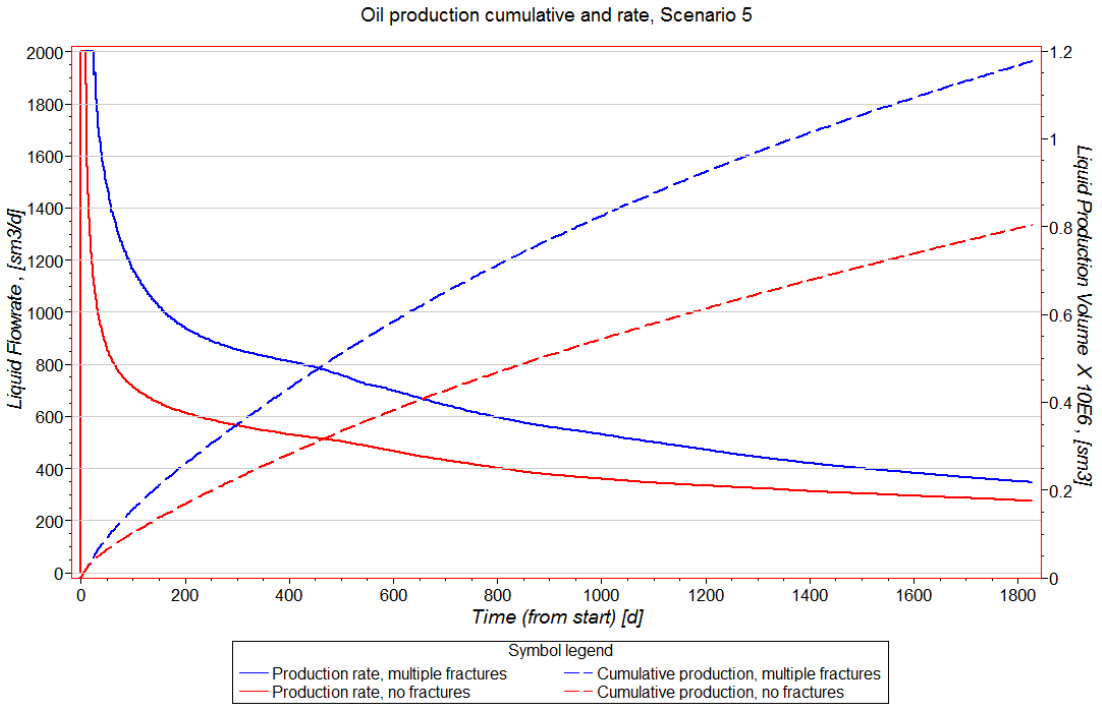

Figure 8-21: Oil production for multiple- and non-fractured runs.

The fractured run indicates the importance of optimising the early production, as the performance of the fractures reduced significantly after the first couple of years. This reduction was probably due to water breakthrough in the producer. As more water was produced, a corresponding decrease in oil production through the fractures is evident from the figure. The oil production then decreased more rapidly.

The oil production rate is shown together with the water cut on the secondary y-axis in Figure 8-22. The figure states that water breakthrough occurred at approximately the same time in both runs. They produced the same amounts of water until about 1000 days. Afterwards, the water production increased more for the fractured case. The reduction in oil rate was due to an increasing water cut.

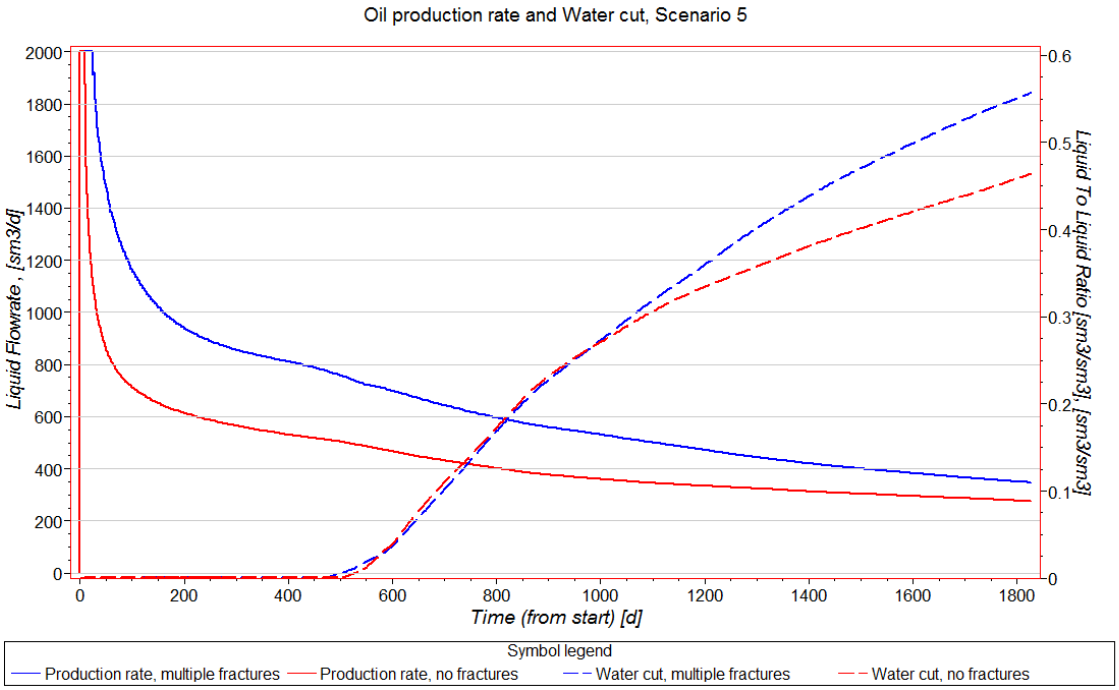

Figure 8-22: Oil production rate and water cut for multiple- and non-fractured runs.

The equal time for water breakthrough in both runs indicate that the fractures were not placed too close. More likely, the possibility of a highly connected region in the wellbore heel area, not reached by the fractures, could be the explanation.

By studying water saturation maps of the entire sector at a time after water breakthrough, for both runs, this suspicion was confirmed. The maps are given in Figure E-1 and E-2 in Appendix E. The circles created around the injecting fractures is visible, as well as the large area swept in the heel-section, which was equal for both runs. This result also justifies the choice of fracturing the toe-sections of the wells. Fracturing in the connected areas would probably have contributed to even earlier water production.

8.5.1 Summary of Scenario 5

The following conclusions can be made from two parallel multiple-fractured horizontal wells in this reservoir:

- Connected high permeability regions should not be fractured, only disconnected regions.
- High early production rate is critical to maximise recovery
- An extra volume of 400 000 Sm^3 (2.5 million Sbbl) can be recovered by hydraulic fracturing of one well-couple in the Talisman discovery.

8.6 Problems and simplifications

One of the main challenges in this thesis was to get Eclipse to run the simulations exported from Petrel. A large part of the available time has been spent on learning to use the software and to get satisfactory results. This was mainly due to the complexity of the model which provided large local variations in grid properties. Many cases terminated due to problems with convergence of the linear equations in the simulator. By troubleshooting, combined with trial and error, several solutions were tested in order to eliminate numerical problems.

One of the problems experienced was to get Eclipse to read the fractures created in Petrel. If the fractures were randomly placed along the wellbore, the chance of them intersecting inactive grid blocks was large. Grid blocks are inactive if zero pore volume is specified in terms of zero porosity or Net-to-Gross ratio, and the model contained large amounts of such blocks. If a fracture LGR contains inactive grid blocks, these will not be a part of the high conductivity fracture; hence they become flow barriers inside it. This is not acceptable and could lead to the fracture not being connected to the well at all. Therefore, in the model, this issue was solved by manually assigning porosity and Net-to-Gross values equal to model averages, to all grid blocks within the fracture LGR's. The main drawback with this procedure, however, is that more pore volume is introduced to the model resulting in a small increase in oil volume in place (STOOIP).

Secondly, when performed simulations including fractures, the desired fracture permeability of 100 000 mD was too large for the model to handle. It seemed that the producing well did fine, but the injector had problems at once. This was believed to be due to the surrounding tight grid cells representing the shale. When the injector constantly pushed fluid into tight blocks the linear equations within the simulator did not converge, and finally terminated the runs. The first move to cope with this problem was to decrease the injection rate by reducing the BHP limit in the injector. The fracture permeability was then reduced by an order of 10, to 10 000 mD without improvement. The final step was to reduce the fracture permeability even further down to a value of 1000 mD. This setting made it possible to run the simulations for the desired period without major problems, and all analyses was able to be performed.

Due to long simulation time experienced in each run during the analysis, LGR and perforations were only created in the toe sections of the wells, for Scenarios 2 to 4. This was mainly from 4200 mMD. Since only the interaction between two fractures was the interesting part of the analyses, inflow to the whole wellbore was not considered important for the results. However, lengths of the perforation intervals were maintained equal for all the runs in order to compare them, in terms of produced and injected volumes. By reducing the perforated interval the amount of refined grid blocks was reduced to a minimum, consequently providing more efficient simulations.

Finally, the refined grids were solved independent of the global grid, meaning that local time stepping was applied. Thus, the LGRLOCK keyword, activating simultaneous solution of both local and global grid blocks, was disabled. Possible instabilities due to this can be seen as small oscillations in the production rates.

8.7 Uncertainty and sources of error

The results obtained in this study have some degree of uncertainty due to the simplifications and assumptions made in the establishment of the model, and throughout the simulations. The following points could have contributed to less accuracy of this model compared to a realistic case.

8.7.1 Fracture properties

The fracture properties applied in the model were based on several hydraulic fracturing design simulations, stress measurements and log-data gathered from the drilled wells. The best estimate of the most likely fracture properties to occur were determined by taking the average values of the different runs provided by the Drilling Department. Therefore, the properties may vary from fracture to fracture, dependent on the surrounding formation, but equal properties had to be assumed in order to simplify the model. However, as discussed in the analysis, fracture length has limited effects on production.

The fracture height depends on the fracture length, as described in Section 3.4, but in the analysis this was kept constant. The effect of this is that fewer layers would be connected for deep fractures in the reality, due to fracture height termination.

Furthermore, regarding vertical fracture termination, lack of information on the geology and the lateral extent of local stress barriers within Unit 2 and 3, make equal properties to each fracture a reasonable estimate. Due to a large amount of thin shale layers in the reservoir, it is uncertain whether they would terminate vertical fracture growth or not. In reality, thin shale layers would probably not withstand the fracturing pressure, resulting in vertical growth. Thicker layers, however, are also present in the fractured areas where fracture termination would probably occur, creating deeper fractures. Again, this would only affect the vertical communication, since change in fracture lengths did not significantly reduce performance for properly spaced fractures.

As described previously, the optimal fracture permeability of 100 000 mD was not feasible in this model, and the study had to be performed with 1000 mD. This most likely resulted in under-prediction of the productivity increment in the multiple-fractured scenarios. For the rest of the analysis it was believed that the flow behaved equal for both permeability values. The difference, however, could be a less remarkable effect of the fracture compared to the perforations, for the 1000 mD case. Although the fracture permeability was reduced by an order of 100, it still had significantly higher permeability than the rest of the reservoir. Therefore, a highly conductive path was, nevertheless, providing sufficient drawdown and oil transfer from the formation to the producer.

To understand the consequences of reducing the fracture permeability, an analysis was performed where one fracture was placed in the producer. The fracture permeability were given values of 100 000, 10 000 and 1 000 mD in three separate runs. The oil production rates and cumulative production for the three runs is given in Figure 8-23. Surprisingly, the effect was not as large as expected and the maximum difference in oil rate between 100 000 and 1000 mD was only around 70 Sm^3/d for one fracture. This could indicate that a fixed portion of the layers was connected to the fracture, such that limited amounts were produced and the fracture conductivity does not provide critical effects. However, this comparison only concerned one fracture. If multiple fractures occurred, the difference in cumulative production could be severe for the same permeability difference.

It must be mentioned that the run of 100 000 mD terminated just after a year of production. So that a more complex fracture setting, using the designed fracture permeability, were not obtainable within this model.

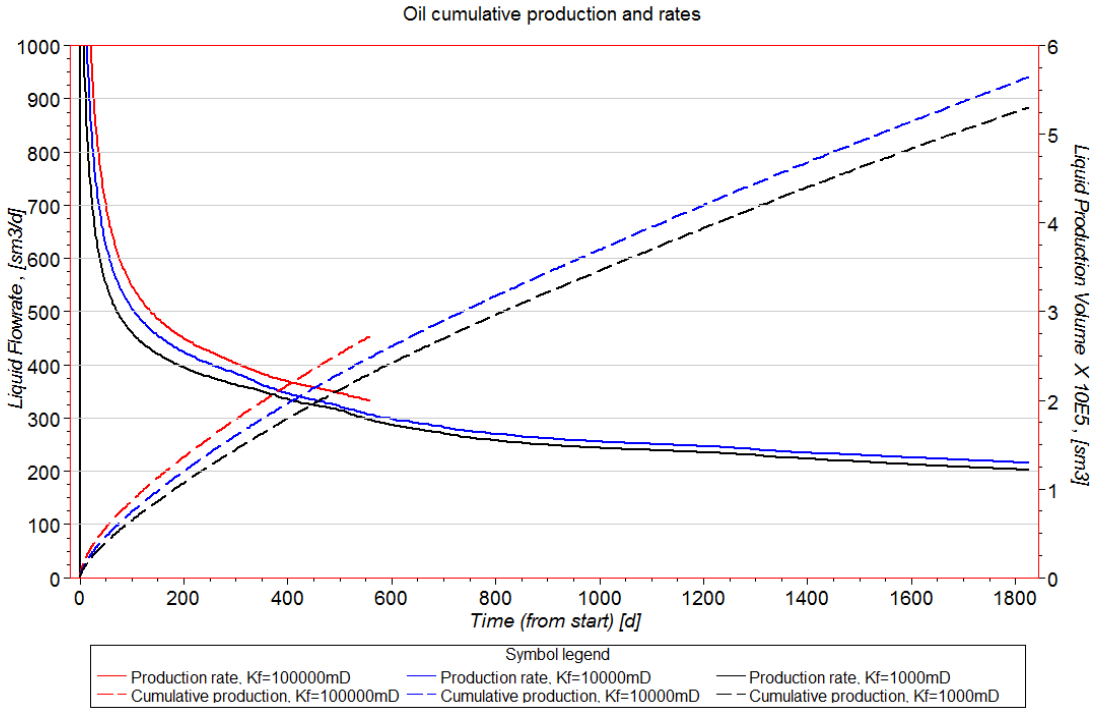

Figure 8-23: Oil production for different fracture permeability in one producing fracture.

8.7.2 Inactive grid blocks

In order to activate the local inactive grid blocks within the hydraulic fractures, the host cells had to be activated by modifying zero net-to-gross and porosity values. This process thereby increased the total pore volume of the model and consequently the STOOIP. Therefore, the difference in volumes produced between the non-fractured and multiple fractured run has the possibility of overestimation.

Ideally, only the centre LGR-grid representing the fracture should be made active, such that as few grid blocks as possible is introduced to new pore volumes. This was not feasible within the time limit, but should be evaluated in later studies

8.7.3 Effects on post-fracturing performance

Changes in fracture performance will concern fracture closure, non-Darcy pressure drop, stresses change due to depletion, multiphase effects and fracture filtrate cleanup.

Reliable sources states that fracture cleanup in this field probably would occur within a week of fracture production; hence this is not important when doing multiple-year simulations as in this thesis. In addition, it is not time-economic to model this with the available tools.

Fracture closure and proppant crushing, due to depletion and increased effective stress in the produced sands, could often decrease the fracture performance by reducing its conductivity. The available model did not take this into account, but could theoretically be simulated using updated restart files with reduced fracture permeability through different years. This is a heavy process and would have taken too much time to perform in this thesis.

Non-Darcy pressure drop due to high flow rates was not accounted for. However, this was not likely to occur since the fluid flowing is viscous oil above the bubble point. The same goes for multiphase effects where the relative permeability decreases in a fracture due to gas presence. Since BHP limits was applied in the producer, keeping the pressure above the bubble point, gas was not present in the model. Therefore, such effects have minor implication on the result.

9. Conclusions

The aim of this thesis was to estimate the enhancement on production by hydraulic fracturing of parallel horizontal wells in a Talisman discovery. The reservoir consists of fluvial dominated geology and strongly varying permeability. The main objectives was to determine if the production could be estimated through numerical simulation, using available reservoir modelling tools, as well as to identify important factors affecting an optimised fracture setting in fluvial reservoirs.

Based on the results the following general conclusions can be made for a fluvial dominated reservoir and parallel hydraulically fractured horizontal wells:

- Numerical simulation of hydraulic fractures in a complex reservoir, using local grid refinement, is difficult due to long simulation time and excessive numerical problems caused by large amount of tight grid blocks.
- By using Petrel to create local grid refinements, the model needs to be manually edited in order to represent hydraulic fractures.
- By performing simplifications to the model, in terms of reducing the fracture permeability and activating inactive grid-blocks in the fracture area, results can be obtained.
- The reservoir used in this study is sensitive to small variations in permeability which indicate a potential for sufficient productivity enhancement from hydraulic fracturing.
- Flow barriers, mainly faults, rather than permeability variations, is the main factor affecting the communication between the fractures.
- Closely spaced fractures, either in the same or in different wells, can negatively affect oil production in terms of early water production and reduced sweep area between the wells.
- Long distance between fractures, either in the same or in different wells, can negatively affect early oil production due to delay in pressure communication and unswept areas between the fractures.
- Vertical communication is established by hydraulic fracturing in a fluvial reservoir, but uncertainty exists in fracture height and length.
- Changes in fracture length do not affect the production unless the fracture spacing becomes too narrow.
- Optimal distances are evident from the study, but due the reservoir complexity these will vary throughout the field.
- Small changes in injection pressure do not significantly affect optimal fracture distance.
- High, early oil production rates in hydraulic fractured wells are critical in fluvial dominated reservoirs to achieve an optimal recovery.

Based on these points, it has been shown that hydraulic fracturing can severely increase the production of a fluvial dominated reservoir, if the fracture placement is optimised, in terms of fracture communication, flow restrictions and permeability contrasts. Multiple hydraulic fracturing of two parallel horizontal wells, one injector and one producer, can increase the oil production with at least 400 000 Sm^3 (2.5 million Sbbl) during a period of 5 years, in the Talisman discovery.

10. Recommendations for further work

- A full field study containing many multiple fractured wells should be performed to capture the interference between all wells and to get an overall volume.
- Simpler methods for representation of hydraulic fractures should be tested and compared to the LGR method applied in this thesis. If small changes in result are evident, a larger fracture permeability value could be used to give productivity estimates.
- Fracture modelling, trying to determine the maximum shale thickness which can be fractured, should be performed and then place the fractures in such areas.
- Effects as thermal fracturing, filtrate cleanup and stress changes around the fractures could be incorporated to increase the accuracy of the results.
- LGR should be created between the wells to get more accurate knowledge of fluid movement in the analyses.
- Varying distances between the wells should be investigated to determine any relationship between fracture spacing and well spacing.
- The fracture analysis should be performed in regions having larger permeability contrasts to get more distinct results and more general conclusions.
- Establishment of an understanding of fracture propagation across faults would be important in this reservoir.
- Effect of inactive grid blocks and flow barriers on production and fracture distance should be investigated by running simulations where all blocks were activated.

References

[1] Clark, J.B.; *"A Hydraulic Process for Increasing the Productivity of Wells"*, 1949, SPE 949001

[2] <www.britannica.com>, Keyword search: "calcrete" [Downloaded 07.05.2011]

[3] Economides, M.J., Nolte, K.G.; *"Reservoir Stimulation, Third Edition"*, Wiley, England, 2000

[4] Lake, L.W., Clegg, J.D.; *"Petroleum Engineering Handbook Volume 4: Production Operations Engineering, Chapter 8: "Hydraulic Fracturing"*, Holditch, S.A., SPE, 2007

[5] Fjær, E., Holt, R.M, Horsrud, P., Raaen, A.M., Risnes, R.; *"Petroleum Related Rock Mechanics – 2nd Edition"*, Elsvier, Netherland, 2008

[6] Schlumberger presentations by Mark Norris on the Hydraulic Fracturing Seminar at the Oil Museum in Stavanger, 30th November 2010

[7] Norris, M.R., Berntsen, B.A., Myhre, P., Winters, W.J.; *"Multiple Proppant Fracturing of a Horizontal Wellbore: an integration of two techniques"*, SPE 36899, 1996

[8] Valkó, P., Economides, M.J.; *"Hydraulic Fracture Mechanics"*, Wiley, England, 1995

[9] Myrvang, A.; *"Bergmekanikk"*, NTNU, Trondheim, 2001

[10] Brown, J.E.; Economides, M.J.; *"An Analysis of Hydraulically Fractured Horizontal Wells"*, SPE 24322, 1992

[11] Olsen, K.E., Haidar, S., Milton-Tayler, D., Olsen, E.; *"Multiphase Non-Darcy Pressure Drop in Hydraulic Fracturing"*, SPE 90406, 2004

[12] Davies, D.R., Kuiper, T.O.H.; *"Fracture Conductivity in Hydraulic Fracture Stimulation",* Journal of Petroleum Technology, p.550-552, May 1988

[13] Sadrapanah, H., Charles, T., Fulton, J.; *"Explicit Simulation of Multiple Hydraulic Fractures in Horizontal Wells"*, SPE 99575, 2006

[14] Soleimani, A., Lee, B., Ghuwaidi, Y., Dyer, S.; *"Numerical Modelling of Multiple Hydraulically Fractured Horizontal Wells"*, SPE 120552, 2009

[15] Hegre, T.M.; *"Hydraulically Fractured Horizontal Well Simulation"*, SPE 35506, 1996

[16] Ehrl, E., Schueler, S.K.; *"Simulation of a Tight Gas Reservoir with Horizontal Multifractured Wells"*, SPE 65108, 2000

[17] Ding, Y.; *"Modelling of Fractured Wells in Reservoir Simulation"*, SPE 36668, 1996

[18] Fjerstad, P.A., Sikandar, A.S., Cao, H., Liu, J., Da Sie, W.;"*Next Generation Parallel Computing for Large-Scale Reservoir Simulation"*, SPE 97358, 2008

[19] Iwere, F.O., Moreno, J.E., Apaydin, O.G.; *"Numerical Simulation of Thick, Tight Fluvial Sands"*, SPE 90630, 2006

[20] Y. Abacioglu, Sebastian, H.M., Oluwa, J.B.; "*Advancing Reservoir Simulation Capabilities for Tight Gas Reservoirs"*, SPE 122793, 2009

[21] Soliman, M.Y., Hunt, J.L., El Rabaa, A.M.; *"Fracturing Aspects of Horizontal Wells"*, SPE 18542, 1990

[22] Al-Kobaisi, M., Ozkan, E., Kazemi, H.; *"A Hybrid Numerical/Analytical Model of a Finite-Conductivity Vertical Fracture Intercepted by a Horizontal Well"*, SPE 92040, 2006

[23] Karcher, B.J., Giger, F.M., Combe, J.; *"Some Practical Formulas to Predict Horizontal Well Behaviour"*, SPE 15430, 1986

[24] Schulte, W.M.; "*Production From a Fractured Well With Well Inflow Limited to Part of the Fracture Height"*, SPEPE, p. 333-343, 1986

[25] Larsen, L., Hegre, T.M.; *"Pressure Transient Analysis of Multifractured Horizontal Wells",* SPE 28389, 1994

[26] Wan, J., Aziz, K.; *"Semi-Analytical Well Model of Horizontal Wells With Multiple Hydraulic Fractures"*, SPE 81190, 2002

[27] Paceman, D.W.; *"Interpretation of Well-Block Pressures in Numerical Reservoir Simulation with Non-Square Grid Blocks and Anisotropic Permeability"*, SPE 10528, 1983

[28] Lolon, E.P., Shaoul, J.R., Mayerhofer, M.J.; *"Application of 3-D Reservoir Simulator for Hydraulically Fractured Wells"*, SPE 110093, 2007

[29] Shaoul, J.R., Behr, A.; *"Developing a Tool for 3D Reservoir Simulation of Hydraulically Fractured Wells"*, IPTC 10182, 2005

[30] Miranda, C., Soliman, M.Y., Settari, A., Krampol, R.; *"Linking Reservoir Simulators with Fracture Simulators"*, SPE 137752, 2010

[31] PETREL manual

[32] ECLIPSE manual

[33] Discussions with Schlumberger consultants and Petrel support.

Nomenclature

Symbols

Δp_s	=	Skin pressure drop
q	=	Flow rate
μ	=	Viscosity
S	=	Skin factor
k	=	Formation permeability
h	=	Formation height
$\bar{p}$	=	Average reservoir pressure
p_{wf}	=	Bottom hole flowing pressure
r_e	=	Reservoir radius
r_w	=	Wellbore radius
F_c	=	Fracture conductivity
F_{cD}	=	Dimensionless fracture conductivity
k_f	=	Fracture permeability
x_f	=	Fracture half-length
h_f	=	Propped fracture height
w	=	Propped fracture width
σ_h	=	Minimum horizontal stress
σ_H	=	Maximum horizontal stress
σ_v	=	Vertical overburden stress
υ	=	Poisson's ratio
k_G	=	Grid permeability
w_G	=	Grid width

d = Wellbore longitudinal distance between two transverse hydraulic fractures in each parallel horizontal well

s = Wellbore longitudinal distance between two transverse hydraulic fractures in the same horizontal well

Abbreviations

ESP	=	Electric Submersible Pumps
LGR	=	Local Grid Refinement
ECD	=	Equivalent Circulating Density
PI	=	Productivity Index
PEBI	=	Perpendicular Bisector
STOOIP	=	Stock-Tank Oil Originally In Place
BHP	=	Bottom-hole pressure
MD	=	Measured Depth
TVD	=	True Vertical Depth

Units

mD	=	milli-Darcy
Sm^3	=	Standard cubic meters
Sbbl	=	Standard barrels
d	=	Days

Appendix A: Results from Scenario 1

A.1 Water saturation profiles for different formation permeability

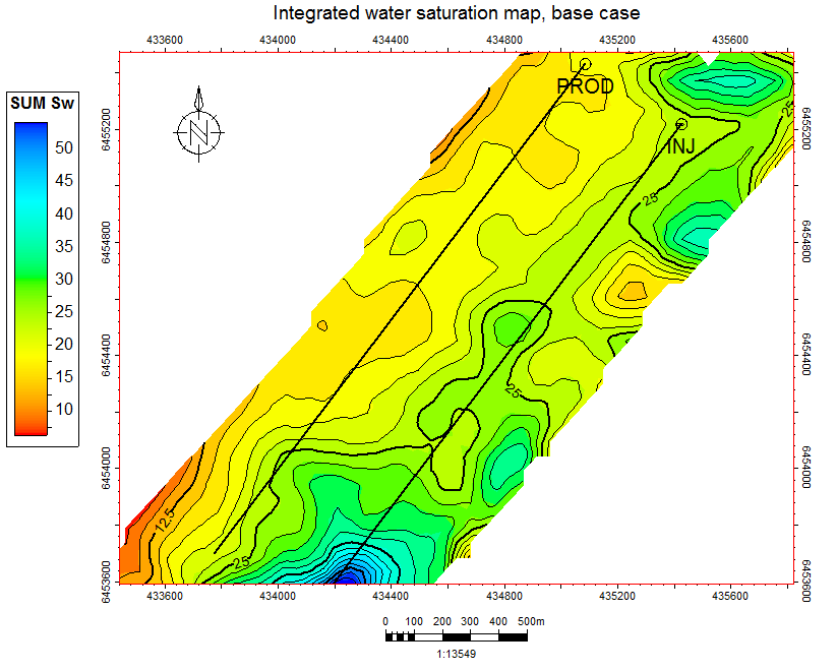

Figure A-1: Water saturation profile after 3 years for base case run.

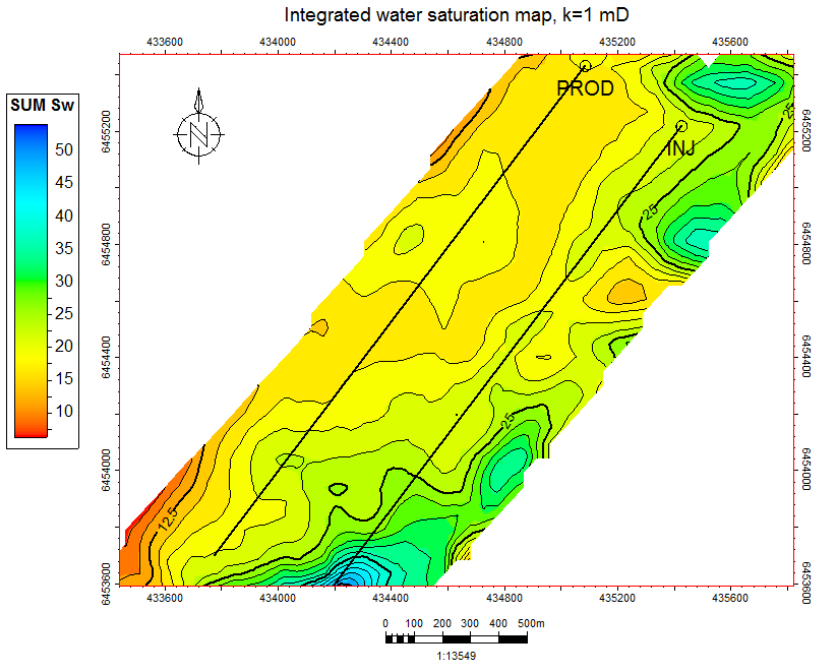

Figure A-2: Water saturation profile after 3 years for 1 mD run.

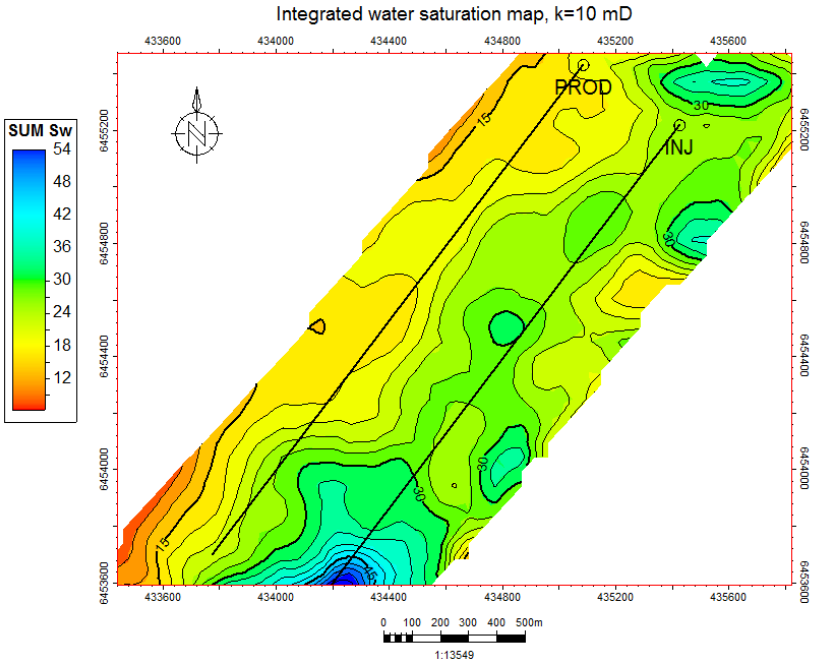

Figure A-3: Water saturation profile after 3 years for 10 mD run.

Appendix B: Results from Scenario 2

B.1 Horizontal water saturation profiles for Case 1

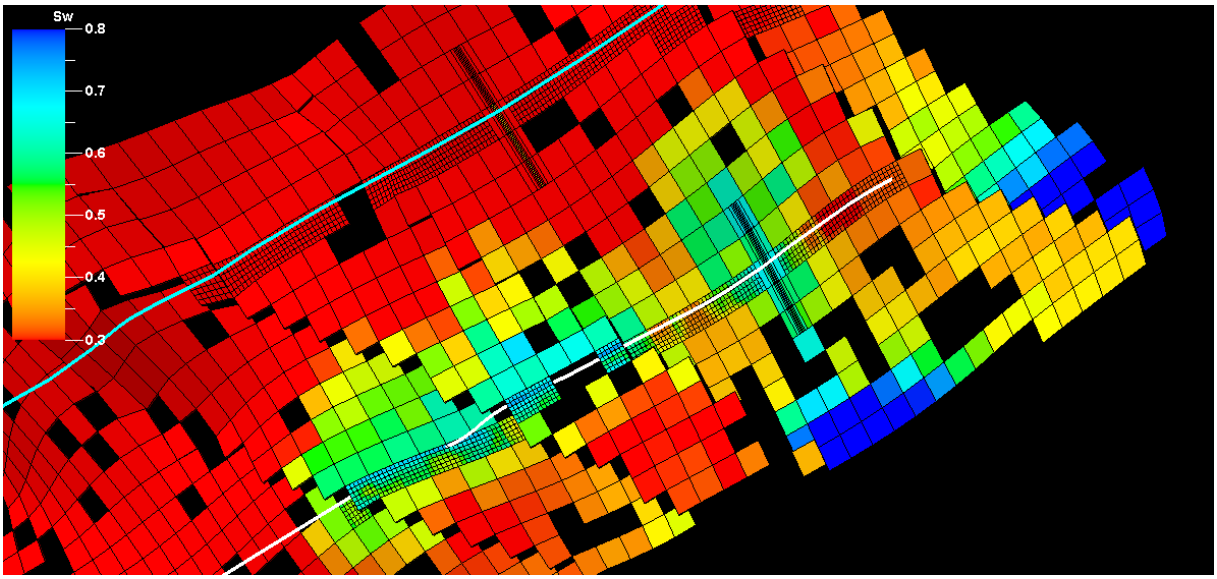

Figure B-1: Water saturation profile after 2 years along plane K=89 for d=300m.

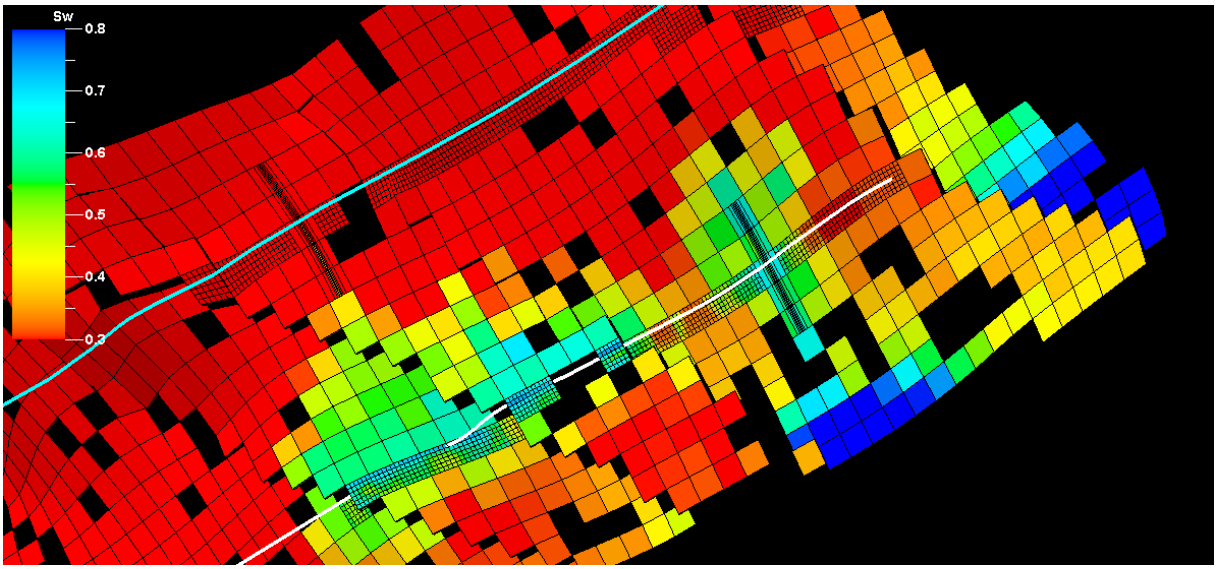

Figure B-2: Water saturation profile after 2 years along plane K=89 for d=700m.

B.2 Vertical water saturation profiles for Case 1

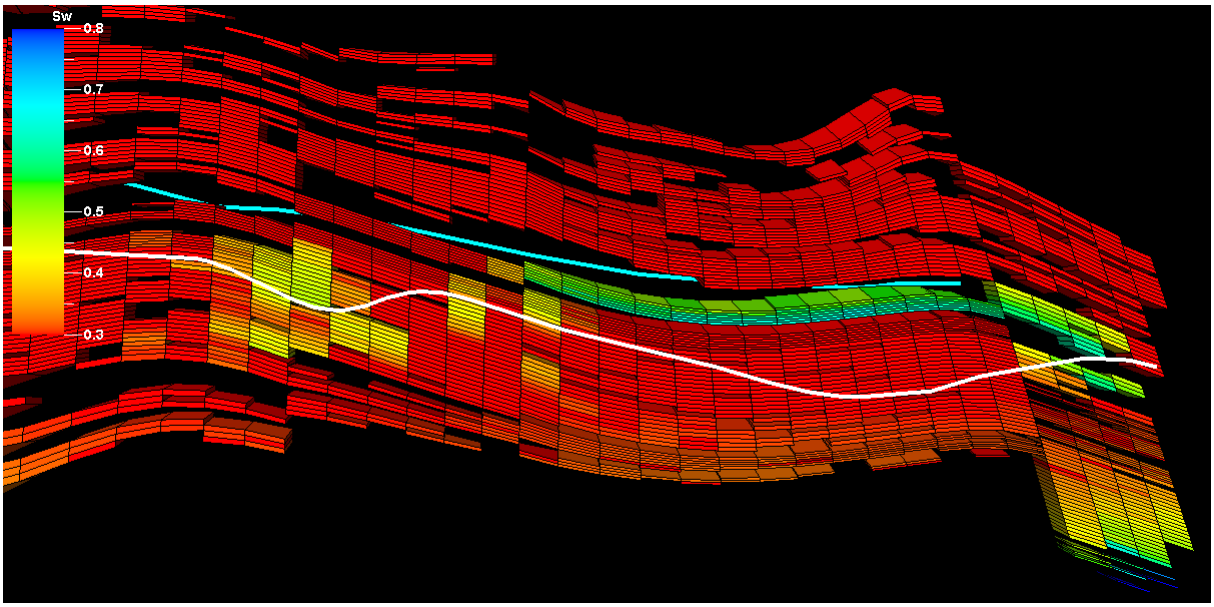

Figure B-3: Water saturation profile after 3 years along plane J=63 for non-fractured case.

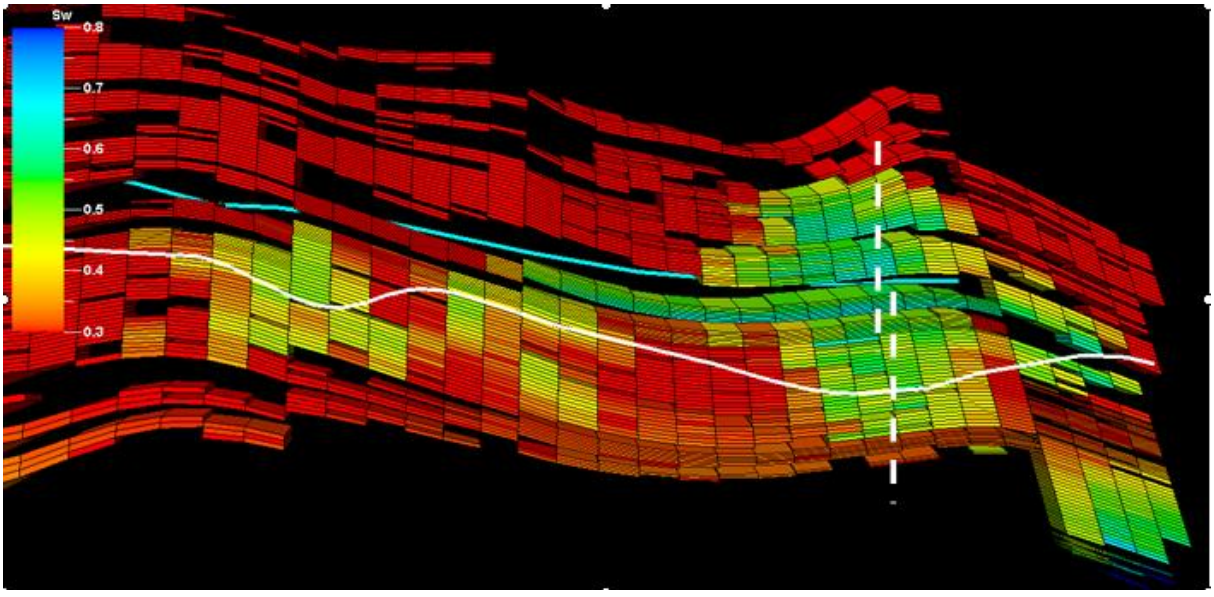

Figure B-4: Water saturation profile after 3 years along plane J=63 for d=0m.

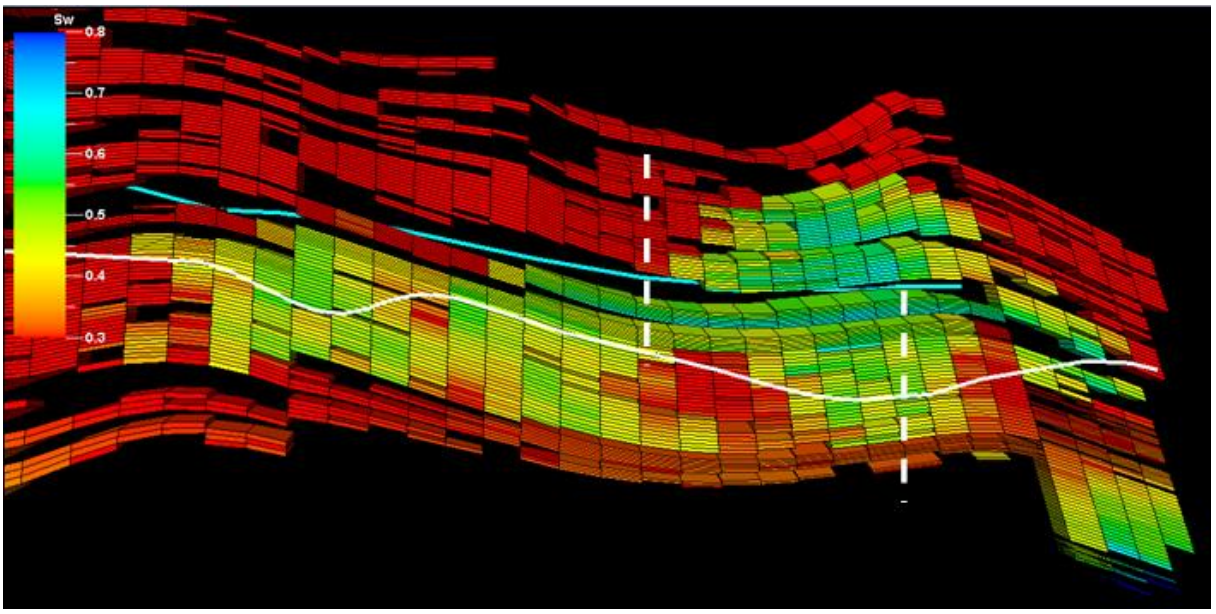

Figure B-5: Water saturation profile after 3 years along plane J=63 for d=300m.

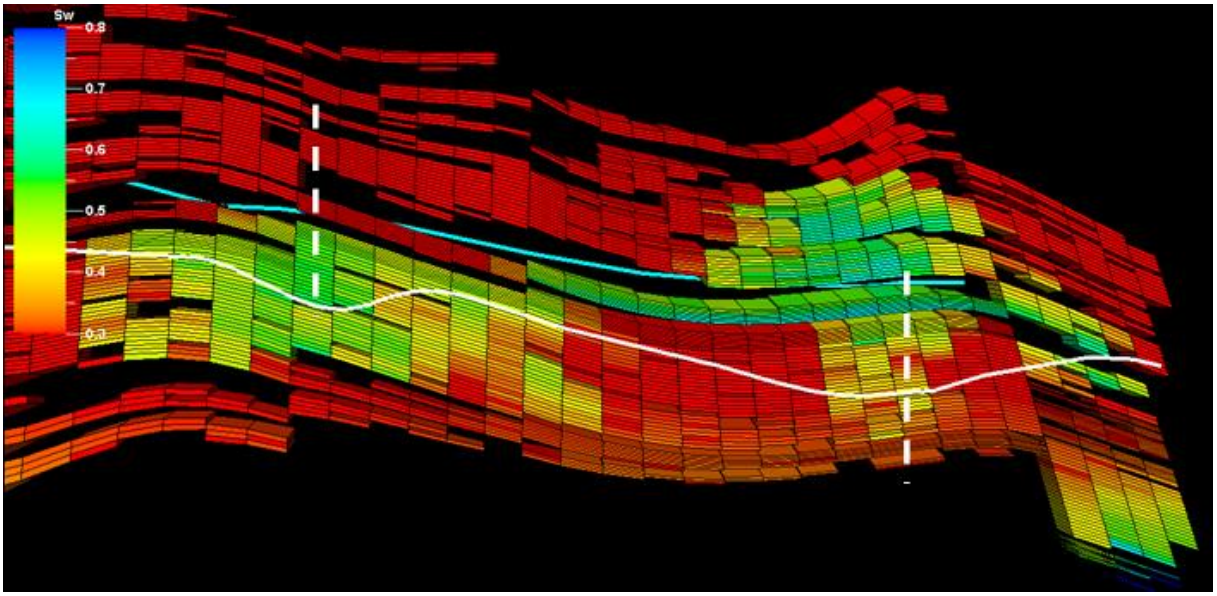

Figure B-6: Water saturation profile after 3 years along plane J=63 for d=700m.

B.3 Horizontal pressure profiles for Case 1

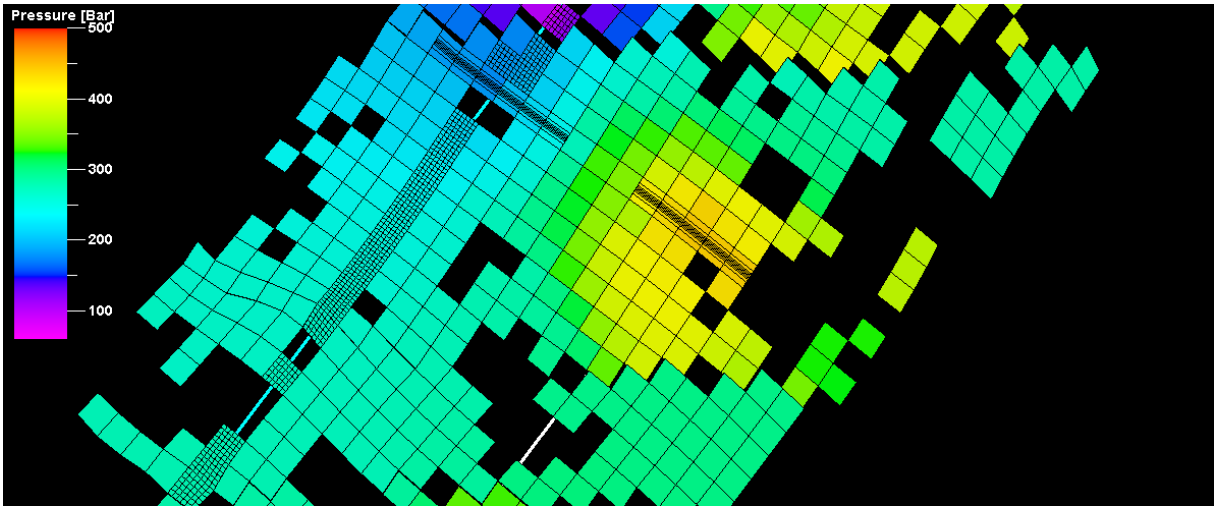

Figure B-7: Pressure profile after 3 years along horizontal plane K=47 for d=0m.

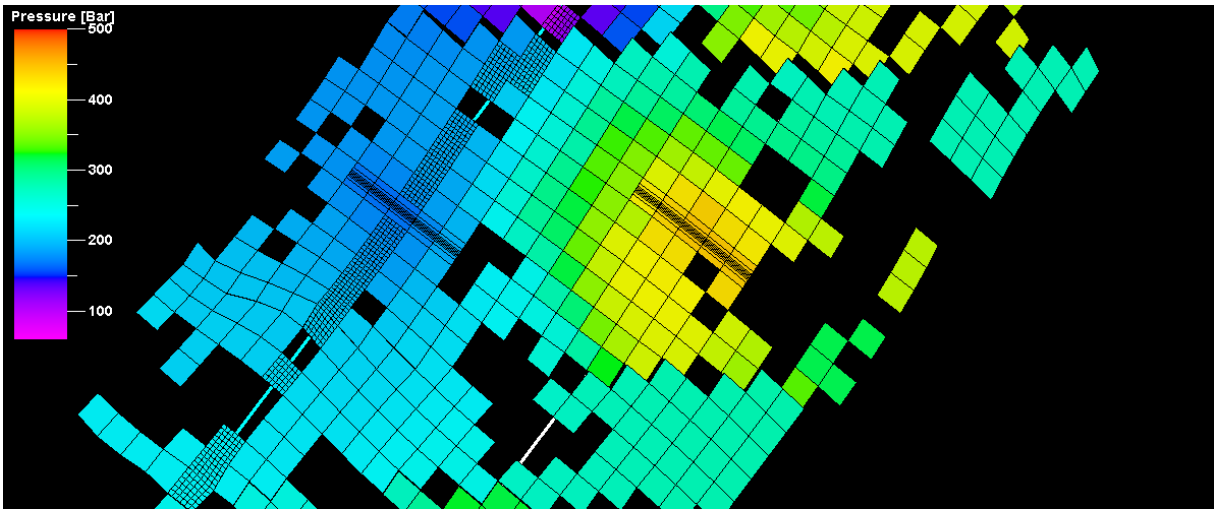

Figure B-8: Pressure profile after 3 years along horizontal plane K=47 for d=300m.

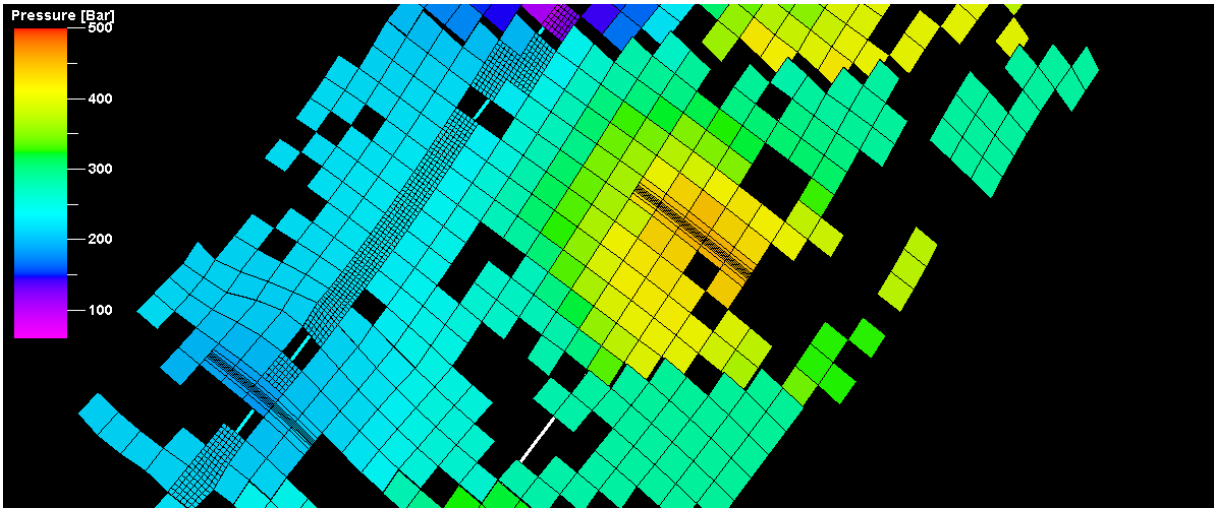

Figure B-9: Pressure profile after 3 years along horizontal plane K=47 for d=700m.

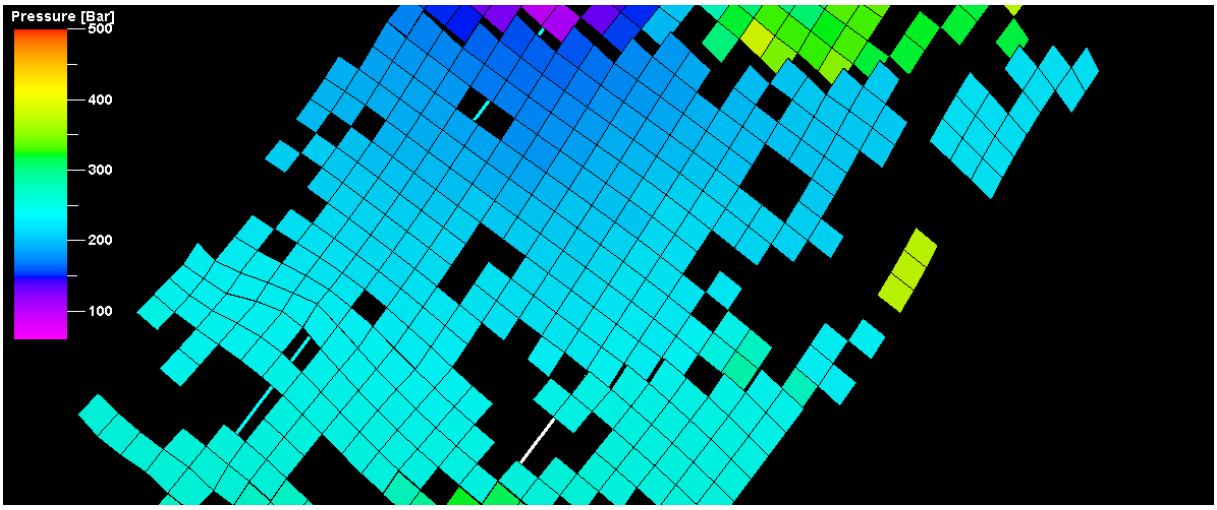

Figure B-10: Pressure profile after 3 years along horizontal plane K=47 for non-fractured run.

B.4 Effect of reversed fracture setting on oil production in Case 2

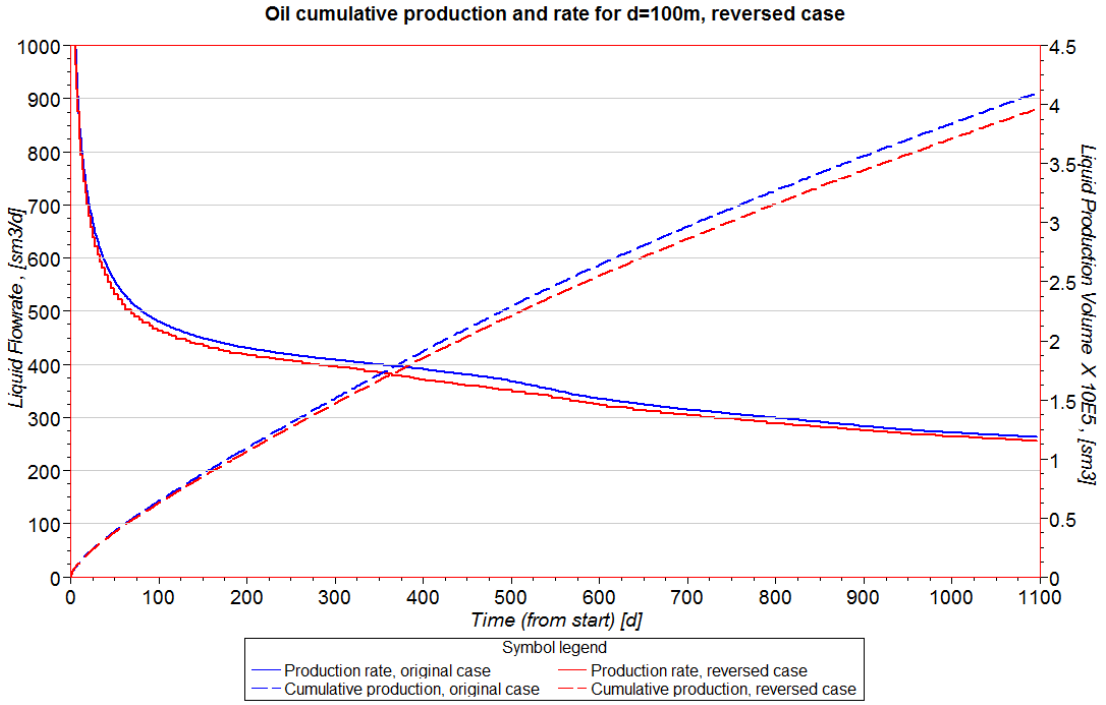

Figure B-11: Effect of moving injecting or producing fracture for d=100m.

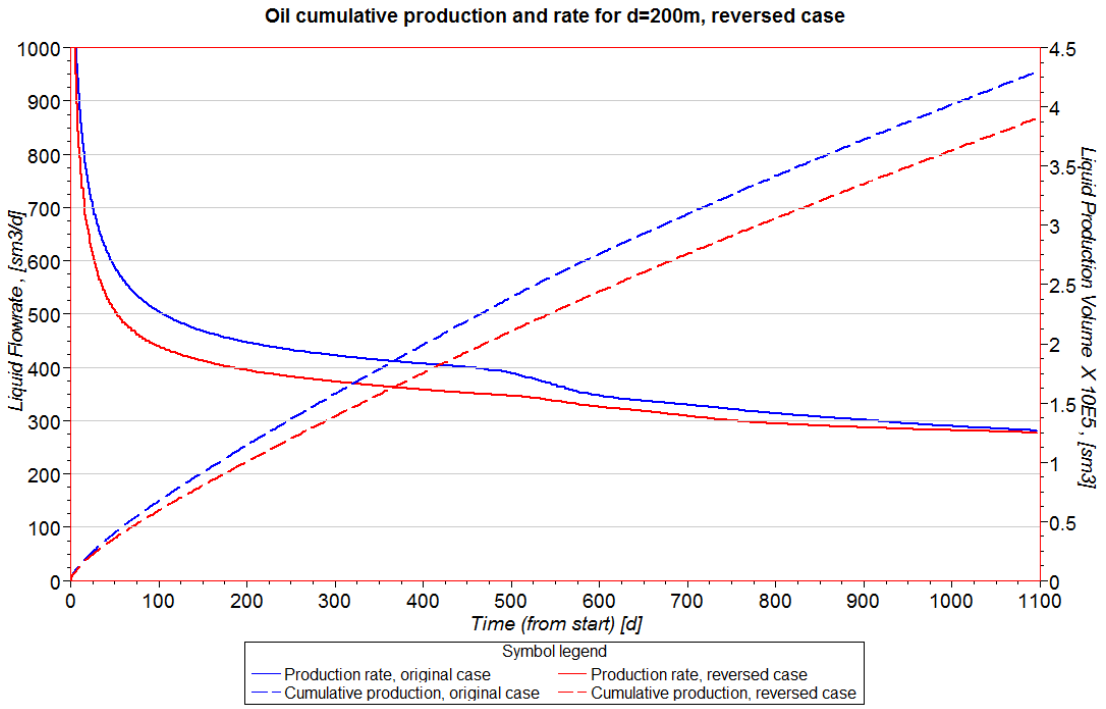

Figure B-12: Effect of moving injecting or producing fracture for d=200m.

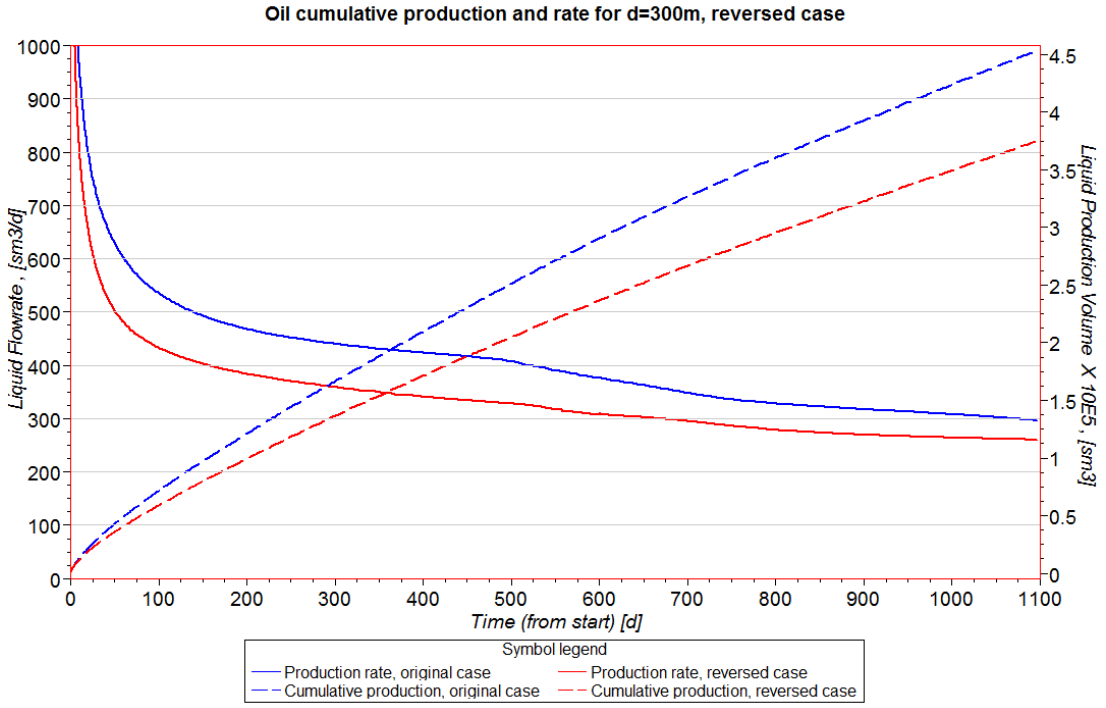

Figure B-13: Effect of moving injecting or producing fracture for d=300m.

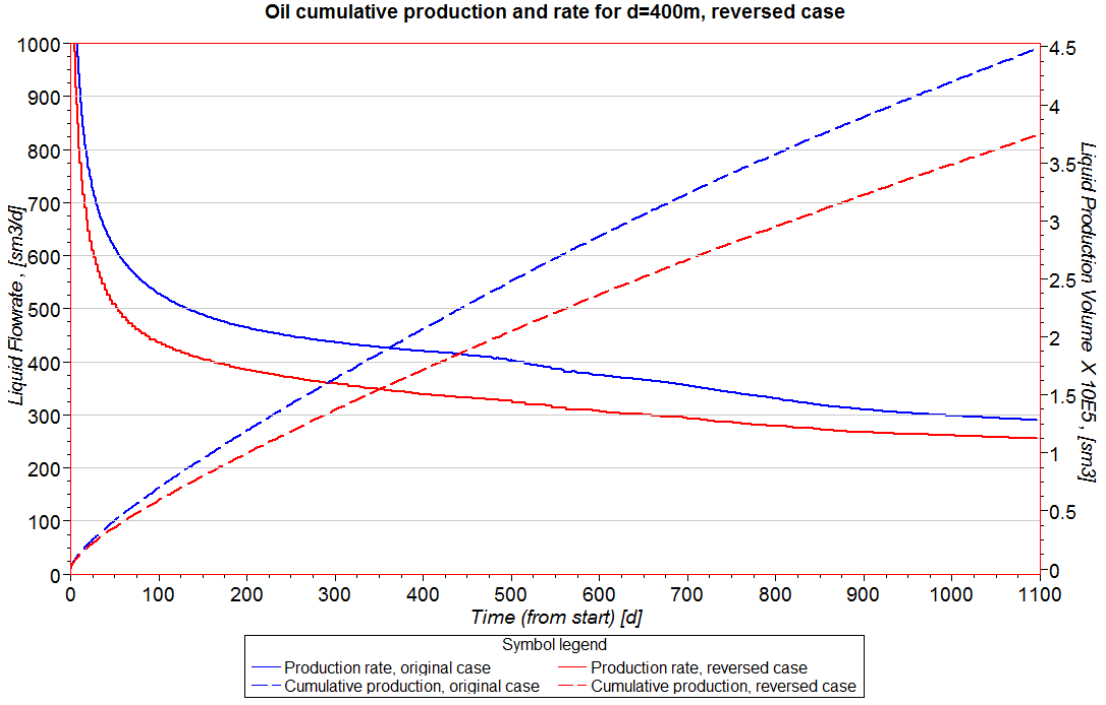

Figure B-14: Effect of moving injecting or producing fracture for d=400m.

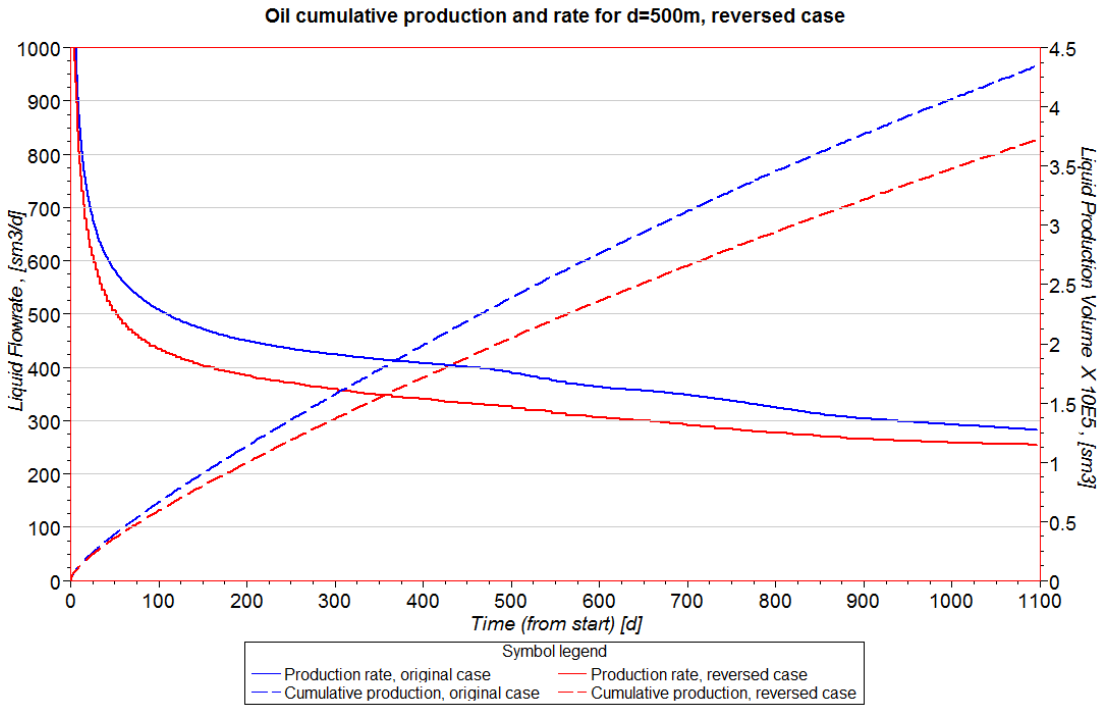

Figure B-15: Effect of moving injecting or producing fracture for d=500m.

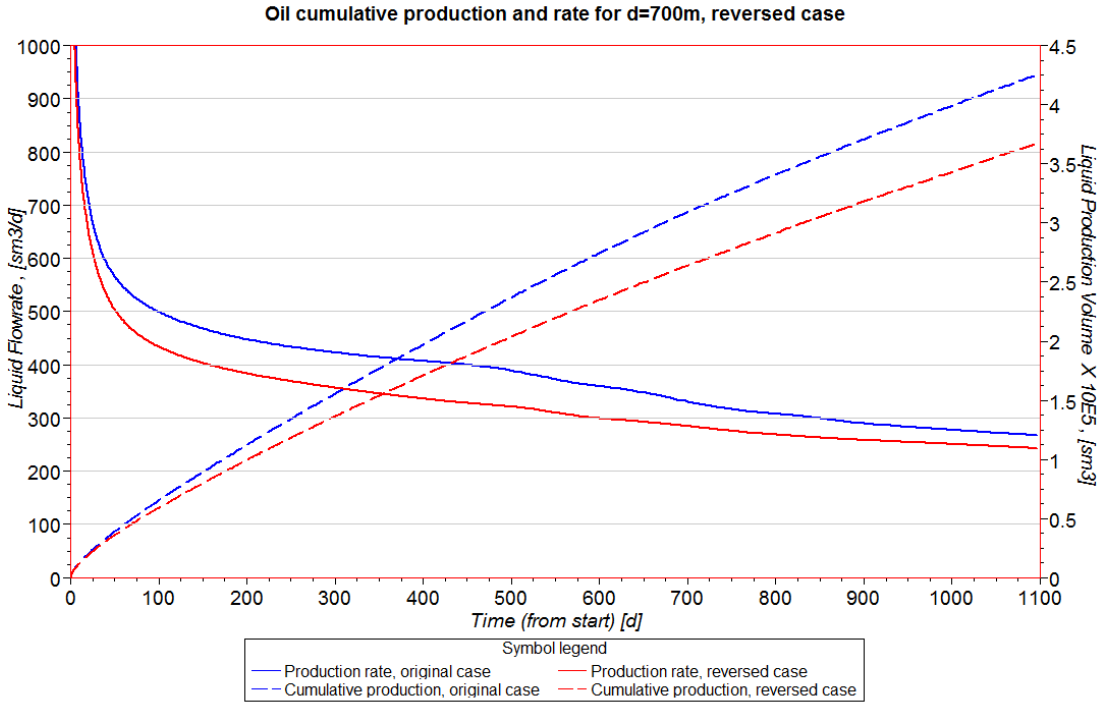

Figure B-16: Effect of moving injecting or producing fracture for d=700m.

B.5 Sensitivity to injection to bottom hole pressure in Case 5

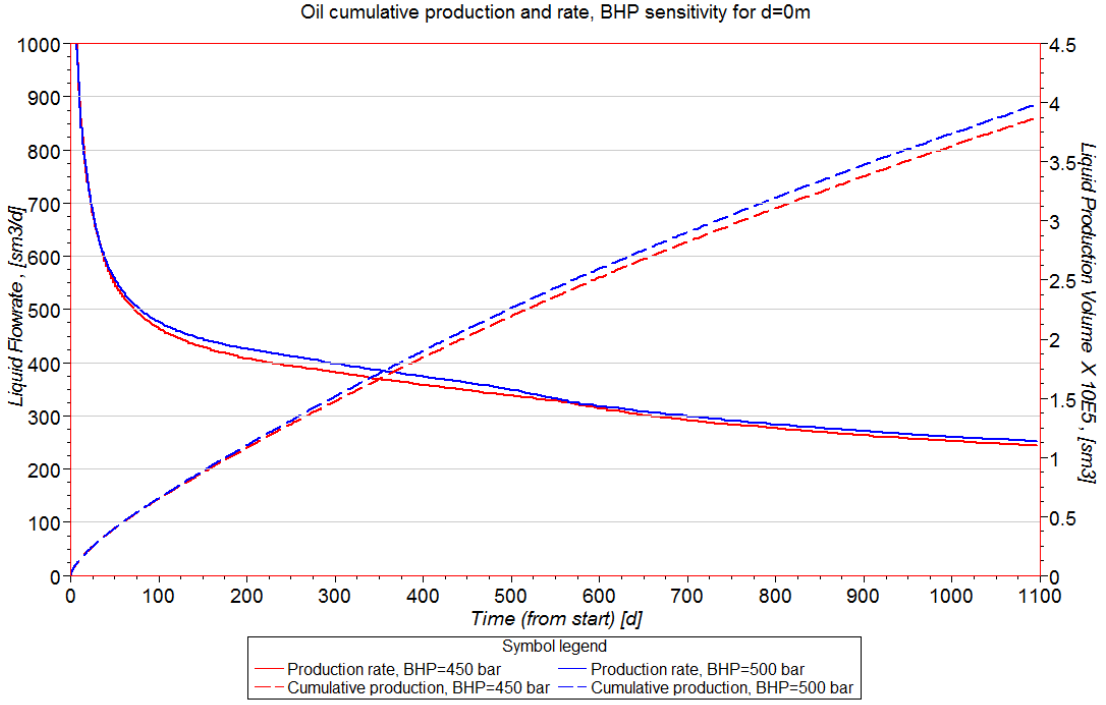

Figure B-17: Comparison of 500 and 450 bars injection pressure for d=0m.

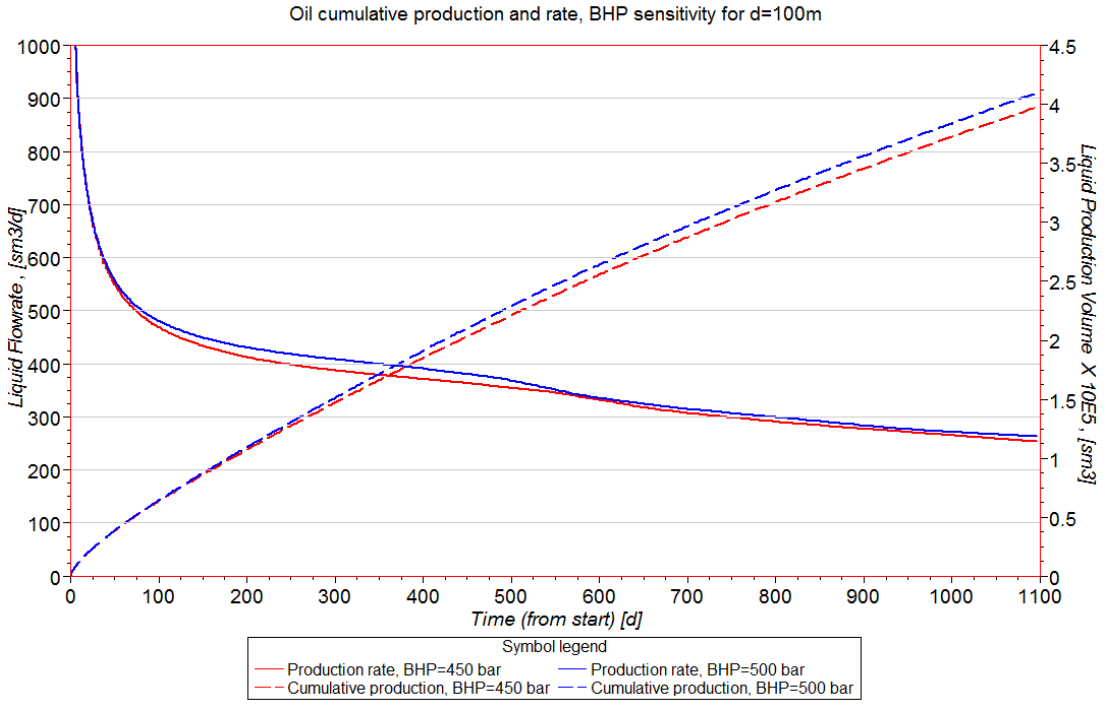

Figure B-18: Comparison of 500 and 450 bars injection pressure for d=100m.

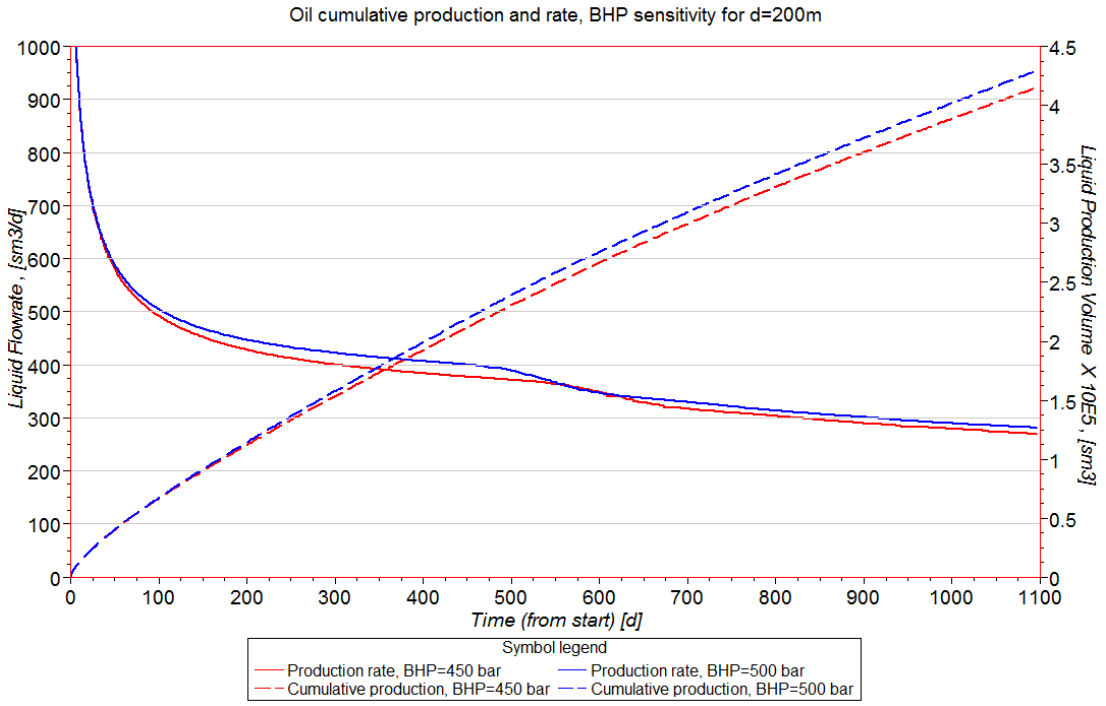

Figure B-19: Comparison of 500 and 450 bars injection pressure for d=200m.

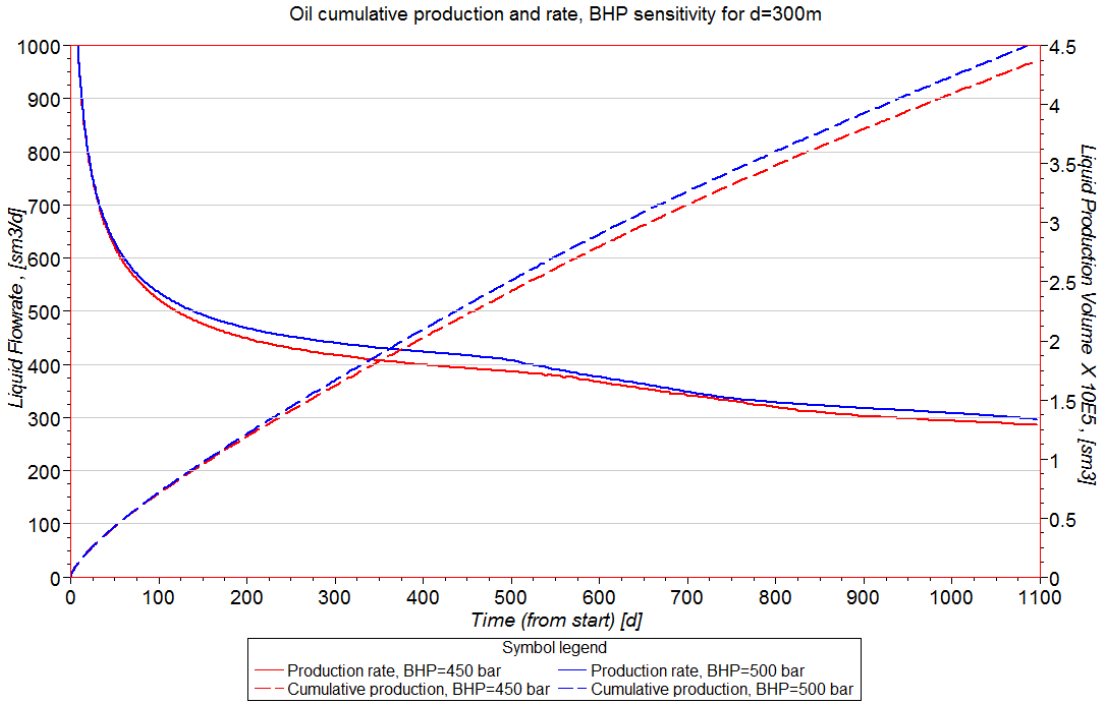

Figure B-20: Comparison of 500 and 450 bars injection pressure for d=300m.

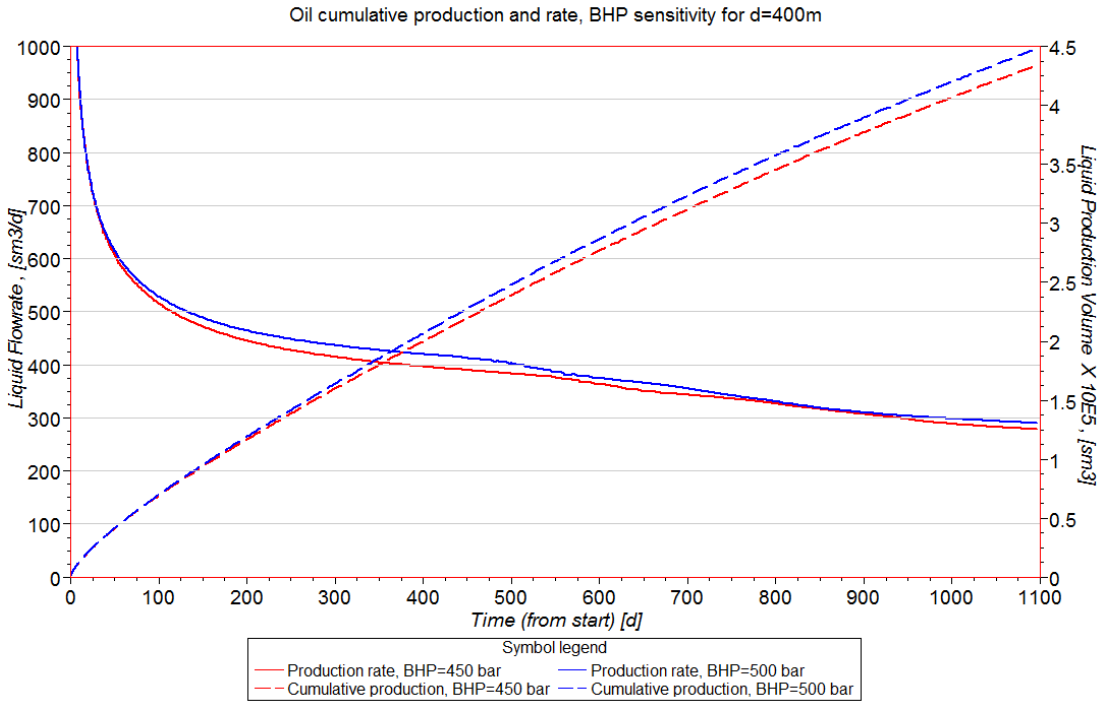

Figure B-21: Comparison of 500 and 450 bars injection pressure for d=400m.

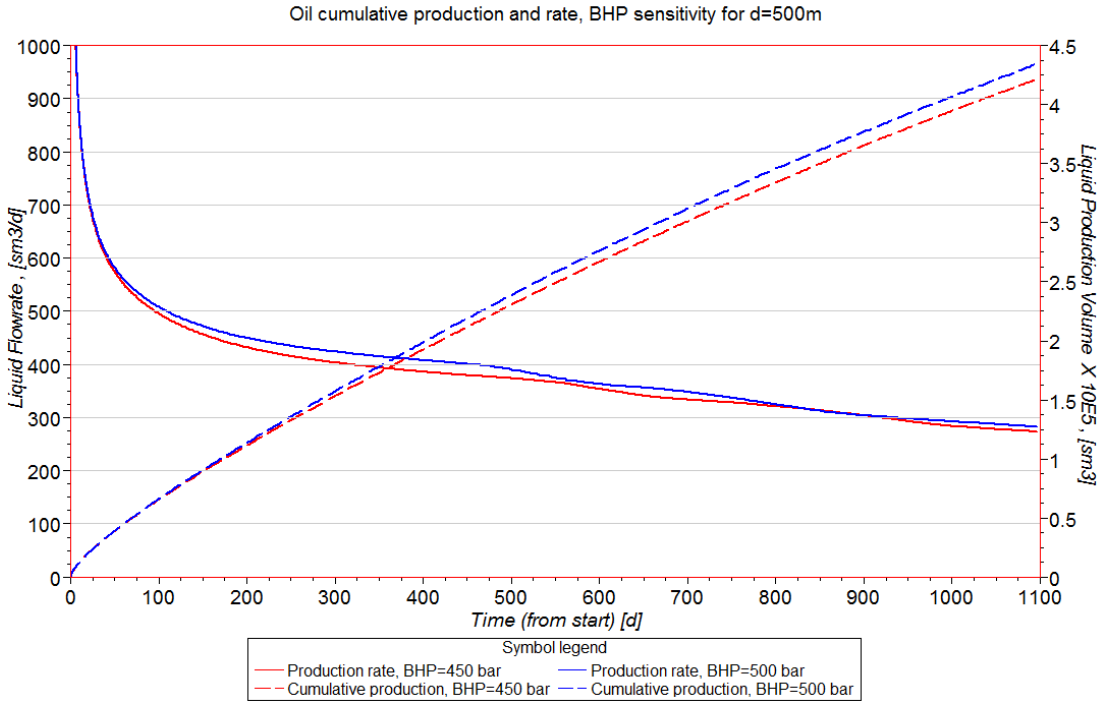

Figure B-22: Comparison of 500 and 450 bars injection pressure for d=500m.

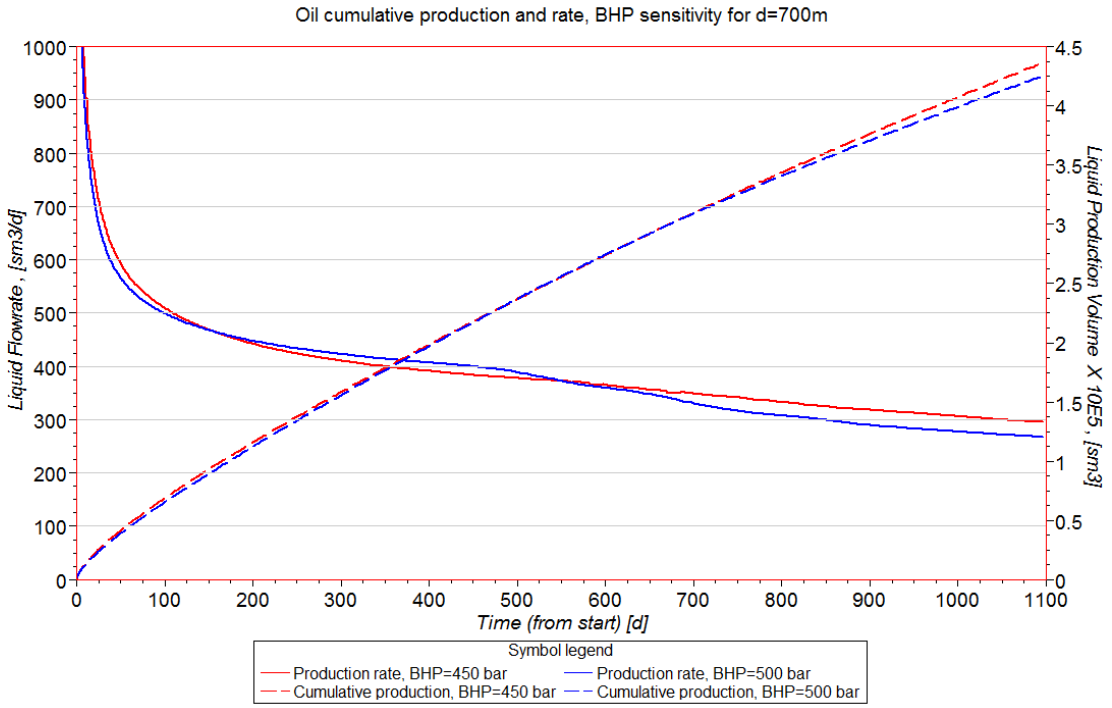

Figure B-23: Comparison of 500 and 450 bars injection pressure for d=700m.

Appendix C: Results from Scenario 3

C.1 Saturation maps for different fracture spacing in the injector

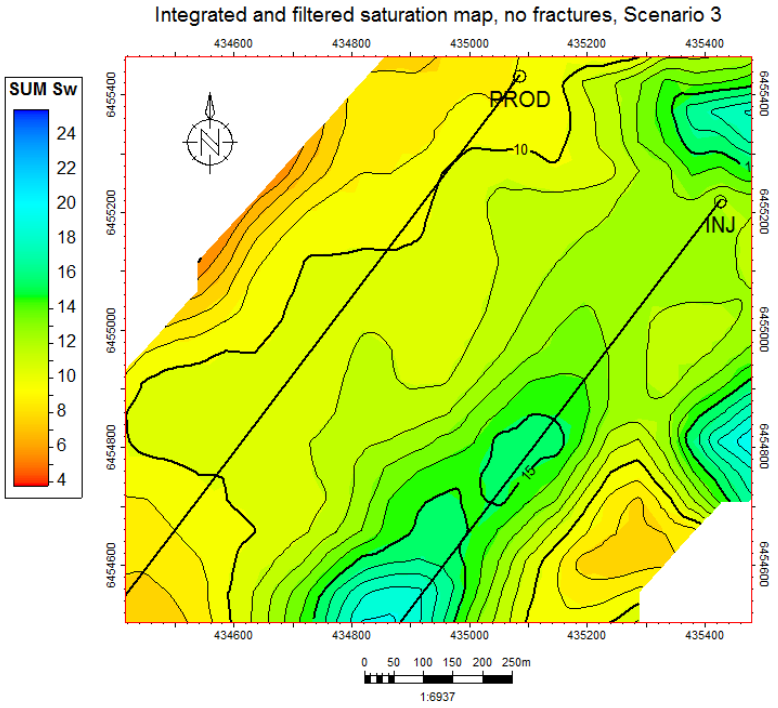

Figure C-1: Integrated saturation map after 3 years for non-fractured run.

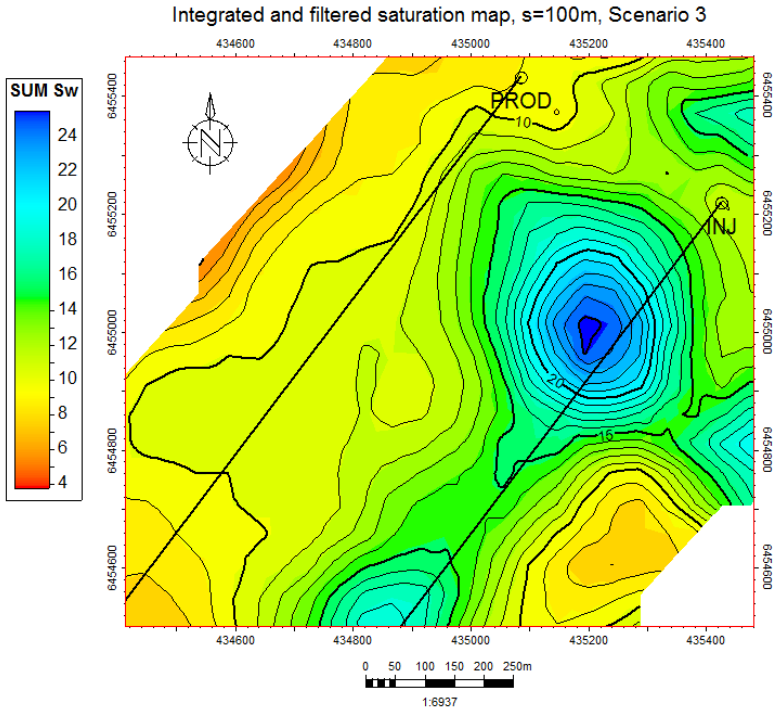

Figure C-2: Saturation map after 3 years for s=100m.

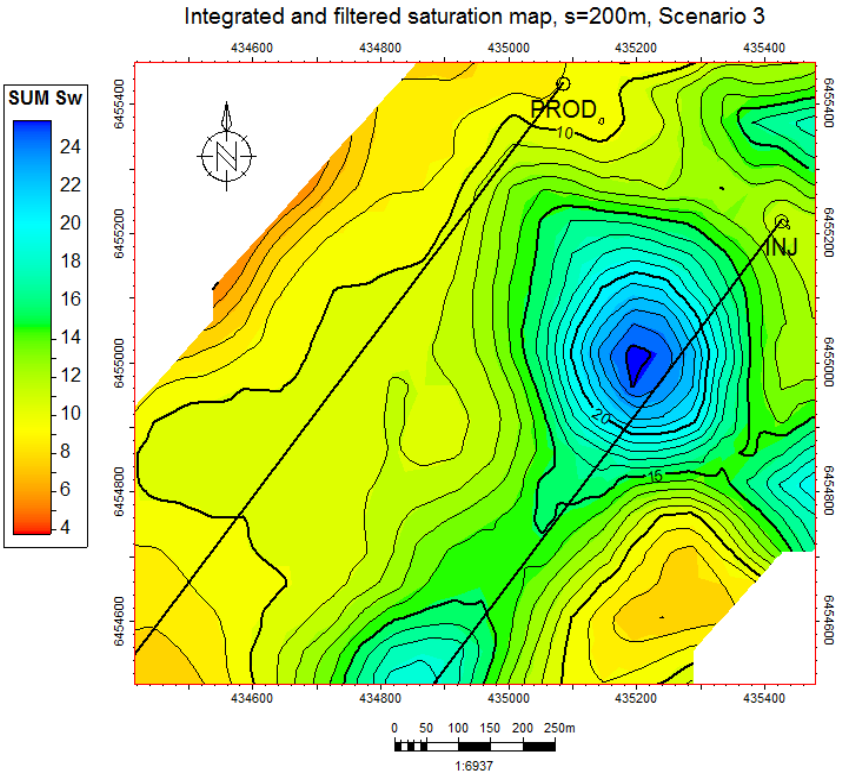

Figure C-3: Integrated saturation map after 3 years for s=200m.

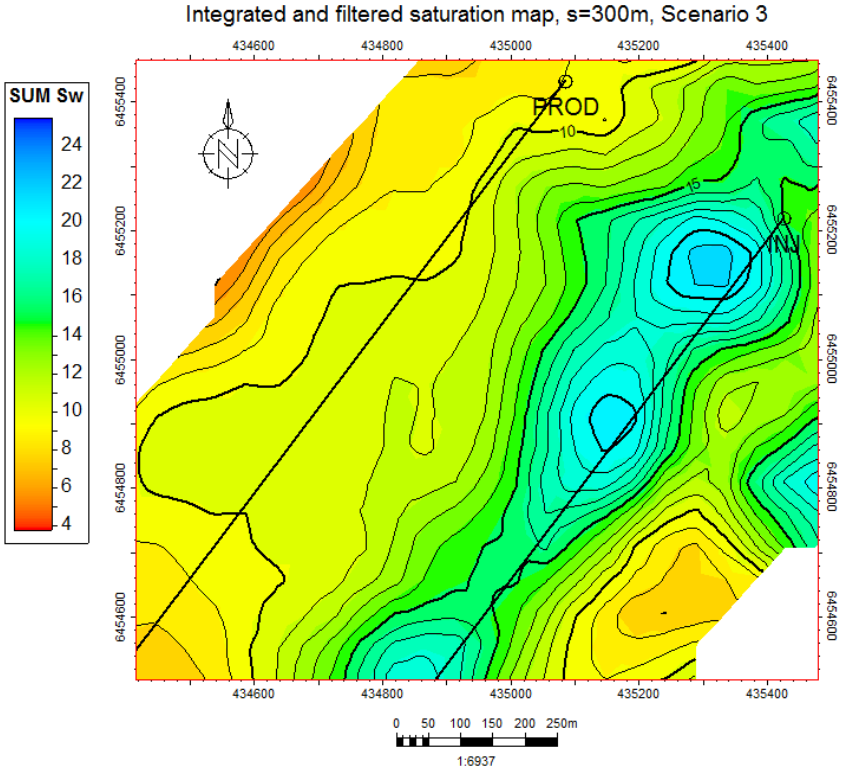

Figure C-4: Integrated saturation map after 3 years for s=300m.

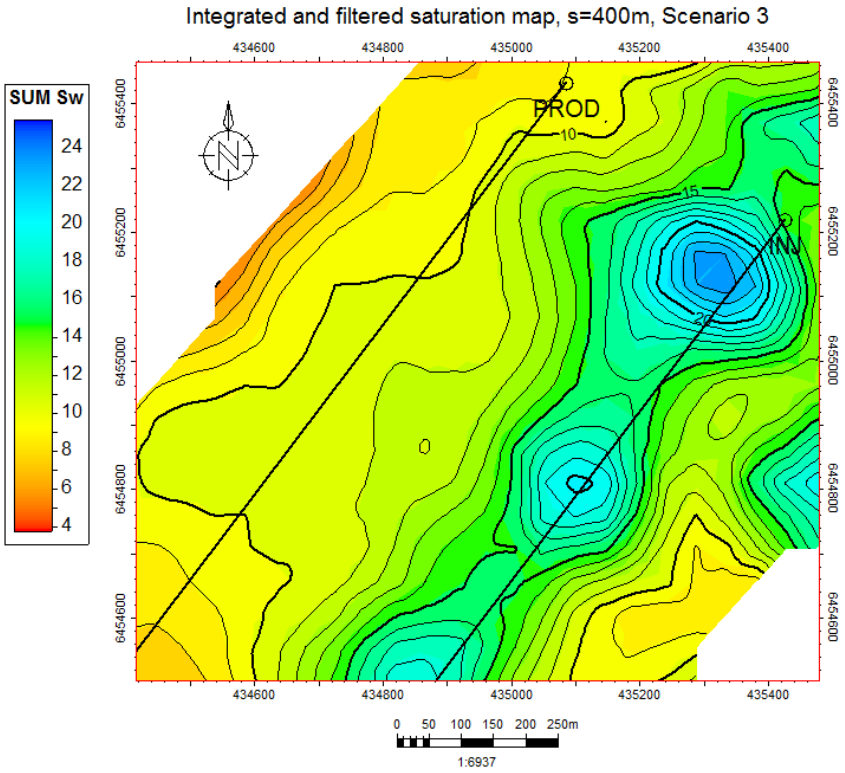

Figure C-5: Integrated saturation map after 3 years for s=400m.

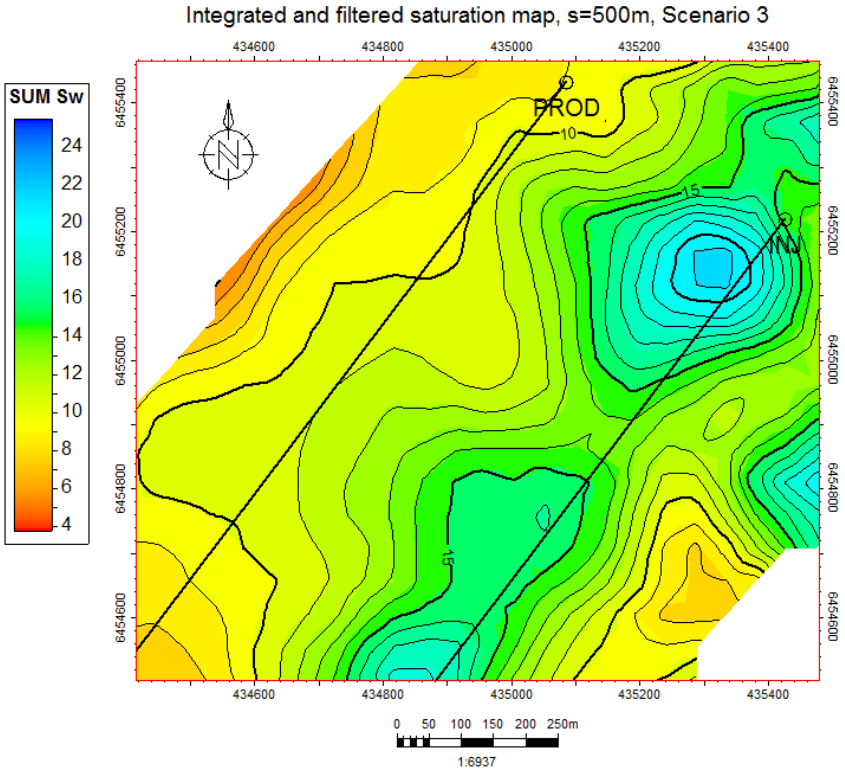

Figure C-6: Integrated saturation map after 3 years for s=500m.

Appendix D: Results from Scenario 4

D.1 Average pressure profile for different fracture spacing in the producer

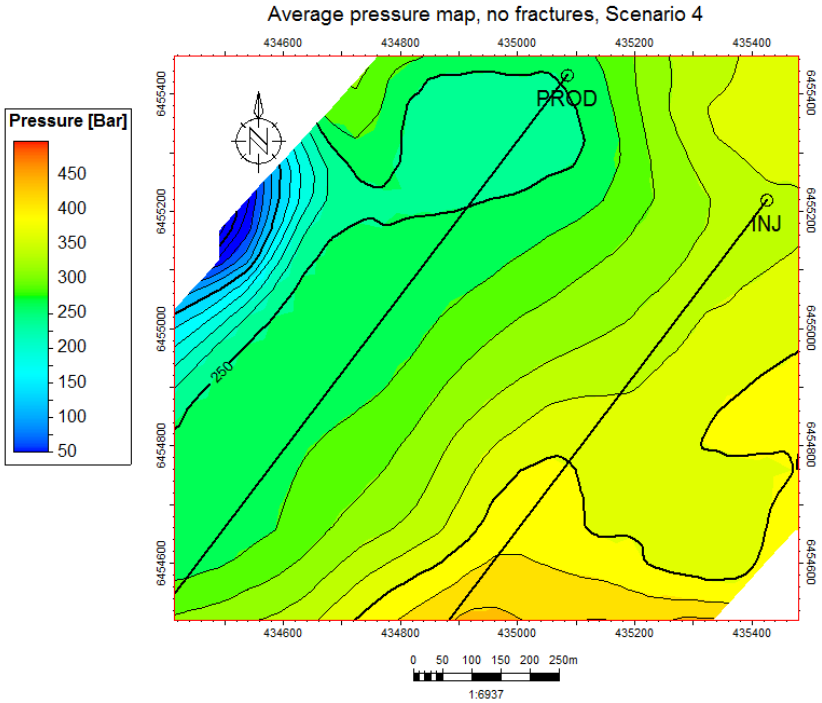

Figure D-1: Average pressure map after 3 years for non-fractured case.

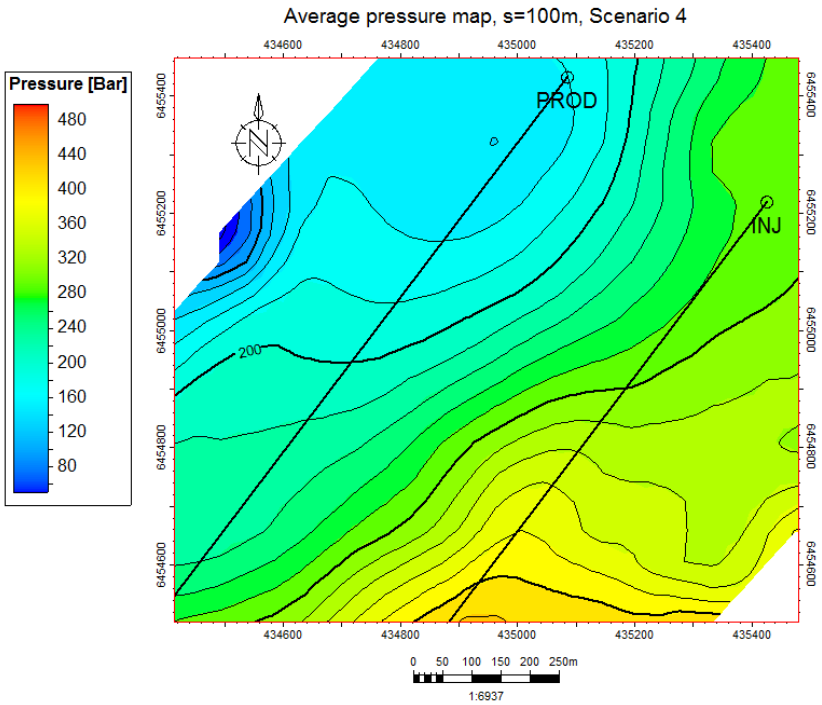

Figure D-2: Average pressure after 3 years map for s=100m.

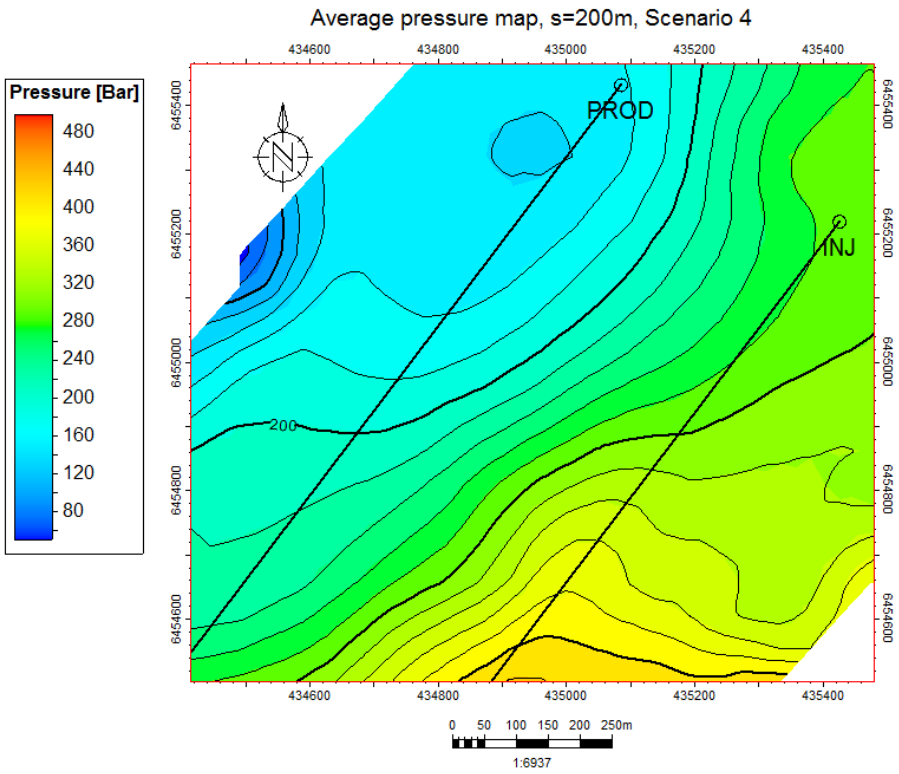

Figure D-3: Average pressure map after 3 years for s=200m.

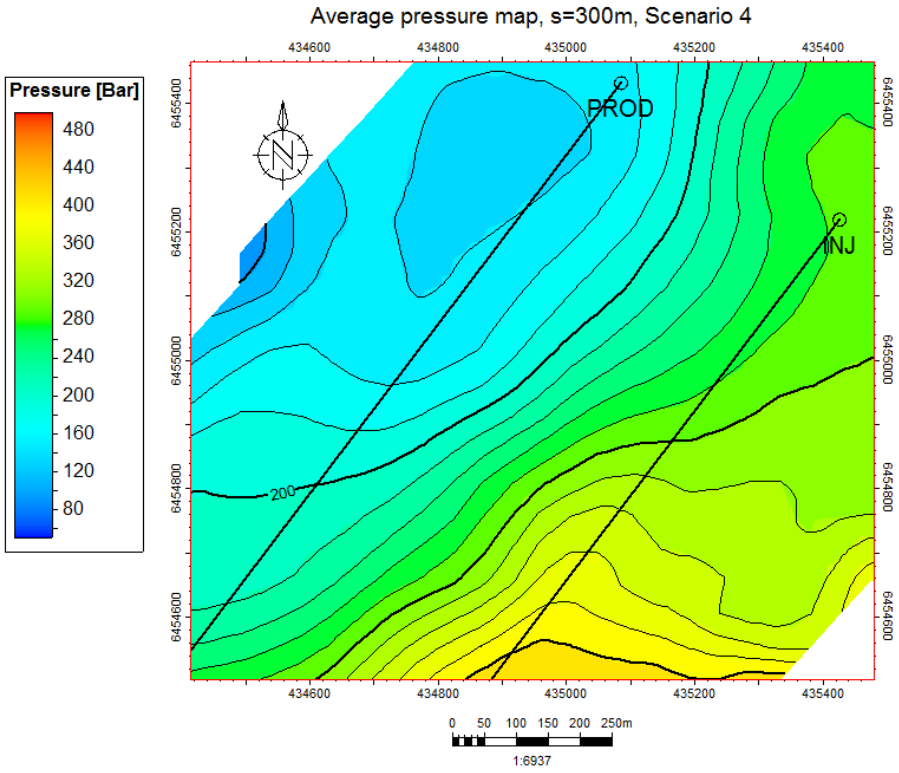

Figure D-4: Average pressure map after 3 years for s=300m.

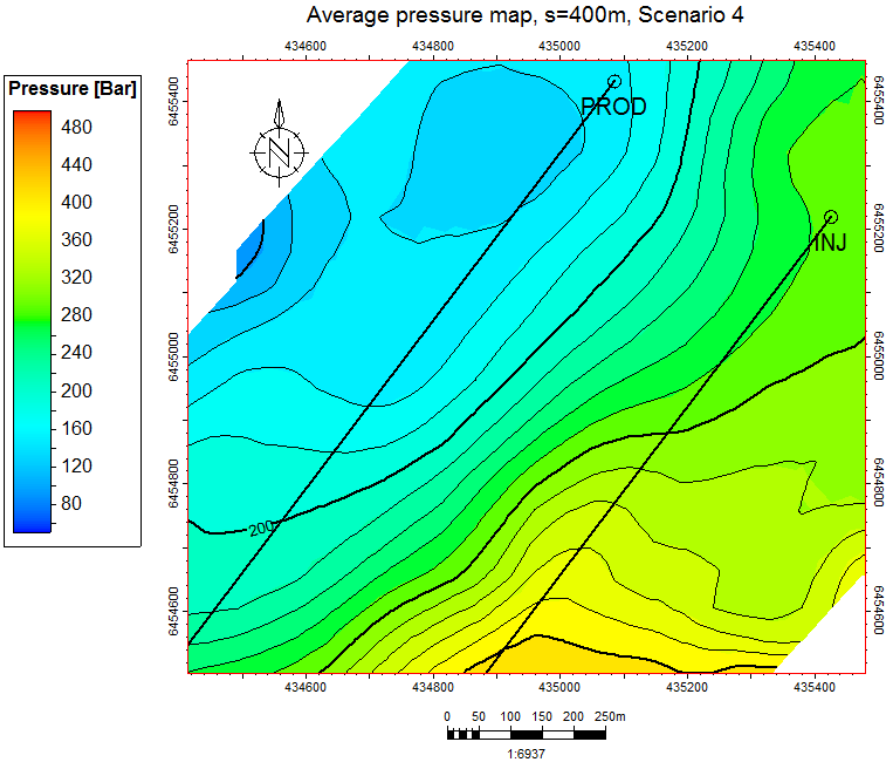

Figure D-5: Average pressure map after 3 years for s=400m.

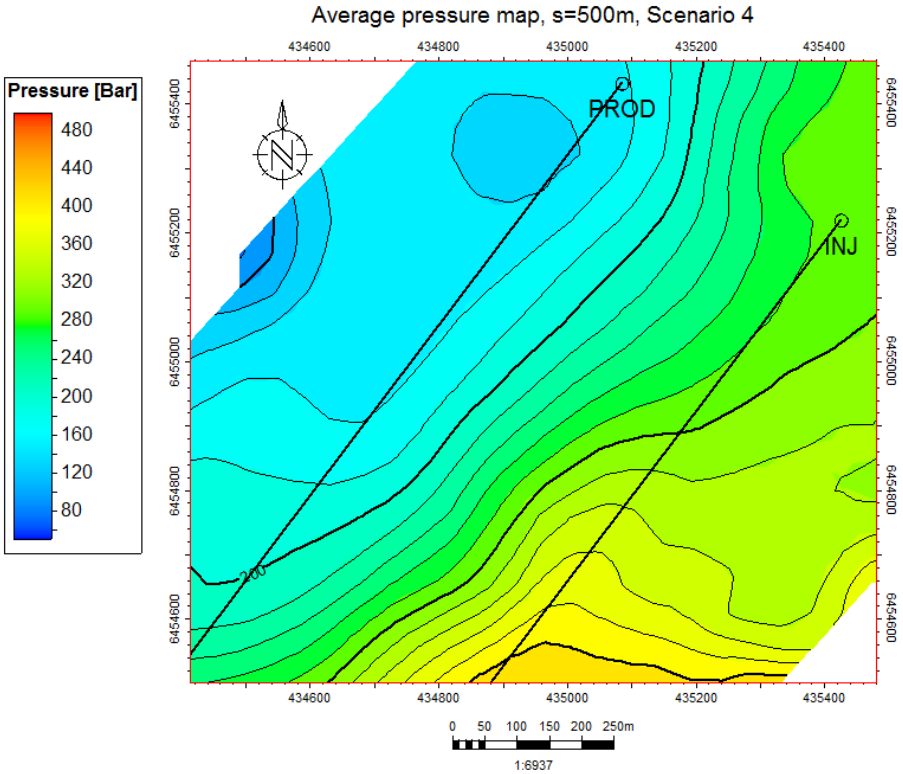

Figure D-6: Average pressure map after 3 years for s=500m.

Appendix E: Results from Scenario 5

E.1 Integrated saturation profiles for multiple- and non-fractured case

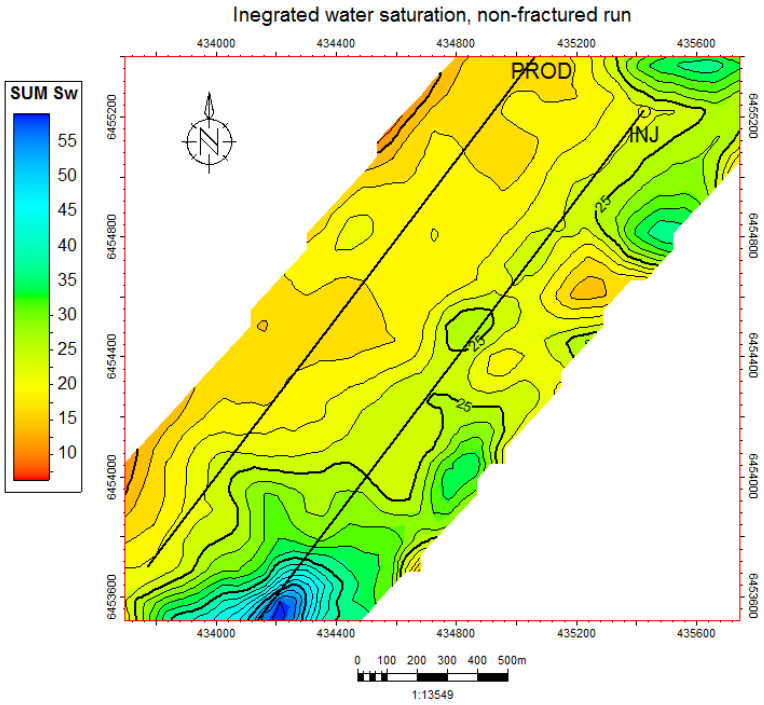

Figure E-1: Saturation map after 2 years for non-fractured run.

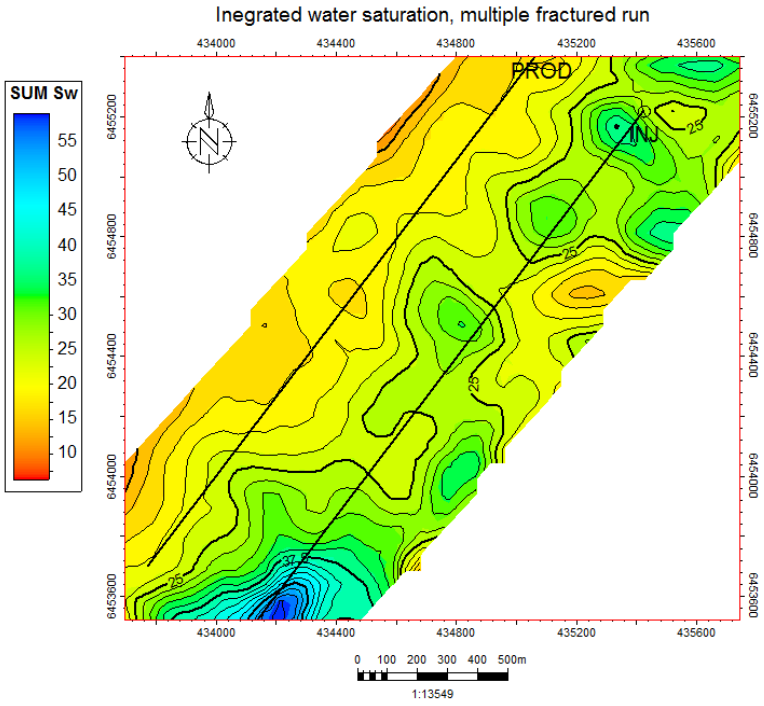

Figure E-2: Saturation map after 2 years for multiple fractured run.